OXYGEN DEPENDENT ELECTRON TRANSFER IN THE CYTOCHROME bc_1 COMPLEX AND THE INTERACTION BETWEEN *RHODOBACTER SPHAEROIDES* bc_1 COMPLEX AND CYTOCHROME c OR c_2

By

FEI ZHOU

Bachelor of Engineering
Jiangsu University
Jiangsu, P.R.China
2000

Master of Science
Lanzhou University
Gansu, P.R.China
2004

Submitted to the Faculty of the
Graduate College of the
Oklahoma State University
in partial fulfillment of
the requirements for
the Degree of

DOCTOR OF PHILOSOPHY
December, 2011

OXYGEN DEPENDENT ELECTRON TRANSFER

IN THE CYTOCHROME bc_1 COMPLEX

AND THE INTERACTION BETWEEN

RHODOBACTER SPHAEROIDES bc_1 COMPLEX

AND CYTOCHROME *c* OR c_2

Dissertation Approved:

Dr. Chang-An Yu

Dissertation Adviser

Dr. Linda Yu

Dr. Andrew Mort

Dr. Robert Burnap

Outside Committee Member

Dr. Sheryl A. Tucker

Dean of the Graduate College

TABLE OF CONTENTS

Chapter Page

Chapter Page

LIST OF TABLES

LIST OF FIGURES

Figure Page

Figure Page

Figure Page

NOMENCLATURE

ADP	Adenosine Diphosphate
ATP	Adenosine Triphosphate
AA	Antimycine A
BAS	Bovine Serum Albumin
bc_1 complex	ubiquinol-cytochrome *c* oxidoreductase
b_H	higher potential cytochrome *b* heme
b_L	lower potential cytochrome *b* heme
CMC	critical micelle concentration
DM	*n*-Dodecyl-ß-D-Maltopyranoside
DMSO	Dimethyl sulfoxide
DSC	Differential Scanning Calorimetry
E. coli	*Escherichia coli*
EDTA	Ethylenediaminetetraacetic acid
FPLC	Fast Protein Liquid Chromatography
ICM	Intracytoplasmic membrane
IM	Inner Membrane
IMS	Inner Membrane Space
ISC	Iron-Sulfur Cluster
ISP	Iron-Sulfur Protein
IPTG	Isopropyl β-D-thiogalactopyranoside
KD	Kilodaltons
kb	kilo base pair

LB	Luria Broth
MCLA	2-Methyl-6-(4-methoxyphenyl)-3, 7-dihydroimidazol [1, 2-α]pyrazin-3-one, hydrochloride
NADH	Nicotinamide Adenine Dinucleotide (reduced form)
Ni-NTA	Nickel-Nitrilotriacetic Acid
NQNO	2-*n*-nonyl-4-hydroxyquinoline *N*-oxide
$O_2^{\cdot -}$	Superoxide anion
OG	*n*-octyl-D-Gluocopyranoside
Pi	Inorganic phosphate
Psi	Pound per Square Inch
PAGE	Polyacrylamide Gel Electrophoresis
PCR	Polymerase Chain Reaction
PMSF	Phenylmethylsulfonyl fluoride
$Q^{\cdot -}$	Ubisemiquinone
Q	Ubiquinone
$Q_0C_{10}BrH_2$	2,3-dimethoxy-5-methyl- 6-(10-bromodecyl)- 1,4- benzoquinol
QCR	Ubiquinol-cytochrome *c* reductase
QH2	Ubiquinol
R.sphaeroides	*Rhodobacter sphaeroides*
ROS	Reactive Oxygen Species
SDS	Sodium Doceylsulfate
SOD	Superoxide Dismutase

TM	Transmembrane
Tm	melting temperature
TMBZ	tetramethylbenzinidine
UHDBT	5-undecyl-6-hydroxy-4,7-dioxobenzothiazole
β-ME	β-mercaptoethanol
[2Fe-2S]	Rieske iron-sulfur center

CHAPTER I

INTRODUCTION

Energy conservation

Energy supply is the most basic activity for all living cells. Chemical-bond energy from the catabolic products is used directly or storted in the energy-rich compound ATP via the process of energy conservation. The energy conservation including oxidative phosphorylation in mitochondria and photosynthetic phosphorylation in bacteria requires the intermolecular electron transfer. During this process, electrons are sequentially transferred through a chain of membrane-bound protein complexes called the electron transfer chain. Meanwhile, protons are translocated over the membrane to create an electrochemical gradient which in its turn is the driving force to the synthesis of ATP by the membrane-bound ATP synthase. Energy conservation takes place in the mitochondrial and chloroplastic inner membrane, and the cell membrane of aerobic and photosynthetic bacteria.

Mitochondrial Electron Transfer Chain

The mitochondrial electron transfer chain is located in the inner membrane. It is composed of four enzyme complexes: NADH:ubiquinone oxidoreductase (complex I),

succinate:ubiquinone oxidoreductase (complex II), ubiquinol:cytochrome c_1 oxidoreductase (cytochrome bc_1 complex or complex III), and cytochrome *c* oxidase (complex IV). Each complex consists of several protein subunits which host a variety of redox active prosthetic groups with successively increasing redox potentials. As illustrated in Figure 1 (Page 3), complexes I and II catalyze the electron transfer from NADH and succinate which are derived from the TCA cycle and the β-oxidation of fatty acids and amino acids to ubiquinone. Then reduced complex III oxidizes ubiquinol and reduces cytochrome *c*. Complex IV oxidizes cytochrome *c* and reduces oxygen to water. During the electron transfer through complexes I, III and IV, protons are translocated across the mitochondrial inner membrane to produce the membrane potential and proton gradient for use in ATP synthesis catalyzed by complex V. This is the central dogma of the chemiosmotic theory proposed by the Nobel Prize laureate Peter Mitchell in 1961 (1). Since then, the chemiosmotic theory has become the general mechanistic principle of oxidative phosphorylation and a paradigm in the intellectual framework of bioenergetics.

The cytochrome bc_1 complex

Ubiquinol-cytochrome *c* reductase (the cytochrome bc_1 complex) is a central component of the electron transfer in mitochondria and many photosynthetic bacteria. In chloroplasts and cyanobacteria, cytochrome b_6f (plastoqinol-plastocyanin oxidoreductase), which is an analogue to the cytochrome bc_1, participates in electron transfer of their oxygenic photosynthesis (2,3). The cytochrome bc_1 catalyzes electron transfer from ubiquniol to cytochrome *c* (c_2 in bacteria) with concomitant proton translocation across the inner mitochondria or bacterial plasma membrane, resulted in the generation of transmembrane proton electrochemical gradient (ΔμH), or proton motive

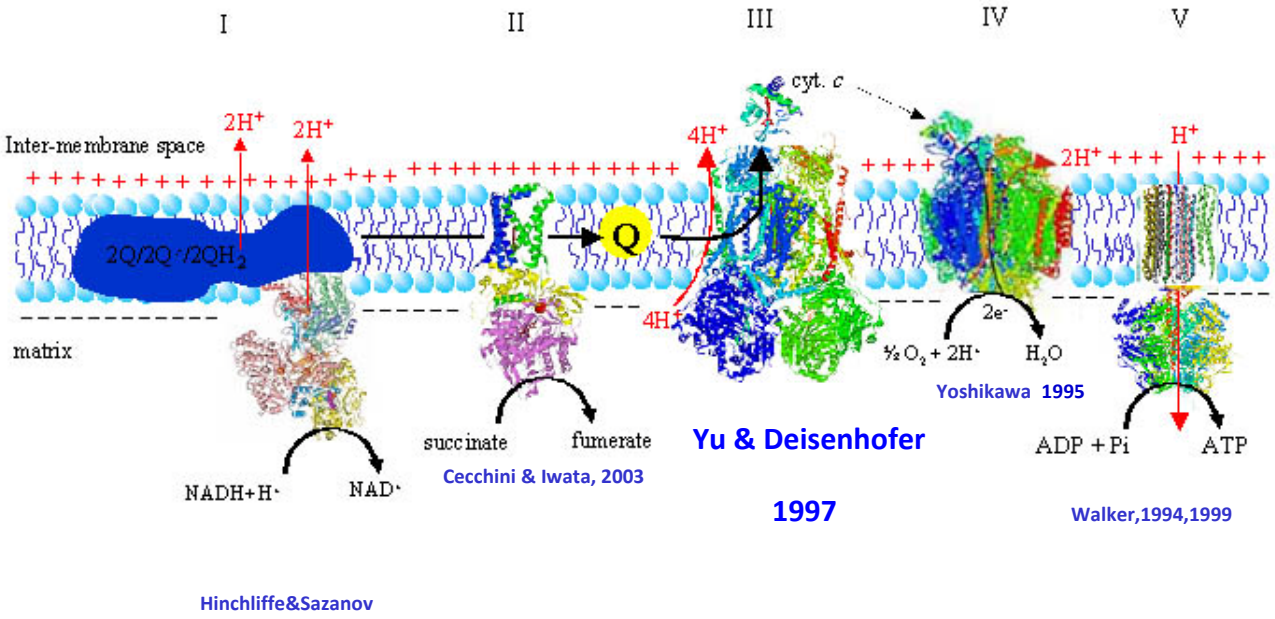

Figure 1. **Mitochondrial electron transfer chain**

force (pmf) for use in synthesis of ATP by ATP synthase (4,5).

The first three-dimensional crystal structure of the bovine mitochondrial bc_1 complexes from was solved with X-ray diffraction at about 2.9 Å by our group in collaboration with Dr. Deisenhofer's lab (4,5). The structures of the mitochondrial bc_1 complex from chicken (6) and yeast (7-9) were also reported since then. The bovine mitochondrial bc_1 complex is a pear-shaped dimer and contains 4330 amino acid residues with total molecular mass of 496 kDa (4,10) (Figure 2, Page 5). The height of the complex is approximately 155 Å, and its diameter at its widest point in the matrix space is about 130 Å. The complex extends 38 Å into the cytoplasmic space, spans the 42 Å inner mitochondrial membranes, and projects 75 Å into the matrix space (4). The matrix region contains more than one half of the molecular mass, including subunits I, II, VI, IX, the N-terminal of subunit VII and the C-terminal of ISP. The trans-membrane region covers thirteen trans-membrane helices in each monomer, including eight from cytochrome *b*, and one each from cytochrome c_1, ISP, subunits VII, X and XI. The inner-membrane space is the region housing soluble and catalytic domains of cytochrome c_1, ISP and subunit VIII as well. Each monomer contains 11 protein subunits; three of them are redox group containing subunits called core subunits and eight of them are non-redox group containing subunits called supernumerary subunits. The three redox group containing subunits are: cytochrome *b* housing hemes b_L and b_H, cytochrome c_1 housing heme c_1 and iron-sulfur protein (ISP) housing the iron-sulfur cluster [2Fe-2S]. They are directly involve in the catalytic function and are found in all the bc_1 complexes, supported by the 3-D crystal structure from different sources. The number of supernumerary subunits varies in different species, seven in chicken and yeast, one in

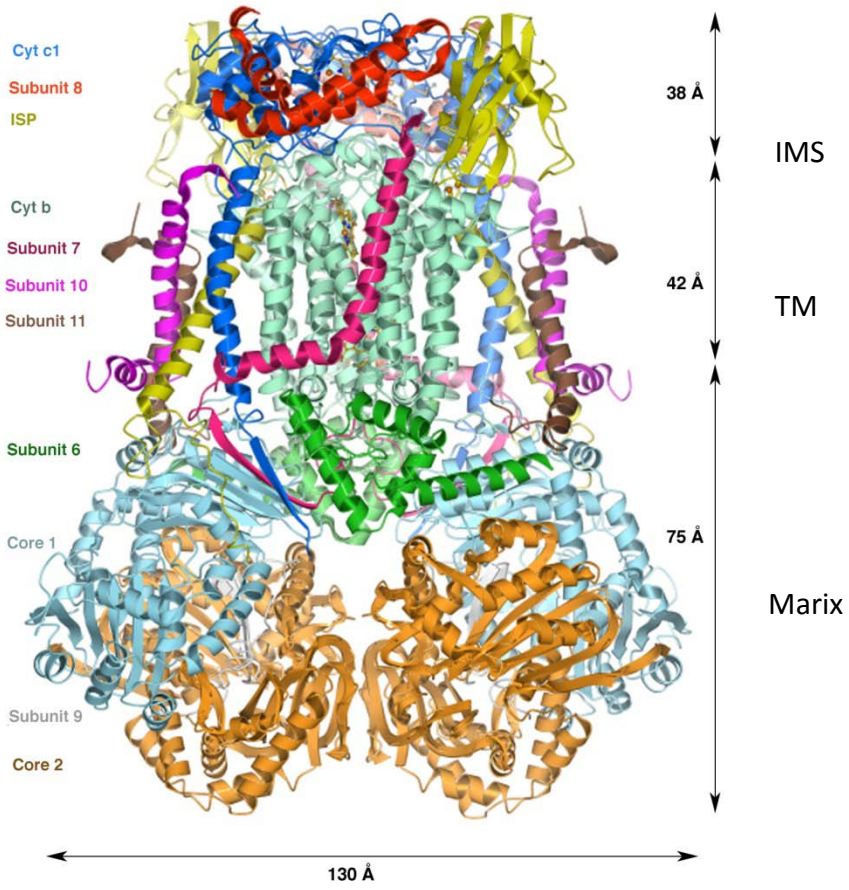

Yu and Deisenhofer's labs. *Science*. 1997

Figure 2. **The structure of the dimeric bovine mitochondrial cytochrome bc_1 complex shown in ribbon form** (4)**.** 11 subunits are represented by different colors. The mitochondrial inter-membrane space (IM), the transmembrane region (TM), and the mitochondrial matrix (Matrix) are as indicated.

Table 1. **The number of subunits, core subunits and supernumerary subunits in cytochrome bc_1 complexes from different species.**

Species	Number of subunits	Core subunit	Supernumerary subunit
Bovine	11	3	8
Chicken	10	3	7
Yeast	10	3	7
Potato	10	3	7
Rhodobacter sphaeroides	4	3	1
Rhodobacter capsulatus	3	3	0

Rodobacter sphaeroides and zero in *Rodobacter capsulatus* (11) (Table 1, Page 6).

The structure of cytochrome b - The cytochrome *b* is the only subunit in the cytochrome bc_1 complex which is encoded by the mitochondrial DNA (12). The cytochromes *b* from more than 900 species have highly conserved secondary structures (2). Bovine cytochrome *b* has 379 amino acid residues and consists of eight trans-membrane helices, named sequentially from A to H with both the N and C terminus located in the matrix side of the inner membrane (4,13-15) (Figure 3, Page 8). The eight helices are divided into two helical bundles. A to E helices belong to one bundle and F to H belong to another. They are connected by four long loops (AB, CD, DE and EF) and three short loops (BC, FG and GH). The bundles converge at the matrix side of the membrane but diverge toward the inter-membrane space side thus forming a pocket called Q_p pocket (or Q_o site) between the heme b_L and the iron sulfur cluster of ISP (ISC). This pocket is where quinol oxidization occurs and closes to heme b_L. Another pocket, Q_N pocket (or Q_i site), is where quinone reduction occurs and is close to heme b_H. Cytochrome *b* house two *b* type hemes: the low potential heme b_L and the high potential heme b_H. Two hemes are incorporated in first helical bundle through the totally conserved histidine residues (His-83 and His-182 for the heme b_L, His-97 and His-196 for the heme b_H). Heme b_H is close to the matrix side of cytochrome *b* while heme b_L is close to the intermembrane space side. The distance of 21Å between two hemes b_L in two monomers is close enough to allow electron transfer between them (16).

The structure of cytochrome c_1 - The cytochrome c_1 is a member of the *c* type cytochrome family (Figure 4, Page 9). The hydrophilic majority of this protein is

A

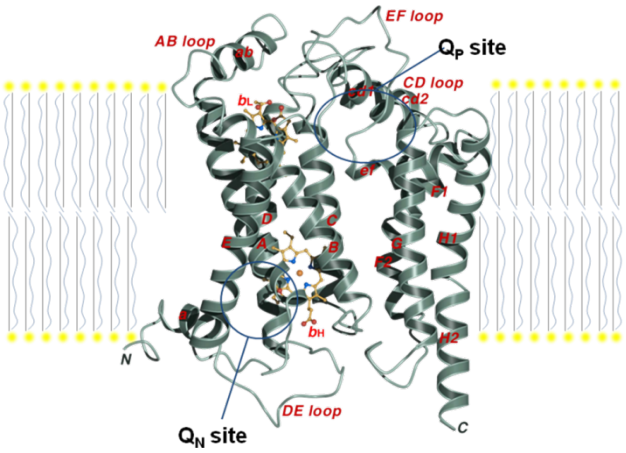

IM

TM

Matrix

B.

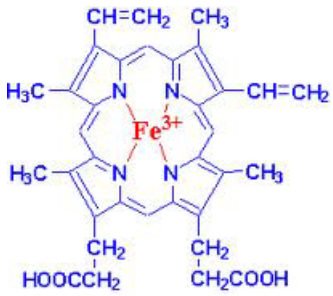

Figure 3. **Structure of the mitochondrial cytochrome *b*. (A)** Ribbon structure of cytochrome b. There are eight helices as labeled from A to H. Four prominent extramembrane loops are labeled as AB, CD, DE and EF. The b_L and b_H hemes are labeled in the ball-and-stick models with the carbon atoms in yellow, nitrogen in blue and oxygen in red. Two active sites are labeled: one is the ubiquinone reduction site (Q_N) and the other is the ubiquinol oxidation site (Q_P). The mitochondrial inter-membrane space (IM), the transmembrane region (TM), and the mitochondrial matrix (Matrix) are as indicated. (B) The structure of heme *b*.

A.

B.

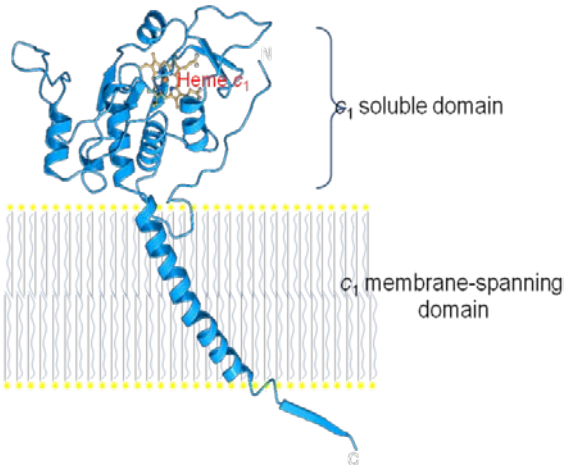

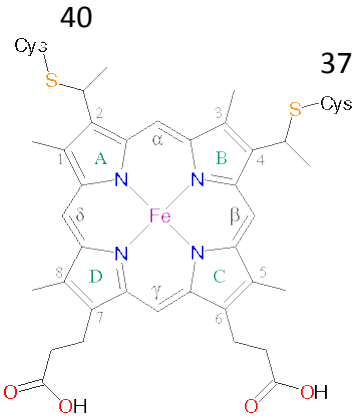

Figure 4**. Structure of the cytochrome c_1.** (A) Overall ribbon structure of cytochrome c_1. The soluble head domain of cytochrome c_1 and transmembrane domain are indicated. Heme c_1 is labeled as a ball-and-stick model with carbon atoms in yellow, nitrogen in blue and oxygen in gray. (B) The structure of heme c_1.

anchored to the periplasmic side of the membrane by a hydrophobic transmembrane helix at its C-terminal. The heme c_1 is covalently attached through thio-ether linkages to two conserved cysteines cys37 and cys40, and is coordinated with His41 and Met160 as well. The carboxy group of one of the propionates of the heme c_1 forms a salt bridge with Arg-120, while the other propionate of the heme c_1 extends toward ISP. The cytochrome c_1 provides three docking sites for cytochrome *c*, ISP and subunit 8 (hinge protein), respectively. Heme c_1 crevice is surrounded by acidic residues that could form a docking site for the positively charged residues around the heme crevice in cytochrome *c* (17).

The structure of Iron-Sulfur Protein (ISP) - The structure of ISP can be divided into three domains: the transmembrane N- terminal domain (tail) including residues 1-62, the soluble C – terminal domain (head) spanning residues 73-196, and the flexible linking domain (neck) covering 63-72 (18,19) (Figure 5, page 11). The iron sulfur cluster is positioned at the tip of the soluble head domain which contains three layers of antiparallel β sheets. There are two cysteine residues (Cys139 and Cys158) and two histidine residues (His141 and His161) coordinate the [2Fe-2S] cluster. Two additional highly conserved cysteine residues Cys-144 and Cys-160 form a disulfide bond stabilizing the protein. Hydrogen bonds around this region contribute to the stability of the protein.

One surprising finding about ISP is its extension across the interface between the two monomers, with membrane-spanning tail domain in one monomer and extrinsic head domain in the other (20-26). Movement of the ISP head domain during bc_1 catalysis has been proved by site-directed mutagenesis in several systems such as *Rodobacter sphaeroides*. Different positions of ISP head domain have been observed in crystal structures from different species, supporting the mechanism of electron transfer by

A.

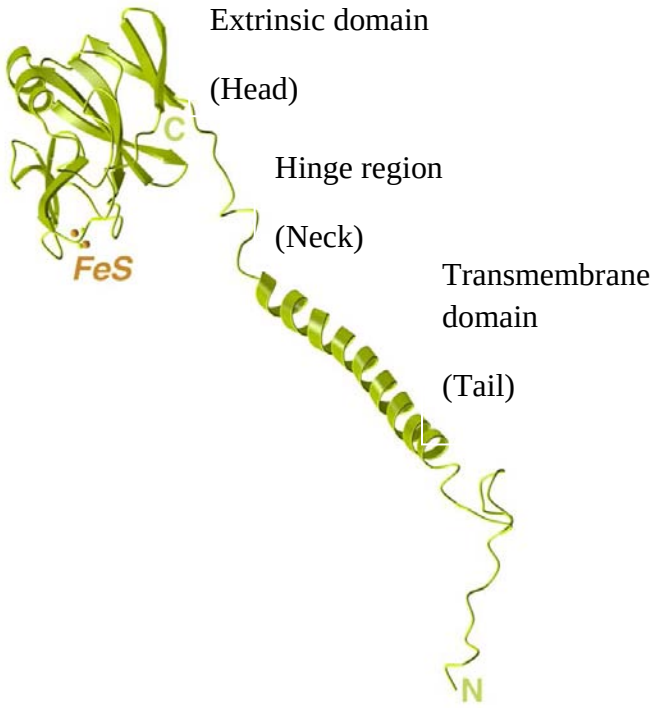

B.

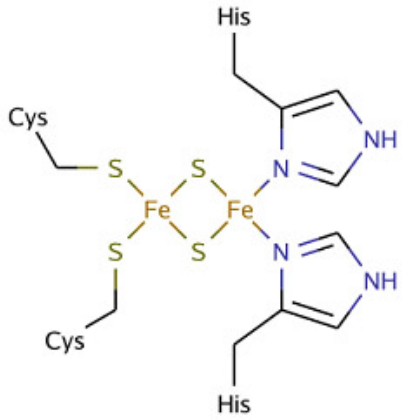

Figure 5. **Structure of the Rieske Iron-Sulfur Protein (ISP).** (A) The overall structure of ISP; The head, neck, tail and the iron-sulfur cluster are indicated. (B) The ligands of the iron-sulfur cluster.

domain movement in the bc_1 complex. During the process of electron transfer, the head domain of ISP moves between a site on the cytochome *b* interface and a site on the cytochrome c_1 interface. These two sites, therefore, are called "*b*" position and "c_1" position. Studies have strongly demonstrated the requirement of mobility of the ISP head domain in the bc_1 catalysis (27,28). Decreasing the flexibility of the neck domain of ISP through proline substitution, deletion, or insertion of amino acid residues can decrease the bc_1 activity. Fixation of the head domain of ISP at the *b* position or c_1 position by engineered disulfide bond also diminished bc_1 activity. However, the β-mercaptoethanol treatment that can release the ISP head domain from the *b* or c_1 positions restored most of the bc_1 complex activity. Although the importance of ISP head domain movement for the bc_1 catalysis has been well proved, the regulation and driving force for this movement is still unknown.

The protonmotive Q-cycle mechanism - The Q – cycle (Figure 6, Page 13), the most convincing hypothesis so far for the mechanism of electron transfer and proton translocation catalyzed by the cytochrome bc_1 complex, was first proposed by Peter Mitchell and later modified by several groups (6,29-31). This mechanism features two key points: (a) the presence of two separate Q binding sites located on opposite sides of the membrane: a site of quinol oxidization, called Q_P or Q_o site, is on the positive side of the membrane; a site of quinone reduction, called Q_N site or Q_i site, is on the negative side of the membrane. (b) The bifurcated reaction at the Q_P site; two electrons from the ubiquinol (QH_2) are transferred to two completely different acceptors, one to the [2Fe-2S] cluster and the other to heme b_L either in a sequential mechanism (32-34) or in a concerted mechanism (35-37).

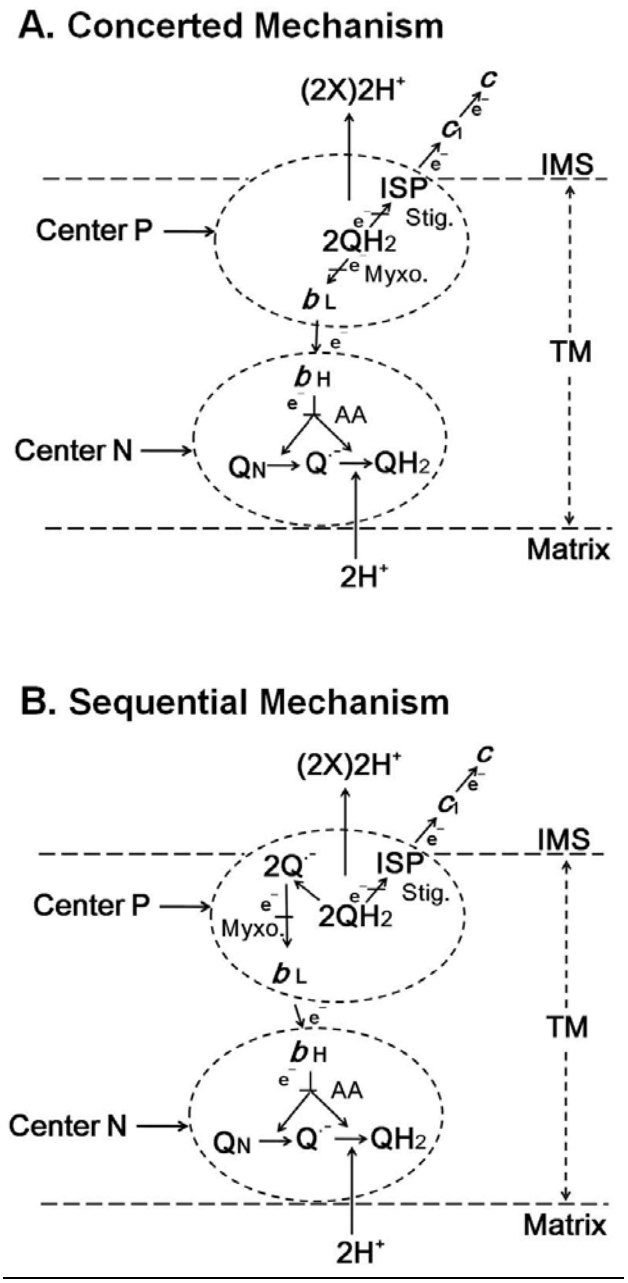

Figure 6. **The protonmotive Q-cycle mechanism.** (A) Concerted bifurcated oxidation of ubiquinol at the Qp site. (B) Sequential bifurcated oxidation of ubiquinol at the Qp site.

In the concerted mechanism, electrons from QH_2 oxidation at the Qp site are transferred simultaneously to heme b_L and the ISP in a bifurcated pathway. In the sequential mechanism, the first electron is transferred from QH_2 to the ISP to generate an intermediate ubisemiquinone at the Q_p site. Then the second electron is transferred from this ubisemiquinone to the heme b_L. Therefore, the existence of the ubisemiquinone at the Q_p site will be a key point to substantiate the sequential mechanism. However, a functional ubisemiquinone has never been observed at the Q_p site although the detection of ubisemiquinone under abnormal conditions has been reported (38,39). Furthermore, the failure to detect ubisemiquinone in a mutant bc_1 complex lacking heme b_L (40) also support the concerted mechanism in the bifurcated QH2 oxidation. In addition to the unsuccessful effort to detect the ubisemiquinone, recently, the study of presteady state kinetics showed the same cytochrome *b* reduction rate as the ISP reduction (32), which also encourages many groups to support the concerted mechanism.

In both mechanisms, the ISP accepts the electron and then transfers it to cytochrome c_1, then to cytochrome *c* (high potential electron transfer chain). On the other hand, the b_L accepts the second electron from QH2 then transfers it to b_H (low potential electron transfer chain) and finally the Q_N site where the ubiquinone is reduced to a stable semiquinone ($Q^{\cdot-}$), concomitant with the release of two protons on the periplasmic side of the membrane, thus finishes the first half catalytic cycle. In the second half of the Q-cycle, all steps in the first cycle are repeated: a second QH_2 is oxidized at the Q_P site, one electron is transferred through the high potential chain to the cytochrome *c*, the other electron travels through the low potential chain to b_H where the semiquinone ($Q^{\cdot-}$) from first cycle is reduced to QH_2, with the uptake of two protons from the negative side of the

membrane. Therefore, in one complete Q - cycle, one molecule of QH_2 is oxidized to Q, two molecules of cytochrome *c* are reduced; two protons are taken from the negative side of the membrane, and four protons are deposited to the positive side of the membrane.

The overall reaction catalyzed by the bc_1 complex is:

$$QH_2 + 2\text{cytchrome } c^{3+} + 2H^+_N \longrightarrow Q + 2\text{cytochrome } c^{2+} + 4H^+_P$$

Inhibitors of the cytochrome bc_1 complex – The inhibitors (Figure 7, Page 16) of the cytochrome bc_1 complex can be divided into two classes (Table 2, Page 17). Class I inhibitors bind to the Q_P site to block the oxidation of QH_2. Class II inhibitors, represented by Antimycin A and heptyldroxyquinoline-N-oxide (HQNO), bind to the Q_N site to block the reduction of ubiquinone. Class I inhibitors can be subdivided into three sub-classes Ia, Ib and Ic based on chemical characteristics, and on spectroscopic and biophysical effects of the b_L heme and the iron-sulfur cluster of ISP upon binding of inhibitors. Class Ia inhibitors, such as myxothiazaol, azoxystrobin, famoxadone and methoxyaxrylate stilbene (MOAS), presumably block the electron transfer from quinol to ISP, accompanying by a red shift in the α and β- bands of the reduced heme b_L spectrum. Class Ib inhibitors, including stigmatallin, usually contain a chromone ring and inhibit electron transfer from the ISP to cytochrome c_1. Binding of class Ib inhibitors to cytochrome bc_1 complex causes an increase in redox potential of ISP and a red shift of the reduced heme b_L spectrum. Class Ic inhibitors which belong to 2 – hydroxy quinon analogues, such as 5-undecyl-6-hydroxy-4,7-dioxobenzothiazole and UHDBT.

Another classification of bc_1 inhibitors was proposed 7 years ago based on the crystal structures of inhibitor bound bc_1 (15). In this modified classification, Qp site inhibitors are called class P inhibitors and Q_N site inhibitors are called class N inhibitors.

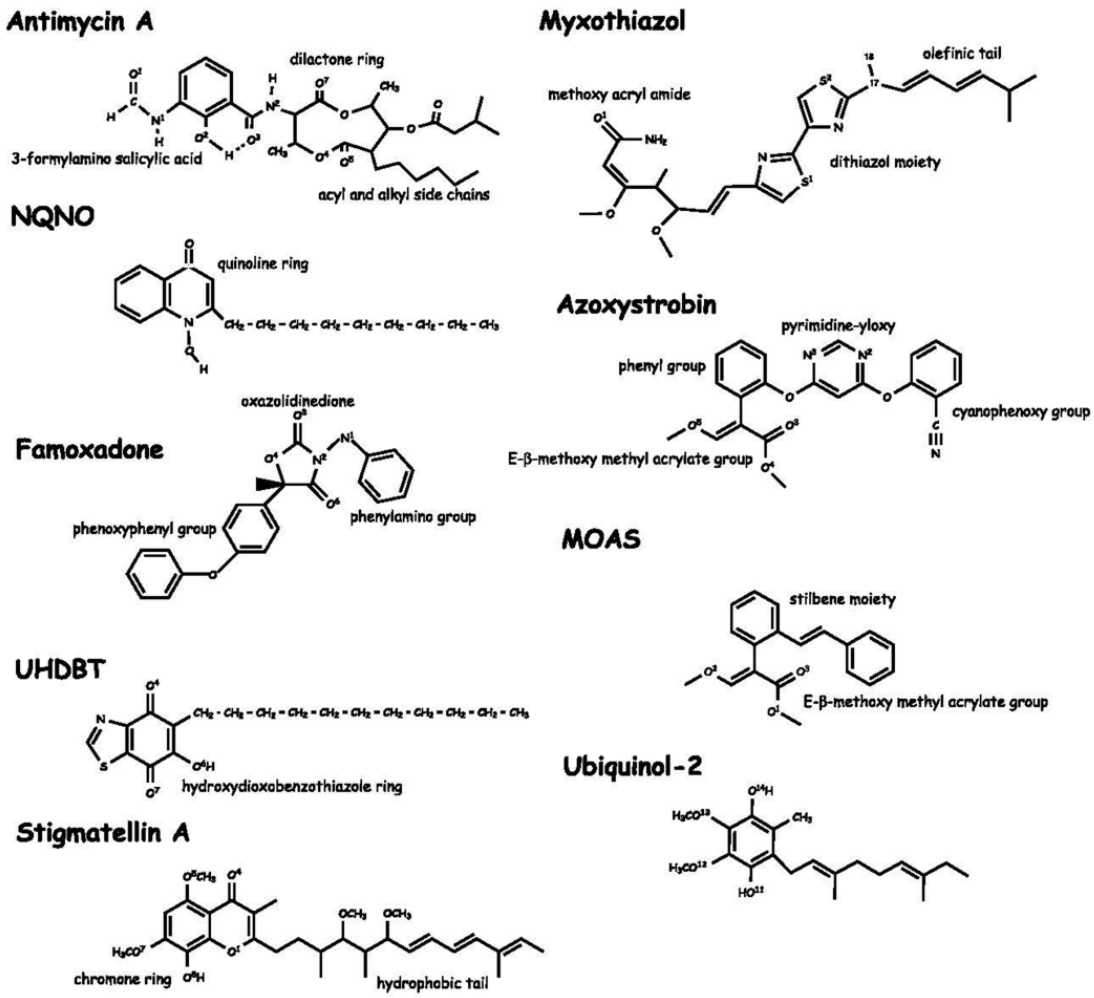

Figure 7. **Chemical structures of cytochrome bc_1 inhibitors** (15).

Table2. **Classification of cytochrome bc_1 inhibitors.**

Class	Sub-class	Site of blocking electron transfer	Inhibitors
	Ia (Pm)	QH2 → ISP	Myxothiazol, famoxadone, MOAS
I (P)	Ib (Pf)	ISP → c_1	Stigmatellin
	Ic (Pf)	ISP → c_1	UHDBT
II (N)		b_H → Q	Antimycin, HONO

Class P inhibitors are defined into two groups. One group is P_f inhibitors which fix the ISP head domain including Stigmatellin and UHDBT, and the other group P_m inhibitors facilitate its mobility including myxothiazol and MOAS. Comparison of co-crystal structures of bc_1 with different inhibitors showed the binding of inhibitors has a little effect on the over complex conformation change but a significant effect on the immediate environment of the binding sites.

The cytochrome bc_1 complex from Rhodobacter sphaeroides - In the aerobic respiratory system of bacteria, the bc_1 complex works similarly as the one in mitochondria. In photosynthetic purple non-sulfur bacterium *Rhodobacter sphaeroides*, the bc_1 complex catalyzes the electron transfer from QH_2 to oxidized cytochrome c_2 instead of cytochrome *c* when bacteria grow photosynthetically (41,42). The function of cytochrome bc_1 complex in photosynthetic bacteria is also well described by the Q-cycle mechanism, which has been demonstrated by intensive biophysical, biochemical and molecular genetic studies. For every complete reaction catalyzed by the bc_1 complex in photosynthetic bacteria, one QH_2 is oxidized, two cytochrome c_2 are reduced, and two protons are picked up from the cytoplasmic side of membrane and four protons are deposited to the bacterial periplasm which is the equivalent to the mitochondrial inter-membrane space (42). Then, the electrons are shuttled by the reduced cytochrome c_2 back to the photosynthetic reaction center to reduce P_{870}. Therefore, there is no exogenous electron donor or final electron acceptor in this cyclic electron transfer pathway. Energy is conserved through the electron recycling between the reaction center and the bc_1 complex to produce a driving force for ATP synthesis.

However, the bc_1 complex is not an essential element for *R. sphaeroides* when it

grows aerobically (Figure 8, Page 20). Under the condition with high oxygen tension, its photosynthetic system is repressed but the bacterial growth switches to an alternative pathway in which the electron can be transferred directly from ubiquinol to oxygen via quinol oxidase (Figure 8). Limited oxygen can induce the synthesis of the photosynthetic apparatus. So, this is an important feature that *R. sphaeroides* cells can grow under semi-aerobic conditions in the dark even with a defective or non-functional bc_1 complex (42,43).

In *R. sphaeroides*, the gene sequence of the cytochrome bc_1 complex is only 3.3kb. Three core subunits are encoded by genes organized in an *fbc*FBC operon (44). A gene *fbc*Q encoding the subunit IV is approximately 278kb away from the *fbc*FBC operon. The strains *BC17* in which the *fbc*FBC operon and RSΔIV in which *fbc*Q operon has been deleted from the chromosome cannot grow photosynthetically but can aerobically due to the alternative bc_1-independent electron transfer pathway. By inserting *fbc*FBC genes into the low copy number expression vector pRKD418, the bc_1 complex can be overexpressed in *BC17*. The well established systems have been utilized to study the structures and functions of the cytochrome bc_1 complex by site directed mutagenesis. Six consecutive histidine residues were tagged on the C-terminus of the *R. sphaeroides* cytochrome c_1 (20). Using a nickle-nitrilotriacetic acid (Ni-NTA) agarose column which has been commercialized, the six-histidine tag greatly facilitated the purification of the bc_1 complexes from *R. sphaeroides* cells.

Therefore, as we mentioned above, the advantages of *Rodobacter sphaeroides* - the flexibility of growth condition, the simplicity of the subunit composition and the well-developed molecular engineering system - make it a valuable model to study the structure

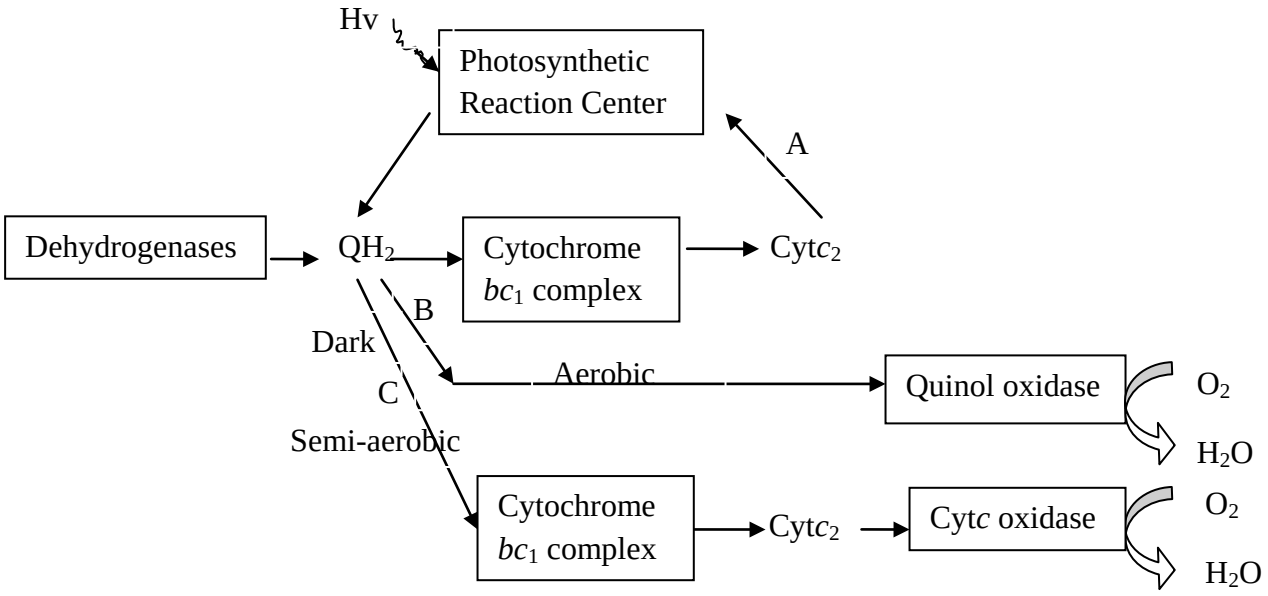

Figure 8. **Electron transfer pathways in *Rodobacter sphaeroides***

Pathway A: photosynthetic cycle. Pathway B: Aerobic growth in the dark. Pathway C: Semi-aerobic growth in the dark.

and function of the cytochrome bc_1 complex.

There are only four subunits in the *R. sphaeroides* bc_1 complex, cytochrome *b* (43KD), cytochrome c_1 (31KD), ISP (23KD), and subunit IV (14KD) (45-47). Three catalytic subunits: cytochrome *b*, cytochrome c_1 and ISP are homologous to their mitochondrial counterparts. In contrast to seven or eight supernumerary subunits in mitochondrial bc_1 complex, the *R. sphaeroides* subunit IV is the only one supernumerary subunit which is functionally homologus to subunit VII in the mitochondrial bc_1 complex (48,49). Corresponding to this simple structure, *R. sphaeroides* cytochrome bc_1 complex only has 10% of mitochondrial bc_1 activity.

The wild type *R. sphaeroides* bc_1 complex had not been crystallized. The structure of a mutant *R. sphaeroides* bc_1 complex with an arginine substitution at the S287 of cytochrome *b*, a cysteine substitution at the V135 of ISP [S287R (cytochrome *b*)/V135S (ISP)], and the inhibitor stigmatellin bound at the Q_P site has been resolved at high resolution, 2.35Å (Figure 9, Page 22). Subunit IV is missing from the crystal during the process of crystal formation for unknown reasons (50) .

X-ray crystal structure reveals that the three core subunits *R. sphaeroides* bc_1 assemble in a manner similar to the corresponding subunits in bovine mitochondrial bc_1. But the bacterial core subunits are larger than their counterparts in the bovine complex and have more insertions on or near the periplasmic or cytoplasmic side of the membrane, which might contribute to the structural stability and functional integrity of the bc_1 complex.

Previous studies on interaction between cytochrome c_1 and c or c_2 – Since the cytochrome c_1 was discovered in mid-last century (51), the study on its structure and

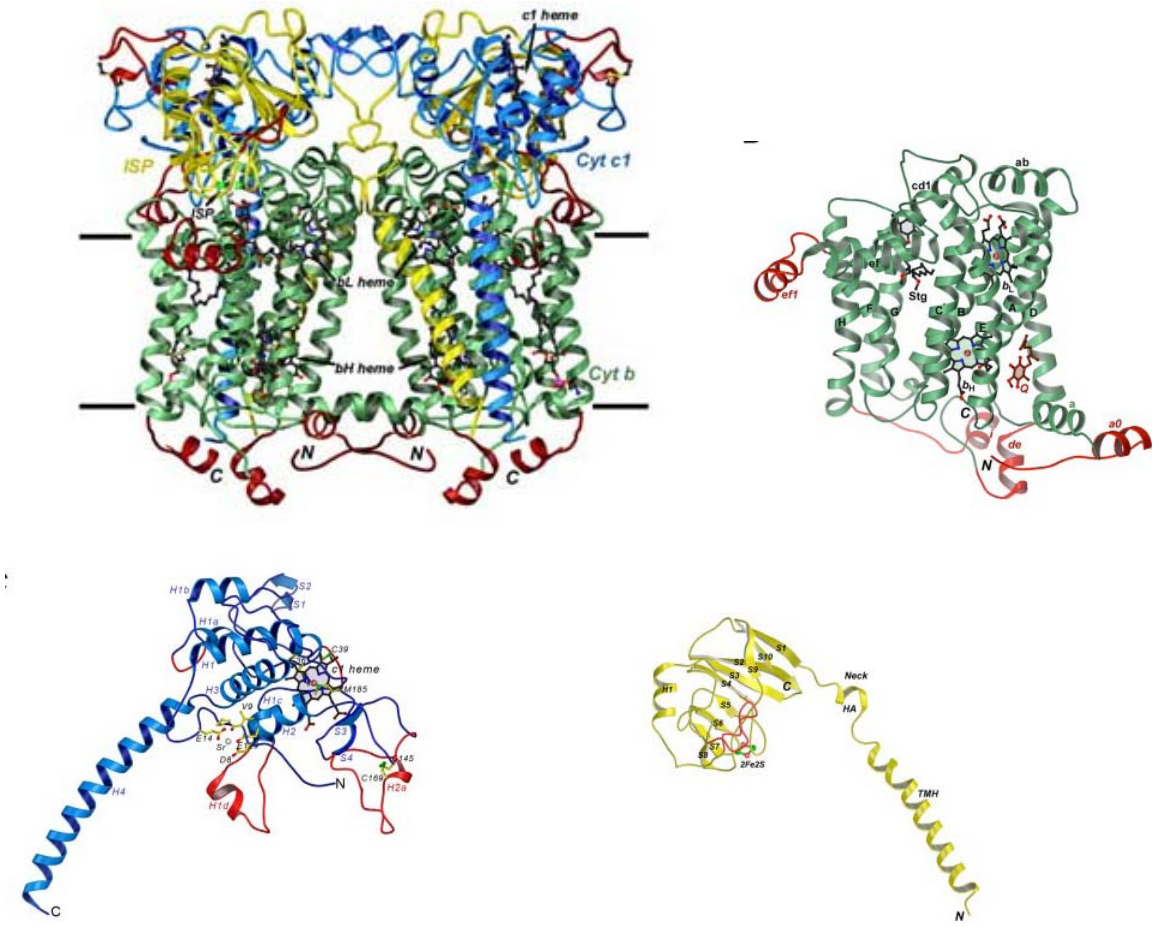

Figure 9. **Structure of the *R. sphaeroides* cytochrome bc_1 complex with a resolution of 2.3 Å (50).** (A). Overall structure of inhibitor bounded of *R. sphaeroides* cytochrome bc_1 complex shown as a ribbon representation. The boundary of lipid bilayer is labeled with two parallel lines. Inhibitor Stigmatellin is indicated. The colors for subunits are: (B) green, cytochrome *b*; (C) blue cytochrome c_1; (D) yellow, ISP. Red: insertions and extensions absent from the bovine cytochrome bc_1 complex.

function has made a great progress. Besides complexed form, the cytochrome c_1 has been isolated from mitochondria and bacteria as well. The cytochrome c_1 belongs to the *c* type cytochrome family which shares the characteristic Cys-X-X-Cys-His heme binding consensus motif. In *R. sphaeroides* bc_1 complex, the cytochrome c_1 has a soluble head domain housing heme c_1 and a trans-membrane helix near the carboxyl terminus to fix it on the membrane in the same way as in bovine bc_1 (52).

The mechanism of interaction between cytochromes c_1 in bc_1 complex and *c* (or c_2 in bacterial system) has been extensively studied but not been determined conclusively. Considerable amount of publications supported the nature of the interaction is hydrophlic. The importance of electrostatic interaction on the complex formation between cytochrome *c* and bc_1 complex has been demonstrated in different species. Biophysical, biochemical and mutagenesis data suggested the lysine amino groups surrounding the heme crevice of cytochrome *c* interact with the carboxyl groups of cytochrome c_1 in the bc_1 complex (4,53-57) during electron transfer from cytochrome c_1 to *c* or c_2. However, the co-crystal structure of yeast cytochrome bc_1 with its substrate cytochrome *c*, an Fv fragment and an inhibitor Stigmatellin bound showed a small hydrophobic interface surrounded by charged residues, which is favorable for transient complex formation (58,59).

How the cytochrome c_1 interacts with cytochrome *c* is still under debate. Why do the co-crystal results differ from the results of biophysical, biochemical and mutagenesis data? Is it possible that the presence of Stigmatellin and antibody caused the conformational change? Is it universal in all species or unique in yeast?

In order to clarify these questions, the construction, purification and characterization of soluble *R. sphaeroides* cytochrome c_1 head domain, and the interaction between *R. sphaeroides* bc_1 complexes and cytochrome *c* or c_2 has been further studied in this study.

Involvement of oxygen in electron transfer catalyzed by cytochrome bc_1 complexes and superoxide anion radical generation – Reactive oxygen species (ROS) are well known as one of the toxicities mediating oxidative stress (60-62). ROS can interact with DNA/RNA, proteins, carbohydrates, lipids, thus causing a number of diseases, such as the aging process, cancers, and inflammations (63-65). Superoxide anion is a progenitor ROS. It is thought that 1-2% of electron leakage from the normal pathway of oxidative phosphorylation is involved in the production of the superoxide anion (66). In addition to its main functions of electron transfer and proton translocation, the cytochrome bc_1 complex has been identified as one of two main reactive oxygen radical generation sites in the electron transfer chain (67-69). Electrons leaked during electron transfer through cytochrome bc_1 are thought to react with molecular oxygen to form superoxide anions which dismutate to H_2O_2 quickly. In the cytochrome bc_1 complex, two electron leakage factors -ubisemiquinone radical at the Qp site and the reduced heme b_L are suggested to be involved in the superoxide production (67,68). Antimycin, one of the cytochrome bc_1 inhibitors which block electron transfer, can cause increased superoxide anions generation activity (60,70,71). However, the lack of detection of ubisemiquinone obscures the mechanism which suggests that the superoxide is caused by the ubisemiquinone radical at the Qp site. A new mechanism has been proposed based on the results in our lab (72): Oxygen participates in the bifurcated ubiquinol oxidation by

acting as a low potential electron acceptor in a hydrophobic environment and in the absence of heme b_L; One electron from QH_2 is transferred to the high potential electron acceptor ISP, another electron goes to oxygen to produce protonated superoxide ($O_2^{\cdot}H$) which diffuses to the intermembrane space or matrix (a hydrophilic environment) to generate $O_2^{\cdot -}$ after deprontonation. The recent crystal structure of bc_1 complex showed an oxygen (Xe) binding site located between heme b_L and QH_2. In this study, the involvement of oxygen in the electron transfer and superoxide generation is further discussed.

References

1. Mitchell, P. (1961) *Nature* **191**, 144-148
2. Trumpower, B. L., and Gennis, R. B. (1994) *Annu. Rev. Biochem.* **63**, 675-716
3. Trumpower, B. L. (1990) *Microbiol Rev* **54**, 101-129
4. Xia, D., Yu, C.-A., Kim, H., Xia, J.-Z., Kachurin, A. M., Zhang, L., Yu, L., and Deisenhofer, J. (1997) *Science* **277**, 60-66
5. Iwata, S., Ostermeier, C., Ludwig, B., and Michel, H. (1995) *Nature* **376**, 660
6. Zhang, Z., Huang, L., Shulmeister, V. M., Chi, Y.-I., Kim, K. K., Hung, L.-W., Crofts, A. R., Berry, E. A., and Kim, S.-H. (1998) *Nature* **392**, 677-684
7. Hunte, C., J, K., C, L., T, R., and H, M. (2000) *Structure* **8**, 669-684
8. Hunte, C., and Michel, H. (2002) *Current Opinion in Structural Biology* **12**, 503
9. Solmaz, S. R. N., and Hunte, C. (2008) *J. Biol. Chem.* **283**, 17542-17549
10. Iwata, S., Lee, J. W., Okada, K., Lee, J. K., Iwata, M., Rasmussen, B., Link, T. A., Ramaswamy, S., and Jap, B. K. (1998) *Science* **281**, 64-71
11. Berry, E. A., Guergova-Kuras, M., Huang, L.-s., and Crofts, A. R. (2000) *Annual Review of Biochemistry* **69**, 1005-1075
12. Voet, D. a. V., J.G. . (2004), 814
13. Gao, X., Wen, X., Esser, L., Quinn, B., Yu, L., Yu, C., and Xia, D. (2003) *Biochemistry* **42**, 9067-9080
14. Gao, X., Wen, X., Yu, C.-A., Esser, L., Tsao, S., Quinn, B., Zhang, L., Yu, L., and Xia, D. (2002) *Biochemistry* **41**, 11692-11702
15. Esser, L., Quinn, B., Li, Y.-F., Zhang, M., Elberry, M., Yu, L., Yu, C.-A., and Xia, D. (2004) *Journal of Molecular Biology* **341**, 281

16. Gong, X., Yu, L., Xia, D., and Yu, C.-A. (2005) *J. Biol. Chem.* **280**, 9251 - 9257

17. Tian, H., Sadoski, R., Zhang, L., Yu, C. A., Yu, L., Durham, B., and Millett, F. (2000) *J Biol Chem* **275**, 9587-9595

18. Iwata, S., Saynovits, M., Link, T. A., and Michel, H. . (1996) *Structure* **4**, 567-579

19. Link, T. A., Saynovits, M., Assmann, C., Iwata, S., Ohnishi, T., and Von Jagow, G. . (1996) *Eur J Biochem* **237**, 71-75

20. Tian, H., Yu, L., Mather, M. W., and Yu, C.-A. (1998) *J. Biol. Chem.* **273**, 27953-27959

21. Tian, H., White, S., Yu, L., and Yu, C.-A. (1999) *J. Biol. Chem.* **274**, 7146-7152

22. Xiao, K., Yu, L., and Yu, C.-A. (2000) *J. Biol. Chem.* **275**, 38597-38604

23. Xiao, K., Chandrasekaran, A., Yu, L., and Yu, C.-A. (2001) *J. Biol. Chem.* **276**, 46125-46131

24. Nett, J. H., Hunte, C., and Trumpower, B. L. (2000) *Eur J Biochem* **267**, 5777-5782

25. Darrouzet, E., Valkova-Valchanova, M., Moser, C. C., Dutton, P. L., and Daldal, F. (2000) *Proc. Natl. Acad. Sci. U.S.A* **97**, 4567-4572

26. Ma, H.-W., Yang, S., Yu, L., and Yu, C.-A. (2008) *Biochim. Biophys. Acta - Bioenergetics* **1777**, 317-326

27. Xiao, K., Yu, L., and Yu, C. A. (2000) *J Biol Chem* **275**, 38597-38604

28. Ma, H. W., Yang, S., Yu, L., and Yu, C. A. (2008) *Biochim Biophys Acta* **1777**, 317-326

29. P, M. (1976) *J. Theor. Biol.* **62**, 327

30. Crofts, A. R. (1985) *The Enzymes of Bioclogical Memebranes* **4**, 347-382

31. Brandt, U. (1996) *Biochim. Biophys. Acta* **1275**, 41-46

32. Zhu, J., Egawa, T., Yeh, S.-R., Yu, L., and Yu, C.-A. (2007) *Proc. Natl. Acad. Sci. U.S.A* **104**, 4864-4869

33. Snyder, C. H., Gutierrez-Cirlos, E. B., and Trumpower, B. L. (2000) *J. Biol. Chem.* **275**, 13535-13541

34. Trumpower, B. L. (2002) *Biochim. Biophys. Acta - Bioenergetics* **1555**, 166

35. Brandt, U. (1998) *Biochim. Biophys. Acta - Bioenergetics* **1365**, 261-268

36. Crofts, A. R. (2004) *Biochim. Biophys. Acta - Bioenergetics* **1655**, 77-92

37. Crofts, A. R. (2004) *Annual Review of Physiology* **66**, 689-733

38. Zhang, H., Osyczka, A., Dutton, P. L., and Moser, C. C. (2007) *Biochim Biophys Acta* **1767**, 883-887

39. Cape, J. L., Bowman, M. K., and Kramer, D. M. (2007) *Proc Natl Acad Sci U S A* **104**, 7887-7892

40. Yang, S., Ma, H. W., Yu, L., and Yu, C. A. (2008) *J Biol Chem* **283**, 28767-28776

41. Ferguson, S. J., Jackson, J. B., and McEwan, A. G. (1987) *FEMS Microbiology Letters* **46**, 117-143

42. Gennis, R. B., Barquera, B., Hacker, B., Doren, S. R., Arnaud, S., Crofts, A. R., Davidson, E., Gray, K. A., and Daldal, F. (1993) *Journal of Bioenergetics and Biomembranes* **25**, 195-209

43. Thony-Meyer, L. (1997) *Microbiol Mol Biol Rev* **61**, 337-376

44. Yun, C. H., Beci, R., Crofts, A. R., Kaplan, S., and Gennis, R. B. (1990) *Eur J*

Biochem **194**, 399-411

45. Ljungdahl, P. O., Pennoyer, J. D., Robertson, D. E., and Trumpower, B. L. (1987) *Biochim. Biophys. Acta - Bioenergetics* **891**, 227

46. Yu, L., Mei, Q. C., and Yu, C. A. (1984) *J. Biol. Chem.* **259**, 5752-5760

47. Katherine M. Andrews, A. R. C., Robert B. Gennis. (1990) *Biochemistry* **29**, 2645-2651

48. Yu, L., and Yu, C.-A. (1991) *Biochemistry* **30**, 4934-4939

49. Yu, L., Tso, S.-C., Shenoy, S. K., Quinn, B. N., and Xia, D. (1999) *Journal of Bioenergetics and Biomembranes* **31**, 251-258

50. Esser, L., Elberry, M., Zhou, F., Yu, C. A., Yu, L., and Xia, D. (2008) *J Biol Chem* **283**, 2846-2857

51. Keilin, D., and Hartree, E. F. (1949) *Nature* **164**, 254-259

52. Yu, L., Mei, Q.C., and Yu, C.A. . (1984) *Biochemical and Biophysical Research Communications* **118**, 964-969

53. Guner S, W. A., Millett F, Caffrey MS, Cusanovich MA, Robertson DE and Knaff DB . (1993) *Biochemistry* **32**, 4793-4800

54. Millett F, D. B. (2004) *Photosynth Res.* **82(1)**, 1-16

55. Clemens BROGER, S. S., and Angelo AZZI. (1983) *Eur. J. Biochem.* **131**, 349-352

56. Samuel H. Speck, S. F.-M., Neil Osheroff, and E. Margoliash. (1979) *Proc. Natl. Acad. Sci. USA* **76,** 155-159

57. Stonehuerner, J., O'Brien, P., Geren, L., Millett, F., Steidl, J., Yu, L., and Yu, C. A. (1985) *J Biol Chem* **260**, 5392-5398

58. Hunte, C. L. a. C. (2002) *PNAS* **99**, 2800-2805

59. Solmaz, S., and Hunte, C. (2008) *J. Biol. Chem.*, M710126200

60. Andreyev, A. Y., Kushnareva, Y. E., and Starkov, A. A. (2005) *Biochemistry (Mosc)* **70**, 200-214

61. Barja, G. (2004) *Trends Neurosci* **27**, 595-600

62. Van Remmen, H., and Richardson, A. (2001) *Exp Gerontol* **36**, 957-968

63. Shigenaga, M. K., Hagen, T. M., and Ames, B. N. (1994) *Proc Natl Acad Sci U S A* **91**, 10771-10778

64. Sadek, H. A., Nulton-Persson, A. C., Szweda, P. A., and Szweda, L. I. (2003) *Arch Biochem Biophys* **420**, 201-208

65. Moro, M. A., Almeida, A., Bolanos, J. P., and Lizasoain, I. (2005) *Free Radic Biol Med* **39**, 1291-1304

66. Boveris, A., Oshino, N., and Chance, B. (1972) *Biochem J* **128**, 617-630

67. Turrens, J. F., Alexandre, A., and Lehninger, A. L. (1985) *Arch. Biochem. Biophys* **237**, 408-414

68. Nohl, H., and Jordan, W. (1986) *Biochem. Bioph. Res. Co* **138**, 533-539

69. McLennan, H. R., and Degli Esposti, M. (2000) *J Bioenerg Biomembr* **32**, 153-162

70. Zhang, L., Yu, L., and Yu, C.-A. (1998) *J. Biol. Chem.* **273**, 33972-33976

71. Quinlan, C. L., Gerencser, A. A., Treberg, J. R., and Brand, M. D. (2011) *J Biol Chem* **286**, 31361-31372

72. Yin, Y., Yang, S., Yu, L., and Yu, C. A. (2010) *J Biol Chem* **285**, 17038-17045

CHAPTER II

OXYGEN DEPENDENT ELECTRON TRANSFER IN THE CYTOCHROME bc_1 COMPLEX

Abstract

The cytochrome bc_1 complex (bc_1) is an essential energy transduction electron transfer complex in mitochondria and many aerobic and photosynthetic bacteria. In the Q-cycle mechanism, the complex catalyzes bifurcated oxidation of QH_2 with concomitant generation of a proton gradient and membrane potential for ATP synthesis. Although it has been well recognized that the bc_1 complex also generates a small amount of superoxide anion during the catalytic reaction, the involvement of molecular oxygen in the regulation of the bc_1 electron transfer reaction was never noticed until now. Oxygen increases the electron transfer activity of the bc_1 complex up to 50%, depending on the intactness of the complex; it has less effect on the complex having lower electron transfer activity and higher superoxide generating activity. Oxygen enhances the pre-steady reduction rate of cytochrome b_L and has no effect on the reduction of cytochrome b_H.

Introduction

On the basis of functional data and structural information of the cytochrome bc_1 complex, the ‘‘protonmotive Q cycle’’ (1-3) is the most favored mechanism for electron and proton transfer in the bc_1 complex. The key step of the Q-cycle mechanism is the bifurcation of electrons from QH_2 at the Q_P site. Two mechanisms, the “sequential” (4-6) and “concerted” (7-10), have been proposed for bifurcated QH_2 oxidation. In the “sequential oxidation” mechanism, the first electron of QH_2 is transferred to ISC**,** then to heme c_1, and the resulting ubisemiquinone is used to reduce heme b_L then b_H. In the “concerted oxidation” mechanism, the two electrons from QH_2 are transferred to ISC and heme b_L simultaneously. The absence of detectable ubisemiquinone radical at the Qp site (SQp) (11,12) questions the validity of the sequential oxidation mechanism. Even though several plausible explanations for the absence of Q-radical have been offered (4,6), such as antiferomagnetic coupling between SQp and ISC or SQp being fast oxidized by heme b_L. It should be noted that the detection of SQp under abnormal conditions has been reported (13,14), but it has not been confirmed by other investigators. The absence of SQp in a mutant bc_1 complex lacking heme b_L further indicates that SQp is not involved in the bifurcated QH_2 oxidation (12). There is no evidence, so far, showing that ISC receives an electron from QH_2 before the other redox components (10).

Taking advantage of the unique EPR signatures of ISC (15), hemes b_L, b_H, c_1 (16-18), and ubisemiquinone radical (19,20), coupled with the use of an ultra-fast microfluidic mixer and the freeze-quenching device, the study of pre-steady state kinetics demonstrated that the reduction of ISC and heme b_L in beef bc_1 by QH_2 was reported (10)

to be similar with a $t_{1/2}$ of 250 μs. These results are consistent with the concerted oxidation mechanism.

In addition to its main functions of electron transfer and proton translocation, the bc_1 complex also produces $O_2^{\cdot-}$ (21,22). The reaction mechanism of $O_2^{\cdot-}$ generation by bc_1 remains elusive. Production of $O_2^{\cdot-}$ during electron transfer through bc_1 is thought to be resulted from the leakage of electrons from their normal pathways to react with molecular oxygen. Under normal catalytic conditions, only a very small amount of electrons leak from bc_1 to form $O_2^{\cdot-}$ (23,24). This $O_2^{\cdot-}$ generating activity increases when electron transfer is blocked by antimycin**,** or when the electron transport chain becomes over reduced (24). Electron leakage (or $O_2^{\cdot-}$ production) has been speculated to occur at SQp (25,26) or reduced cyt b_L (21,27), depending on the mechanism by which bifurcation of ubiquinol proceeds in the Q-cycle model. Since there is no SQp and the mutant complex lacking heme b_L produces as much $O_2^{\cdot-}$ as the wild-type complex in the presence of antimycin (12), neither SQp or reduced heme b_L can be the electron source for $O_2^{\cdot-}$ formation. A new direct mechanism was proposed (28). That is in a hydrophobic environment and in the absence of b_L, O_2 acts as a low potential electron acceptor to participate in bifurcated oxidation of QH_2 with a high potential acceptor, ISP, to produce protonated superoxide ($O_2^{\cdot}H$) which diffuses to a hydrophilic environment (inter-membrane space or matrix) and becomes deprotonated to produce $O_2^{\cdot-}$. In the presence of heme b_L, O_2 may bind to a site between Heme b_L**,** and QH_2 to accept an electron (and H^+) from QH_2 to form O_2H, which then serves as electron donor for heme b_L. In other words, O_2 participates in bifurcated oxidation of QH_2 by mediating electron transfer from QH_2 to b_L. Alternatively**,** both b_L and O_2 can participate in bifurcated oxidation of QH_2 with ISC

separately**,** but the generated O_2H can then be oxidized by b_L effectively. In either scenario, the pre-steady state reduction rate of cytochrome b_L by ubiquinol would be affected by the presence of oxygen. Herein we report the effect of oxygen on the electron transfer activity from QH_2 to cytochrome *c***,** and that from QH_2 to cytochrome b_L in the cytochrome bc_1 complexes from bovine mitochondria and from photosynthetic bacteria *Rhodobacter sphaeroides* (*R. sphaeroides*). By using a heme b_L or b_H knockout *R. sphaeroides* bc_1 mutant complex, the site affected by oxygen in the electron transfer sequence was identified to be cytochrome b_L.

Experimental Procedures

Materials- Cytochrome *c* (horse heart, type III) was purchased from Sigma. The Ni-NTA resin used for purification of the His_6-tagged cytochrome bc_1 was purchased from Sigma. N-Dodecyl-β-D-maltoside (DM) and N-octyl- β-D-glucoside (OG) were purchased from Anatrace. 2-Methyl-6- (4-methoxyphenyl)-3, 7-dihydroimidazol [1, 2-α] pyrazin-3-one, hydrochloride (MCLA) was obtained from Molecular Probes, Inc. 2, 3-Dimethoxy-5-methyl-6-(10-bromodecyl)-1,4-benzoquinol($Q_0C_{10}BrH_2$) was prepared as previously reported (29). All other chemicals were of the highest purity commercially available.

Enzyme preparations and assays - Cytochrome bc_1 complex from beef heart mitochondria (30,31) and from *Rhodobacter sphaeroides* (32,33) were prepared and assayed according to the method previous reported in our lab.

Frozen *R. sphaeroides* cells were suspended in 20mM Tris-succinate, pH7.5 at 4°C, in the presence of 1mM sodium ethylenediamminetetraacetate (EDTA) (3mL of

buffer per gram of cells). After gradually adding a protease inhibitor phenylemethylsulfinyl fluoride (PMSF) dissolved in dimethylsuloxide (DMSO) to 1mM, a grain of DNase and RNase and stirring on ice for 20 minutes, the suspended cells were passed twice through French press with 1,000 psi to break the cells. The unbroken cells and cell debris were spun down and separated from the broken cells after centrifugation at 40,000 x g (18,000rpm with JA-20 rotor) for 30 minutes. After removing the precipitate, the supernatant was centrifuged at 220,000 x g (60,000 rpm with Ti70 rotor or 49,000 rpm with Ti50.2 rotor) for 90 minutes to separate the chromatophore fraction from the soluble protein fraction. The precipitate was homogenized in buffer 50mM TrisCl, pH8.0 at 4°C , containing 1mM $MgSO_4$ then subjected to centrifugation at 220,000xg (60,000 rpm with Ti70 rotor or 49,000 rpm with Ti50.2 rotor) for 90 minutes to recover the chromatophores. The resulting chromatophores were homogenized and suspended in buffer 50mM TrisCl, pH8.0 at 4°C, containing 1mM $MgSO_4$ and 20% glycerol. These chromatophores were ready to use or can be stored at -80°C until use.

To purify the His-tagged *R. sphaeroides* cytochrome bc_1 complex, the freshly prepared chromatophores or frozen chromatophores thawed on ice were adjusted to a cytochrome *b* concentration of 25 µM with buffer 50mM TrisCl, pH8.0 at 4°C, containing 1mM $MgSO_4$. 10% (w/v) Dodecylmaltoside (DM) was added to the chromatophore suspension to 0.56 mg/nmole of cytochrome *b* (0.14145 x volume of suspension) to solubilize the protein. 4M sodium chloride solution was added into the suspension to a final concentration of 0.1M. After stirring on ice for 1 hour, the mixture was centrifuged at 220,000xg (60,000 rpm with Ti70 rotor or 49,000 rpm with Ti50.2 rotor) for 90 minutes. The supernatant was collected and diluted with the same volume of

buffer 50mM TrisCl, pH8.0 at 4°C, containing 1mM $MgSO_4$ followed by passing through the Ni-NTA agarose column (100nmole of cytochrome *b*/ml of resin) equilibrated with buffer 50mM TrisCl, pH8.0 at 4°C, containing 1mM $MgSO_4$ more than two volume of resin. After all the diluted supernatant passed through the column, the column absorbed with bc_1 complex was sequentially washed with following buffer until no greenish effluent, 50mM TrisCl, pH8.0 at 4°C, containing 100mM NaCl and 0.01%DM; 50mM TrisCl, pH8.0 at 4°C, containing 100mM NaCl, 0.01%DM and 5mM Histidine; 50mM TrisCl, pH8.0 at 4°C, containing 100mM NaCl and 0.5%OG; 50mM TrisCl, pH8.0 at 4°C, containing 100mM NaCl, 0.5%OG and 5mM Histidine. The cytochrome bc_1 complex was eluted with buffer 50mM TrisCl, pH8.0 at 4°C, containing 100mM NaCl, 0.5%OG and 200mM Histidine and collected fractionally. The pure fractions were combined and concentrated by using Centriprep-30 concentrator. glycerol was added in the purified bc_1 complex to a final concentration of 20% then stored at -80°C in 100µL aliquots.

The content of cytochrome c_1 was determined from the sodium ascorbate reduced-minus-potassium ferric cyanide oxidized spectrum and the extinction coefficient of 17.5 $cm^{-1}mM^{-1}$ was used for wavelength pair 552 nm and 540 nm (22). To determine the cytochrome *b* content, the spectrum of sodium dithionite reduced-minus-potassium ferrocyanide and the extinction coefficient of 28.5 $cm^{-1}mM^{-1}$ for wavelength pair 560 and 576 nm were used (23).

To determine the activity under anaerobic condition, purified cytochrome bc_1 was diluted in buffer 50 mM TrisCl, pH8.0, containing 200 mM NaCl, and 0.01% DM to a final cytochrome *b* concentration of 1 µM (*R. sphaeroides* bc_1) or 0.1 µM (mitochondrial

bc_1). Assay mixture contains 100 µM cytochrome *c*, 100 mM phosphate buffer, pH7.5, and 1 mM EDTA. Appropriate amount of sample was added to the 1.35 mL of assay mixture in the main compartment of a Thunberg cuvette. 25 µM of $Q_0C_{10}BrH_2$ in 150 µL of aqueous solution containing 1 mM HCl was added in the sidearm of the Thunberg cuvette. To achieve anaerobic condition, both mixtures in the Thunberg cuvette were repeatedly deoxygenated and flashed with argon for three minutes. The mixtures were then mixed. The activity was measured by the reduction of cytochrome *c* in a Shimadzu UV 2101 PC spectrophotometer at room temperature following the increase of OD_{550}. A millimolar extinction coefficient of 18.5 was used to calculate the reduction of cytochrome *c*. The pH and ionic strength of the assay mixture were adjusted if necessary before measuring activity.

Fast Kinetics Study - To determine electron transfer rates between the quinol and heme *b* or heme c_1, the cytochrome bc_1 complex was mixed with ubiquinol ($Q_0C_{10}BrH_2$) in equal volumes at room temperature in an Applied Photophysics stopped-flow reaction analyzer SX.18MV (Leatherhead, United Kingdom) (12). The concentration of bc_1 complex was 10 µM (based on cytochrome *b*) in 100 mM phosphate buffer, pH8.0, containing 1 mM EDTA, 1 mM NaN_3 and 0.01% DM. For use in the stopped-flow, $Q_0C_{10}BrH_2$ in ethanol was diluted to 200 µM in 0.5 mM phosphate buffer, pH 6.0, containing 1 mM EDTA, 1mM NaN_3 and 0.01% DM. Reductions of cytochrome *b* and cytochrome c_1 in wild-type were monitored by the increase of absorption difference of $A_{561–580}$ and $A_{552–540}$, respectively, with a photodiode array scan between 600 and 500 nm. Reductions of cytochrome b_L in H111N and b_H in H198N were determined from the increase in $A_{565–580}$ and $A_{560–580}$. When an inhibitor was used, the cytochrome bc_1 complex

was treated with 3-fold molar excess of inhibitor over heme *b*, for 15 min at 4 °C, prior to the experiment. Because the concentration of $Q_0C_{10}BrH_2$ used was 20 times higher than that of the cytochrome bc_1 complex, the reactions between bc_1 and quinol were treated as pseudo first-order reactions. Time traces of the reaction were fitted with a first order rate equation to obtain the pseudo first rate constants k_1 by Kaleidagraph. To determine electron transfer rates under anaerobic condition, the enzyme and substrate solution were deoxygenated before introducing to the stopped-flow reaction analyzer.

Determination of superoxide generation - Superoxide generated from the oxidation of ubiquinol by cytochrome bc_1 complex was determined by measuring the chemiluminescence of the MCLA-$O^{\cdot -}$ adduct. Equal volumes of solutions A and B (34) were mixed in an Applied Photophysics stopped-flow reaction analyzer SX.18MV (Leatherhead, England), by leaving the excitation light off and registering light emission (35,36). Reactions were carried at 23°C. Solution A contains 50 mM phosphate–buffer, pH 7.4, 1 mM KCN, 1 mM NaN_3, 1 mM EDTA, 0.1% bovine serum albumin, 0.01% DM and 5.0 μM of cytochrome bc_1 complex (based on cytochrome c_1). Solution B contains 50 μM $Q_0C_{10}BrH_2$ and 4 μM MCLA in the same buffer. Concentrated stock solution of $Q_0C_{10}BrH_2$ was made in 95% ethanol containing 1 mM HCl. The final concentration of ethanol in solution B is less than 1%. Once the reaction started, the produced chemiluminescence, in voltage, was consecutively monitored for 5 seconds.

Results and Discussion

Effect of oxygen on the electron transfer activity of the cytochrome bc_1 complex - It has been demonstrated that the electron transfer from ubiquinol to cytochrome *c* catalyzed by the cytochrome bc_1 complex is accompanied with the generation of a minute amount of superoxide. Therefore, some investigators in the field were inclined to believe that cytochrome bc_1 complex has a higher activity under the anaerobic condition than that in the aerobic condition, since no electron leaking would occur in the absence of oxygen. (24,36). Also, the deoxygenated process, which often involves repeated evacuating and flushing with argon, would cause an increase of the concentration and thus enhance the apparent activity. Recently, we have re-examined the effect of oxygen on the electron transfer activity of the cytochrome bc_1 complex from various sources under carefully controlled conditions. All the possible variations in the reactions, including the temperature, enzyme concentration and the degree of the reduction of the substrate, are eliminated. Table 3 (Page 40) summarizes the activities of various bc_1 complex preparations in the presence and absence of oxygen. To our surprise, all of the purified cytochrome bc_1 complexes show higher activity in the presence of oxygen than in the absence of oxygen. The activity of the mitochondrial bc_1 complex decrease about 16% upon removal of oxygen. The bacterial bc_1 complex is more sensitive to the presence of oxygen. In general, a bacterial bc_1 complex preparation with higher activity is more sensitive to the oxygen than that with lower activity. Because the purified bacterial complex is somewhat deficient in subunit IV as the interaction between subunit IV and other core subunit is very sensitive to detergent used during purification, its activity is enhanced substantially upon the addition of recombinant subunit IV.

Table 3. **Summary of electron transfer activities of various cytochrome bc_1 complexes in the presence and absence of oxygen.**

Preparations*	Specific Activity, µmol *c* reduced/ min/nmol *b*			
	Aerobic condition		Anaerobic condition	
	Activity	%	Activity	% remaining
Mit bc_1	21.6	100	18	83
Rsbc_1	2.4	100	2.0	83
Rsbc_1 + IV	4.2	100	2.3	55
#2	3.2	100	1.7	53
#2 + IV	4.8	100	2.9	60
IV fused bc_1	3.7	100	1.5	40
IV fused bc_1+ IV	4.0	100	2.4	60
RsΔIV	0.7	100	0.5	71
Mit SCR (QH2 to Cyt*c*)	17	100	15	88
Mit SCR (Succ to Cyt*c*)	0.67	100	0.8	119

*Mitbc_1, Mitochondrial bc_1; *Rsbc*$_1$, wild-type, 4 subunit complex; #2, *Rsbc*$_1$ mutant S287R(Cyt*b*)/V135S(ISP); *Rs*ΔIV, *Rsbc*$_1$ lacking subunit IV; Subunit IV fused bc_1, *Rsbc*$_1$ with subunit IV fused to Cytc_1 C-terminal through 14 glycine residues; Mit SCR, Mitochondrial Succinate-Cytochrome *c* oxidoreductase. Each data point represents an average of eight experiment results.

In order to avoid artifacts introduced during the sample manipulation in the assay procedure under aerobic and anaerobic conditions, we prepared the assay mixtures and enzyme solution used in both assays under the same conditions. When the bc_1 complex diluted under aerobic condition is introduced to the de-oxygenated assay mixture, one sees that the activity quickly decreased to the same level as that the deoxygenated bc_1 complex is assayed under anaerobic conditions. On the other hand**,** when the deoxygenated bc_1 complex is assayed under aerobic conditions, the activity is almost the same as the bc_1 complex without being subjected to deoxygenated process. This result suggests that oxygen is quickly re-associated to the bc_1 complex. The oxygen effect on the activity observed is real and not due to the artifacts introduced during sample manipulation.

Oxygen concentration dependent electron transfer activity. Figure 10 (Page 42) shows the titration of the electron transfer activity of bacterial cytochrome bc_1 complexes against oxygen concentration in the assay mixture. The electron transfer activity of bc_1 complex increased as the concentration of oxygen in the assay mixture increased. The oxygen concentration of air saturated phosphate buffered assay mixture was assumed to be 250 μM, and that in de-oxygenated assay mixture was assumed to be 0 μM. The concentrations of oxygen in between 250 μM and 0 μM were obtained by mixing varied portions of air-saturated and deoxygenated buffers in a special designed non-air-space mixing cuvette. The activity is proportional to the presented concentration of oxygen, showing a hyperbolic titration curve. The concentration of oxygen for 50% activation was found at 90 μM.

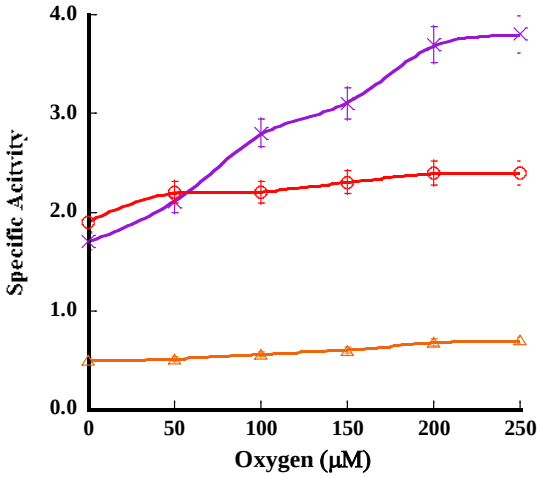

Figure 10. **Oxygen concentration dependent electron transfer activity of *R.sphaeroides* bc_1 complexes.** Wild type (-o-o-, red), Subunit IV-fused complex (-x-x-, purple) and Subunit IV-lacking complex (*Rs*ΔIV) (-Δ-Δ-, orange). Reactions and measurements were performed as described in "Experimental Procedures" except purified *R. sphaeroides* bc_1 with a finial cytochrome *b* concentration of 1μM was deoxygenated and appropriate amounts of sample were added to the 1mL of proportionally mixed air-saturated and deoxygenated assay mixture. Each data point represents an average of six experiment results.

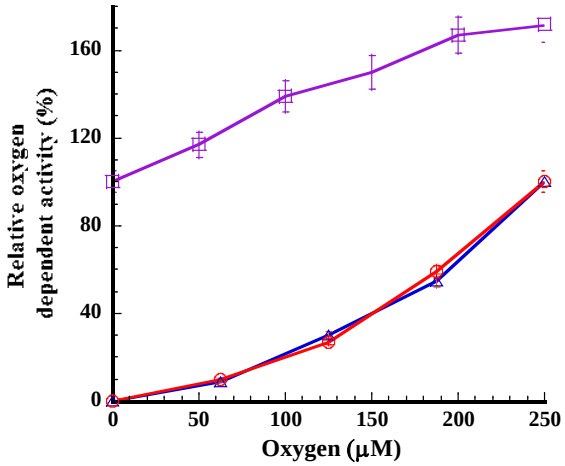

Figure 11. **Relative oxygen dependent activities of the bc_1 complex and its superoxide generation**. The purple (-□-□-) curve represents the increase of cytochrome bc_1 activity and the red (-o-o-) curve is the superoxide generating activity from the oxidation of ubiquinol by wild type *R.sphaeroides* bc_1 and the blue (-Δ-Δ-) curve is the superoxide generating activity by cytochrome *c* in the presence of hydrophobic (detergent) environment under various oxygen concentrations. Reactions and measurements were performed as described in "Experimental Procedures" except for air-saturated and deoxygenated solutions were proportionally mixed before starting reactions. Each data point represents an average of four experiment results.

When the superoxide generations by the bc_1 complex under various oxygen concentrations were examined, a more complicated curve (parabolic) was obtained (see Figure 11, Page 43). A similar behavior was observed when superoxide is generated from the oxidation of ubiquinol by cytochrome *c* in the presence of a hydrophobic (detergent) environment. Little superoxide is generated at low oxygen concentration. When the oxygen concentration is higher (>160μM), then the generation of superoxide is proportional to the concentration of oxygen.

Effect of oxygen on the activity of the succinate-cytochrome c oxidoreductase - As also shown in Table 3 (Page 40), the reaction electron transfer from succinate to cytochrome *c* catalyzed by succinate-cytochrome *c* oxdoreductase is not very sensitive to oxygen. It shows a slightly increased activity under anaerobic conditions (24,36). On the other hand, if ubiquinol is used as substrate, the electron transfer activity from ubiquinol to cytochrome *c* in the succinate-cytochrome *c* oxidoreductase behaves like the purified cytochrome bc_1 complex - the activity is enhanced in the presence of oxygen**,** but only to a lesser extent. Apparently the electron transfer pathway from succinate to cytochrome bc_1 complex via ubiquinol bound to succinate-Q oxidoreductase is different from the pathway from free ubiquinol to cytochrome bc_1 complex.

Effect of the ionic strength and pH on the electron transfer activity of cytochrome bc_1 complex under aerobic and anaerobic conditions - Since a substantial difference in the electron transfer activity of cytochrome bc_1 complex in the presence and absence of oxygen is observed in all bc_1 complexes tested, it is of interest to see whether or not both parts of activities (O_2 sensitive and insensitive) come from the same origin. Figure 12 (Page 45) shows the effect of ionic strength on the activity of cytochrome bc_1 in the

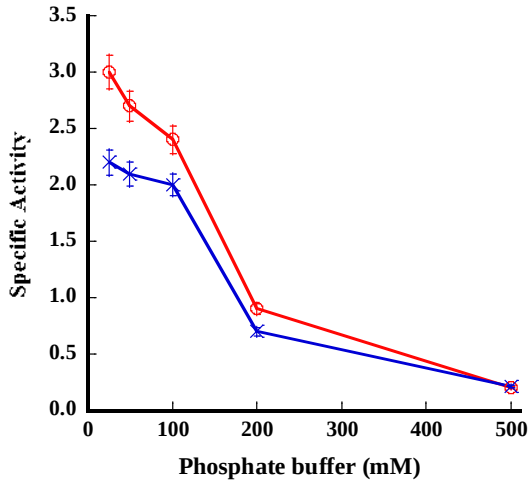

Figure 12. **Effect of ionic strength on the electron transfer activity of wild type *R.sphaeroides* bc_1 complexes under aerobic (-o-o-, red) and anaerobic (-x-x-, blue) conditions.** The ionic strength of the assay mixture was adjusted as indicated. Reactions and measurements were performed as described in "Experimental Procedures." Each data point represents an average of six experiment results.

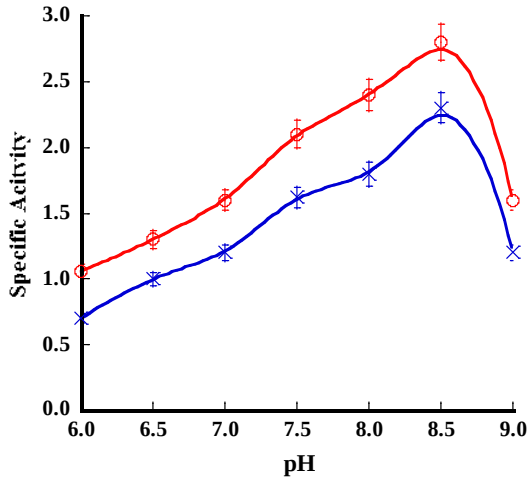

Figure 13. **Effect of pH on the electron transfer activity of wild type *R.sphaeroides* bc_1 complexes under aerobic (-o-o-, red) and anaerobic (-x-x-, blue) conditions**. Experimental conditions were the same as described in Figure 2 expect various pHs were used. Each data point represents an average of six experiment results.

presence and absence of oxygen. Figure 13 (Page 46) shows the pH dependence of electron transfer activity of cytochrome bc_1 in the presence and absence of oxygen. There is no apparent difference in the effect of pH and ionic strength on the activity in presence and absence of oxygen was observed, indicating both activities derived from the same reaction. In other words, both activities share a same rate limiting step in their reaction sequences.

Activation energies of O_2 dependent electron transfer activity of cytochrome bc_1 complex - An effective way to distinguish the difference in the origin of the reactions is to determine their activation energies. Although two different reactions might have the same activation energy, two reactions with different activation energies are definitely not from the same origin. Figure 14 (Page 48) shows the Arrhenius plots for electron transfer reactions carried out by cytochrome bc_1 complex in the presence and absence of oxygen. No significantly different activation energies were obtained from these two conditions, indicating that both reactions involve the same rate limiting step.

Effect of oxygen on the pre-steady reduction of cytochrome b_L by ubiquinol - Since there are multiple steps involved in the electron transfer from ubiquinol to cytochrome *c*, it is of interest to know which step is regulated by oxygen. When the pre-steady reduction rates of cytochromes b_L and b_H by ubiquinol were measured in the presence and absence of oxygen using the stopped-flow apparatus, a significant difference in rates between the two conditions as observed (see Figure 15, page 49). Under anaerobic conditions, the reduction rate of cytochrome b_L, absorption peak at 565 nm, is much smaller than that obtained under aerobic condition in the wild type and Subunit IV-fused cytochrome bc_1 complexes, indicating that the reduction of cytochrome

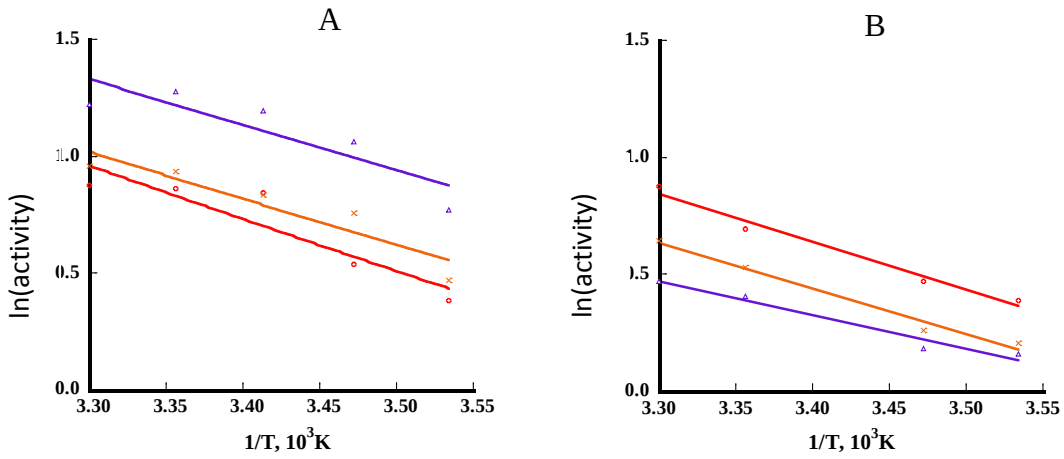

Figure 14. **Arrhenius plots for the electron transfer activities of *R.sphaeroides* bc_1 complexes**. The ubiquinol-cytochrome *c* oxidoreductase activities in wild type (-o-o-, red), mutant S287R(Cyt*b*)/V135S(ISP) (-x-x-, orange) and Subunit IV-fused mutant complex (-Δ-Δ-, purple) were assayed under aerobic (A) and anaerobic (B) conditions as described in "Experimental Procedures." The natural logarithms of activities were ploted against the reciprocal of absolute temperature in Arrhenius plots. The slopes of the least squares fitting straight lines fitted by *Kaleidagraph* were used to estimate their activation energies. Each data point represents an average of eight experiment results.

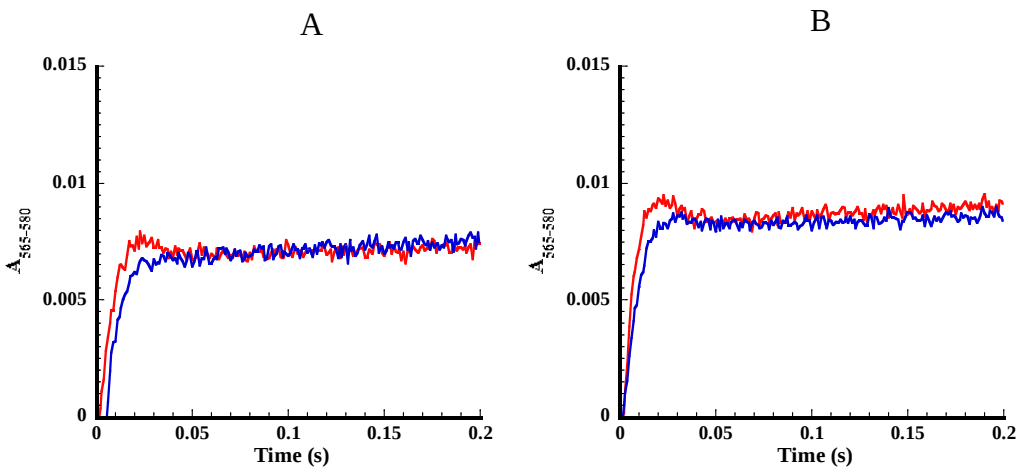

Figure 15. **Time trace of cytochrome *b* reduction by $Q_0C_{10}BrH_2$ in *R.sphaeroides* bc_1 complexes.** The wild type (A) and Subunit IV-fused mutant complex (B) under aerobic (red) and anaerobic (blue) conditions. Reactions and measurements were performed as described under "Experimental Procedures" and monitored by photodiode array. Reductions of cytochrome *b* were determined from the increase at $A_{565-580}$. Each curve represents an average of eight experiment results.

b_L is affected by oxygen. It should be noted that due to spectral overlapping there is some b_H contribution at 565 nm absorption as a result of rapid electron flow from b_L to b_H.

According to the Q-cycle mechanism, cytochrome b_H can be reduced by ubiquinol via two different routes: one from the forward reduction via cytochrome b_L through bifurcated oxidation of ubiquinol with the iron-sulfur cluster at the Qp site, and the other route is the reversed reduction via bound ubisemiquinone at the Q_N site. If the reversed reduction is involved, no participation of molecular oxygen is needed, it would be, therefore, not sensitive to oxygen. When bc_1 complex is treated with Qp site inhibitor, such as stigmatellin, no bifurcated oxidation of ubiquinol takes place, and no electron is transferred from ubiquinol to heme b_H via b_L, all the b_H reduction must be achieved through bound ubisemiquinone at the Q_N site. Under this condition**,** the reduction of b_H will not be sensitive to oxygen. As you can see in Figure 16A (Page 51). The reduction rate of b_H in the bc_1 treated with Stigmatellin is the same regardless oxygen is presence or not.

When the bc_1 complex is reduced by ubiquinol in the presence of antimycin**,** the electron transfer from b_H to ubiquinone or ubisemiquinone is blocked so as reversed reduction, all the electron accumulated at b_H come from b_L as the result of the bifurcated oxidation of ubiquinol, the extent of *b* reduction is larger but rate is slower (12).The degrees of the effect of oxygen on the cytochrome *b* reduction in the antimycin inhibited bc_1 complex by ubiquinol are the same as that in the uninhibited complex (see Figure 16B, Page 51). Since the rate of electron transfer from b_L to b_H is very fast, the effect of oxygen must be at the reduction of b_L.

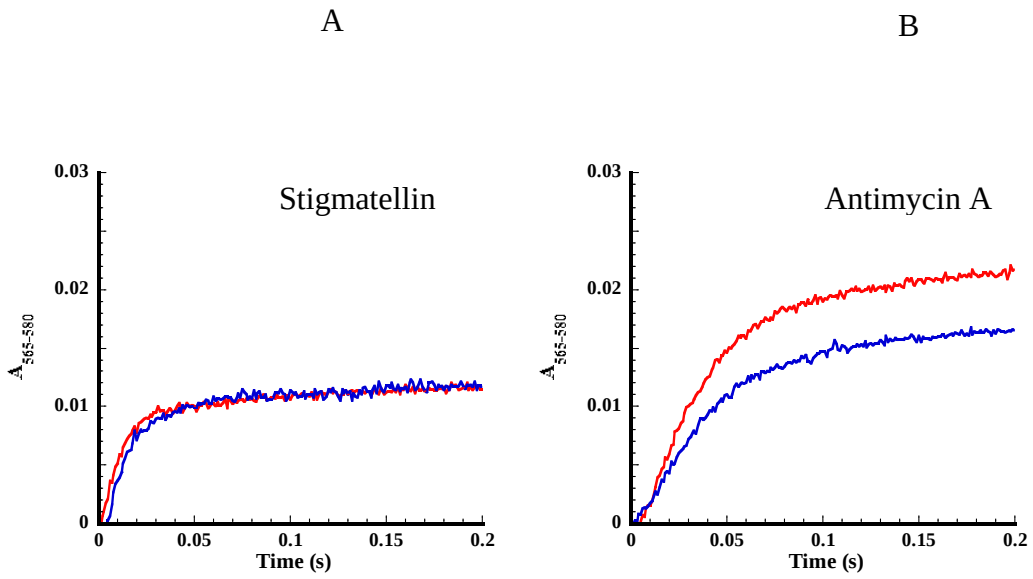

Figure 16. **Time trace of cytochrome *b* reduction by $Q_0C_{10}BrH_2$ in wild type *R.sphaeroides* bc_1 complex in the presence of inhibitor Stigmatellin (A) and Antimycin A (B) under aerobic (red) and anaerobic (blue) conditions**. Reactions and measurements were performed as described under "Experimental Procedures" and monitored by photodiode array. Reductions of cytochrome *b* were determined from the increase at $A_{565\text{-}580}$. Each curve represents an average of eight experiment results.

Effect of oxygen on the pre-steady reduction of cytochrome b_L in H111N and b_H in H198N mutant complexes by ubiquinol - It has been reported that heme b_H is knocked out when the ligand, histidine -111, is replaced with asparagine (12). The b_H knock - out mutant bc_1 complex, which contains hemes b_L, and c_1, and ISC, can be purified from the mutant cells grown semiaerobically but has little electron transfer activity. The spectral property and reduction kinetics of heme b_L in this mutant complex are, however, very similar to those of the wild-type enzyme (12). This mutant complex provides a good opportunity to test the effect of oxygen on heme b_L reduction by ubiquinol as the heme b_L and ISC will be the only components participate in bifurcated oxidation of ubiquinol. Figure 17 (Page 53) shows the time tracings of the heme b_L reduction by ubiquinol in the presence and absence of oxygen. As expected, the heme b_L is reduced at a much higher rate when oxygen is present. Since there is no heme b_H available in the mutant complex, the effect observed must be on heme b_L only. When cytochrome b_H in the heme b_L knock-out mutant (H198N) complex is reduced by ubiquinol, as expected, the reduction kinetics was not affected by oxygen (data not shown), the reduction is proceeding through the Q_N site.

Effect of superoxide dismutase on the pre-steady reduction of cytochrome b_L in the b_H knock-out complex (H111N) in the presence of oxygen - Since it has been reported that mutant complex of H111N generates more superoxide than that of the wild-type complex, it is of interest to see whether or not the heme b_L reduction rate enhancement in the presence of oxygen is due to more superoxide production. If it is due to the superoxide, then the reduction rate of cytochrome b_L would become slower when superoxide dismutase is present. The reduction rate of cytochrome b_L by ubiquinol was

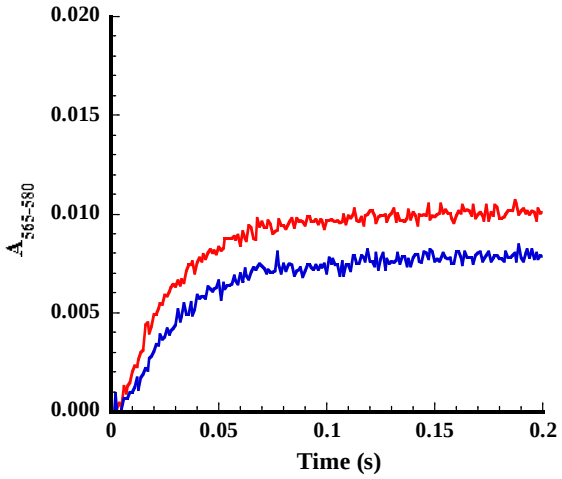

Figure 17. **Time trace of cytochrome *b* reduction by $Q_0C_{10}BrH_2$ in *R.sphaeroides* bc_1 mutant H111N under aerobic (red) and anaerobic (blue) conditions.** Reactions and measurements were performed as described under "Experimental Procedures" and monitored by photodiode array except for the concentration of bc_1 complex was 10μM based on cytochrome c_1. Reductions of cytochrome b_L were determined from the increase at $A_{565\text{-}580}$. Each curve represents an average of eight experiment results.

not affected by superoxide dismutase (data not shown) suggesting that a free superoxide anion is not involved in the reduction of cytochrome b_L. This, however, does not exclude the participation of O_2H in bc_1 complex in the hydrophobic environment, where it is generated (30). O_2H in the hydrophobic environment is not expected to be easily dismutated by superoxide dismutase.

Effect of oxygen on the pre-steady reduction of cytochrome c_1 by ubiquinol - When the pre-steady reduction rate of cytochrome c_1 by ubiquinol was measured in the stopped-flow apparatus under aerobic and anaerobic conditions, a significant difference in rates between these two conditions was observed. The rate of cytochrome c_1 reduction is faster in the presence of oxygen than in the absence of oxygen (see Figure 18, Page 55). The reduction rates were directly correlated with the electron transfer activities.

Oxygen plays a regulatory role on the bifurcated oxidation of ubiquinol and the redox signaling - Aerobic organisms rely on oxygen for the generation of energy, that is required for cells growth and maintain cellular functions. Energy is produced by a coupling reaction between electron transport chain and ATP synthase complex. When oxygen is limited, the activity of cytochrome *c* oxidase will be decreased and the supply of reduced cytochrome *c* is diminished. Consequently**,** less activity of complex III is needed to consume reduced ubiquinol, succinate and other NADH-linked substrates. When the concentration of O_2 decreases (hypoxia), cells respond by activating hypoxia inducible factor (HIF) (37,38) dependent gene transcription to overcome the hypoxia condition. Under the hypoxia condition, the concentration of cytosolic reactive oxygen species (ROS) increased. ROS stabilizes HIF by inhibiting a hydroxylation on an asparagine residue in one of the subunit of HIF. The ROS has been shown to originate

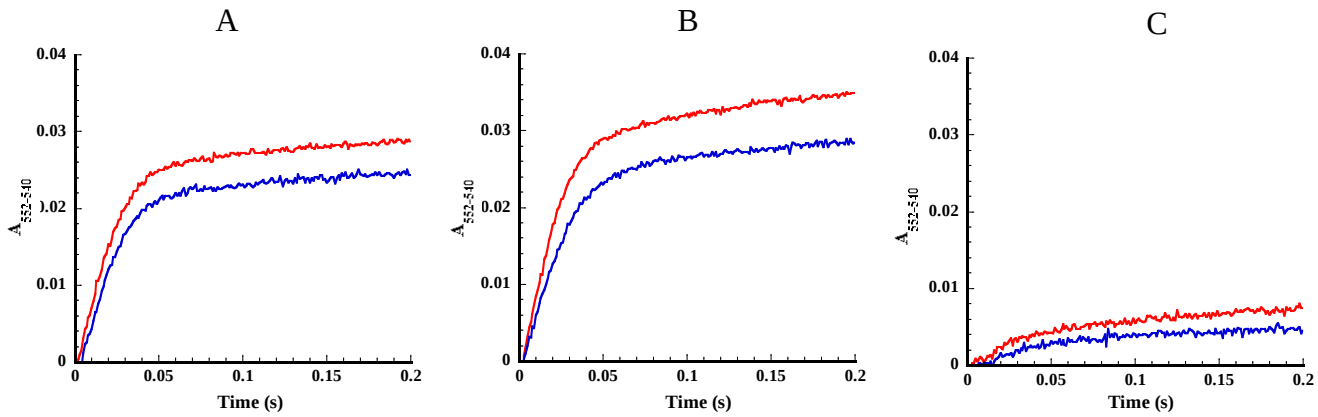

Figure 18. **Time trace of cytochrome *c* reduction by $Q_0C_{10}BrH_2$ in *R.sphaeroides* bc_1 complexes.** Wild type (A), Subunit IV-fused complex (B) and H111N mutant complex (C) under aerobic (red) and anaerobic (blue) conditions. Experimental conditions were the same as those in Figures 5 and 7. Reductions of cytochrome $c_1$were determined from the increase at $A_{552\text{-}540}$. Each curve represents an average of eight experiment results.

from the mitochondrial electron transfer chain (39) and lately the site of its generation has been established to be at the Qo site (40) in the complex III (41,42). Although the site for the ROS generation is well established, it is difficult to understand how more ROS is found in the cytosol under hypoxia. One plausible explanation is the hypoxia condition causes a modification of mitochondrial inner membrane or some components of complex III that results in preference of releasing superoxide into the inter membrane space and then to the cytosol from its generation site (Qo site). As described in the previous sections, electron transfer activity of cytochrome bc_1 (complex III) is greatly affected by the concentration of oxygen**.** When oxygen is abundant in the mitochondria, oxidation of succinate and NADH proceeds smoothly through the electron transfer chain to reduce oxygen to H_2O. The $\Delta\mu H^+$ generated is used to drive ATP synthesis, therefore the inner membrane potential is not high. When oxygen becomes limited**,** the electron transfer chain will become more reduced, more positive charge on the inter membrane space side of the inner membrane will result and the matrix side of the inner membrane will become more negatively charged**.** According to the proposed mechanism (28), protonated superoxide (O_2H) is generated at Qo site, upon bifurcated oxidation of ubiquinol. O_2H is diffusible in the hydrophobic region of membrane; it undergoes deprotonation at either side of the inner membrane. The probability for O_2H to be released into the inter-membrane space or matrix depends on the conditions on both sides of the inner membrane. Apparently, under the hypoxia condition, more O_2H is release to inter-membrane space and becomes H_2O_2 upon the action of Cu/Zn-superoxide dismutase (Cu-Zn-SOD) (43). The activity of the cytosolic Cu-Zn-SOD is pH independent and matrix Mn-SOD is pH sensitive (44). The difference in pH dependency between the Cu-Zn-SOD

(cytosolic) and Mn-SOD (matrix) may promote the release of O_2H to intermembrane space under hypoxia condition. More exploration is needed before we can explain why more O_2H is diffused to the intermembrane side to exert its regulatory function.

References

1. Mitchell, P. (1976) *J Theor Biol* **62**, 327-367
2. Crofts, A. R., Shinkarev, V. P., Kolling, D. R., and Hong, S. (2003) *J Biol Chem* **278**, 36191-36201
3. Brandt, U., and Trumpower, B. (1994) *Crit Rev Biochem Mol Biol* **29**, 165-197
4. Link, T. A. (1997) *FEBS Lett* **412**, 257-264
5. Hong, S., Ugulava, N., Guergova-Kuras, M., and Crofts, A. R. (1999) *J Biol Chem* **274**, 33931-33944
6. Crofts, A. R. (2004) *Annu Rev Physiol* **66**, 689-733
7. Snyder, C. H., Gutierrez-Cirlos, E. B., and Trumpower, B. L. (2000) *J Biol Chem* **275**, 13535-13541
8. Trumpower, B. L. (2002) *Biochim Biophys Acta* **1555**, 166-173
9. Hunte, C., Palsdottir, H., and Trumpower, B. L. (2003) *FEBS Lett* **545**, 39-46
10. Zhu, J., Egawa, T., Yeh, S. R., Yu, L., and Yu, C. A. (2007) *Proc Natl Acad Sci U S A* **104**, 4864-4869
11. Junemann, S., Heathcote, P., and Rich, P. R. (1998) *J Biol Chem* **273**, 21603-21607
12. Yang, S., Ma, H. W., Yu, L., and Yu, C. A. (2008) *J Biol Chem* **283**, 28767-28776
13. Zhang, H., Osyczka, A., Dutton, P. L., and Moser, C. C. (2007) *Biochim Biophys Acta* **1767**, 883-887
14. Cape, J. L., Bowman, M. K., and Kramer, D. M. (2007) *Proc Natl Acad Sci U S A* **104**, 7887-7892

15. Orme-Johnson, N. R., Hansen, R. E., and Beinert, H. (1971) *Biochem Biophys Res Commun* **45**, 871-878

16. de Vries, S., Albracht, S. P., and Leeuwerik, F. J. (1979) *Biochim Biophys Acta* **546**, 316-333

17. Salerno, J. C. (1984) *J Biol Chem* **259**, 2331-2336

18. McCurley, J. P., Miki, T., Yu, L., and Yu, C. A. (1990) *Biochim Biophys Acta* **1020**, 176-186

19. Yu, C. A., Nagoaka, S., Yu, L., and King, T. E. (1980) *Arch Biochem Biophys* **204**, 59-70

20. Ohnishi, T., and Trumpower, B. L. (1980) *J Biol Chem* **255**, 3278-3284

21. Chance, B., Sies, H., and Boveris, A. (1979) *Physiol Rev* **59**, 527-605

22. Turrens, J. F., Alexandre, A., and Lehninger, A. L. (1985) *Archives of Biochemistry and Biophysics* **237**, 408-414

23. Sun, J., and Trumpower, B. L. (2003) *Arch Biochem Biophys* **419**, 198-206

24. Zhang, L., Yu, L., and Yu, C. A. (1998) *J Biol Chem* **273**, 33972-33976

25. Muller, F. L., Roberts, A. G., Bowman, M. K., and Kramer, D. M. (2003) *Biochemistry* **42**, 6493-6499

26. Drose, S., and Brandt, U. (2008) *J Biol Chem* **283**, 21649-21654

27. Nohl, H., and Jordan, W. (1986) *Biochem Biophys Res Commun* **138**, 533-539

28. Yin, Y., Yang, S., Yu, L., and Yu, C. A. (2010) *J Biol Chem* **285**, 17038-17045

29. Yu, C. A., and Yu, L. (1982) *Biochemistry* **21**, 4096-4101

30. Yu, C. A., and Yu, L. (1980) *Biochim Biophys Acta* **591**, 409-420

31. Yu, L., Yang, S., Yin, Y., Cen, X., Zhou, F., Xia, D., and Yu, C. A. (2009) *Methods Enzymol* **456**, 459-473

32. Tian, H., Yu, L., Mather, M. W., and Yu, C. A. (1998) *J Biol Chem* **273**, 27953-27959

33. Tso, S. C., Yin, Y., Yu, C. A., and Yu, L. (2006) *Biochim Biophys Acta* **1757**, 1561-1567

34. Nakano, M. (1990) *Method Enzymol* **186**, 585-591

35. Denicola, A., Souza, J. M., Gatti, R. M., Augusto, O., and Radi, R. (1995) *Free Radic Biol Med* **19**, 11-19

36. Gong, X., Yu, L., Xia, D., and Yu, C. A. (2005) *J Biol Chem* **280**, 9251-9257

37. Maxwell, P. H., Pugh, C. W., and Ratcliffe, P. J. (1993) *P Natl Acad Sci USA* **90**, 2423-2427

38. Wang, G. L., and Semenza, G. L. (1993) *Proc Natl Acad Sci U S A* **90**, 4304-4308

39. Bunn, H. F., and Poyton, R. O. (1996) *Physiol Rev* **76**, 839-885

40. Bell, E. L., Klimova, T. A., Eisenbart, J., Moraes, C. T., Murphy, M. P., Budinger, G. R., and Chandel, N. S. (2007) *J Cell Biol* **177**, 1029-1036

41. Guzy, R. D., and Schumacker, P. T. (2006) *Exp Physiol* **91**, 807-819

42. Klimova, T., and Chandel, N. S. (2008) *Cell Death Differ* **15**, 660-666

43. Ellerby, L. M., Cabelli, D. E., Graden, J. A., and Valentine, J. S. (1996) *Journal of the American Chemical Society* **118**, 6556-6561

44. Yamakura, F., Kobayashi, K., Ue, H., and Konno, M. (1995) *European Journal of Biochemistry* **227**, 700-706

CHAPTER III

PRUIFICATION AND CHARACTERIZATION OF *RHODOBACTER SPHAEROIDES* CYTOCHROME c_1 HEAD DOMAIN

Abstract

Cytochrome c_1, the electron exit point in the cytochrome bc_1 complex, transfers electrons from a hydrophobic environment to its electron acceptor, cytochrome c_2, in a hydrophilic environment in the photosynthetic electron transfer chain. As a functional domain providing the docking site for cytochrome c_2, the head domain of cytochrome c_1 from *Rhodobacter sphaeroides* bc_1 complex was isolated by using site-directed mutagenesis. The purified water-soluble cytochrome c_1 head domain has identical properties to those of the membrane-bound cytochrome c_1, providing a valuable resource to study the structure and function of the cytochrome c_1.

Introduction

As the last station of electron transfer in the cytochrome bc_1 complex, the cytochrome c_1 connects the bc_1 complex and cytochrome *c* by passing electron from ISP to cytochrome *c* in mitochondria or c_2 in bacteria. Cytochrome c_1 is composed of 263 amino acids with an apparent molecular weight of 31KDa on SDS-PAGE (1). It is encoded by the *fbc*C gene of the *fbc*FBC operon encoding iron-sulfur protein, cytochromes *b* and c_1, respectively (2). After being synthesized as a precursor with 285 amino acids, a 22 residue amino-terminal signal sequence is removed and the mature polypeptide is translocated to the periplasm (3). Cytochrome c_1 has a water soluble head domain and a trans-membrane helix. The head domain of cytochrome c_1 houses a *c* type heme and contains the conserved CXXCH heme-binding consensus sequence (4).

Although the X-ray crystal structure of cytochrome c_1 in the bc_1 complex has been obtained from different species and its function has been clarified by biochemical, biophysical and molecular genetic studies, some detailed information still remains inconclusive, such as the mechanism of the interaction between cytochrome c_1 and other subunits. One approach to study a protein complex is to work on individual subunits and their functional domains. Full length cytochrome c_1 from bovine (5-7), yeast (8) and *Rhodobacter sphaeroides* (9) has been isolated in the presence of detergent and the properties of purified c_1 have been studied.

Herein, we report the method for generation of *Rhodobacter sphaeroides* mutant expressing the His-tagged water soluble *R. sphaeroides* cytochrome c_1 (c_1 head domain). A procedure for purification of the fully functional head domain of cytochrome c_1 was developed. The spectroscopic and thermodynamic properties of the purified water

soluble head domain of the cytochrome c_1 were examined and compared with the native membrane-bound cytochrome c_1.

Experimental Procedures

Materials – Horse heart cytochrome *c* (type III) was purchased from Sigma and re-purified through Superdex 200 FPLC column purchased from Pharmacia. The Ni-NTA resin used for purification of the His_6-tagged cytochrome c_1 head domain was purchased from Sigma. DEAE-Cellulose resin was purchased from Sigma. N-Dodecyl-β-D-maltoside (DM) and N-octyl- β-D-glucoside (OG) were purchased from Anatrace. pGEM7ZF(+) vector was purchased from Promega. The *PfuTurbo* DNA polymerase, *Dpn* I and XL 1-Blue *E.coli* strain used in the QuickChange mutagenesis system was purchased from Stratagene. Restriction endonucleases and other DNA-modifying enzymes were purchased from Promega, Life Technologies, Inc., Stratagene, and New England Biolab. All other chemicals were of the highest purity commercially available. DNA sequencing was carried out at the Recombinant DNA/Protein Core Facility at Oklahoma State University.

Generation of R. sphaeroides strains expressing the truncated His_6-tagged cytochrome c_1 mutant (c_1 head domain) - The double stranded pGEM7ZF(+)-C_{6H}Q was used as the template to amplify the fragment containing subunit IV sequence flanked by one fragment of cytochrome c_1 N- terminus at one side and one fragment of cytochrome c_1 N- terminus with a His-tag attached to it at other side. The oligonucleotides used in polymerase chain reaction are below:

Oligonucleotides1:

5’ - GATCACAGAATTCCTGCTTGCGGGCCATCAG – 3’

Oligonucleotides 2:

5’ – GATCGCAGAATTCCATCACCACCACCATC – 3’

Underlined sequences in primers are *E.co*RI restriction site.

PCR product was digested with *Eco*RI to generate two sticky ends. After purification with a Sigma gel extraction kit the amplified sequence was ligated, T4 DNA ligase, through two *Eco*RI sticky ends. The ligation product was digested with DpnI, which can get rid of the methylated nonmutated parental DNA template pGEM7ZF(+)-$C_{6H}Q$. A nick was introduced into the mutated plasmid pGEM7ZF(+)-/$C_{\Delta(229\text{-}263)\ 6H}$ Q which contains the truncated cytochrome c_1 gene but keeps six-Histidine tag and subunit IV sequence. Circular nicked dsDNA was transformed into XL-1 Blue competent cells. After transformation, the XL-1 Blue competent cells repair the nicks in the mutated plasmid.

After DNA sequencing to confirm the deletion of the C-terminus of cytochrome $c_{1,}$ plasmid bearing the successful deletion was digested with XbaI and HindIII to generate the fragment $C_{\Delta(229\text{-}263)\ 6H}Q$ to be ligated to pRKC418-*fbc*FB vector digested with XbaI and HindIII from plasmid pRKC418-*fbc*$FBC_{6H}Q$ (10). The successfully ligated plasmid pRKC418-*fbc*$FBC_{\Delta(229\text{-}263)\ 6H}Q$ was chemically transformed into *E.coli* S17cells. The mutant plasmid was mobilized into *R. sphaeroides* BC17 from S17 cells through a plate mating procedure (10,11). The ex-conjugatant *R. sphaeroides* is resistant to and Tetracycline and Trimethoprim which conferred by the pRK plasmid and resistant to Kanamycin which conferred by the host strain *BC*17.

Growth of Bacteria - *E.coli* cells were grown at 37℃ in LB medium. *R. sphaeroides* BC17 cells bearing pRKD418-f*bc*F*BC*$_{6H}$Q plasmid and *R. sphaeroides* strains (wild type and mutants) were grown photosynthetically or semi-aerobically at 30℃ in an enriched Sistrom medium containing 5mM glutamate and 0.2% casamino acids (12). Cells were transferred to a larger batch when OD_{600} reached 1.6 and harvested at OD_{600} 2.0.

Antibiotics were added to the following concentrations: 125μg/mL ampicillin, 20μg/mL Kanamycin sulfate, 25μg/mL Trimethoprim, 10μg/mL Tetracycline for *E.coli* and 1μg/mL for *R. sphaeroides* strains.

The mutant $\Delta C_{(229\text{-}263)}$ cannot grow photosynthetically but semi-aerobically in 800 ml Sistrom medium in 2-Liter shake flasks at 30℃. Because the trans-membrane helix has been deleted, truncated cytochrome c_1 cannot be assembled into the complex with cytochrome *b* and ISP to form a functional protein complex on the membrane. After the cells were harvested, a very small amount of cell pellet was used to purify the plasmid to confirm the DNA sequence through PCR.

Purification of cytochrome c_1 head domain - The harvested cells were suspended in 20mM Tris-Succinate buffer, pH8.0 at 4℃ (3 mL buffer/g cell). After stirring on ice for 20 minutes with addition of DNase, RNase and 1mM PMSF, the cells were passed through a French Press twice with a pressure of 1000-1500 psig. The broken cells were centrifuged at 40,000xg (18,000rpm with JA-20 rotor) for 30 minutes and the cell debris was discarded. Then the supernatant was ultracentrifuged at 220,000xg (60,000 rpm with Ti70 rotor or 49,000 rpm with Ti50.2 rotor) for 90 minutes. The resulting supernatant was applied to Ni-NTA column which was equilibrated with 50 mM TrisCl, pH8.0 at

4℃, containing 1mM $MgSO_4$. The flow-through was collected and saved for the purification of cytochrome c_2. The column was washed in sequence with 5 gel volumes of 50 mM TrisCl, pH8.0 at 4℃, containing 200mM NaCl (Buffer B), 8 gel volumes of Buffer B with 5mM Histidine, 2 gel volumes Buffer B with 10mM Histidine, 1 gel volume of Buffer B with 20mM Histidine sequentially. The protein was eluted with Buffer B with 200mM Histidine. The fractions with high purities (soret/UV>1.8) were combined and concentrated with YM-10 Amicon ultrafiltration membrane, then subjected to ammonium sulfate fractionation by adding pulverized solid ammonium sulfate from 35% to 100% saturation at 4℃. The precipitates between 50% to 80% ammonium sulfate saturation was collected, which contained most of the soluble cytochomre c_1, were dissolved in 50 mM TrisCl buffer, pH8.0 at 4℃. These fractions were then combined and applied to the Ni-NTA column equilibrated with 50 mM TrisCl buffer, pH8.0 at 4℃, containing 1mM $MgSO_4$. The column was washed with 50 mM TrisCl buffer, pH8.0 at 4℃ until the effluent was clear. Then the column was washed with 50 mM TrisCl buffer, pH8.0 at 4℃, with a histidine gradient of 5 to 20 mM. The protein was eluted with 50 mM TrisCl buffer, pH8.0 at 4℃ containing 40mM Histidine. The fractions with high purity were combined and applied to DEAE-cellulose column equilibrated with 25 mM TrisCl buffer, pH8.0 at 4℃. The column was washed with 25mM TrisCl, pH8.0 at 4℃, containing KCl with a gradient from 0mM to 250mM. The protein was eluted out with 25mM TrisCl pH8.0 at 4℃ containing 300mM KCl. The fractions which had high purity (soret/UV>4) were combined and desalted by changing buffer to 25mM TrisCl, pH8.0 at

4℃ then concentrated with YM-10 Amicon ultrafiltration membrane. The purified protein was divided into aliquots and saved at -80℃ until used.

The concentration of the isolated cytochrome c_1 head domain was determined by using the same method as that in the complexed form c_1. A milimolar extinction coefficient of 17.5mM-1cm-1 was used for the wavelength pair 552 and 540 to calculate the cytochrome c_1 content.

Gel electrophoresis and TMBZ heme staining - Sodium Dodecyl Sulfate – polyacrylamide gel electrophoresis (SDS-PAGE) performed according to Laemmli (13) using a Bio-Rad Mini-Protean dual slab vertical cell. Samples were diluted in 10mM TrisCl buffer, pH 6.8 containing 1% SDS, 3% glycerol and 0.4% β – mercaptoethanol for 10 minutes at room temperature before being applied to electrophoresis.

The TMBZ heme staining was performed as previously reported (14) with minor modifications. After SDS-PAGE electrophoresis, the polypeptides separated during SDS-PAGE were transferred to a polyvinylidene difluoride membrane. 35 mL of 0.25M sodium acetate (pH 5.0) was mixed with 15mL of freshly prepared 6.3 mM TMBZ and added to the blotted membrane. After the membrane was incubated shaking for 1 hour, 1mL 30% cold hydrogen peroxide was added to the solution. Color development was observed immediately after the addition of hydrogen peroxide.

Carbon monoxide binding experiment - Carbon monoxide (CO) binding experiment was performed at room temperature. Fully oxidized purified protein (2.5 μM), diluted with 100 mM TrisCl (pH 8.0) containing 100 mM NaCl, was first reduced with dithionite and the spectrum was recorded (specR), followed by a short bubbling with

carbon monoxide after which the spectrum was also recorded (specR+CO). Carbon monoxide binding was analyzed based on specCO which was calculated from (specR+CO *minus* specR) spectra. No spectral change is expected if no binding of CO is taking place.

Determination of Redox potential of cytochrome c_1 - The potentiometric titrations of cytochrome c_1 head domain were essentially done according to the previously published method (15,16) using the following redox mediators (final concentration): diaminodurol (70 µM), duroquinone (50 µM), Pyocyanine (25 µM), Anthroquinone-2-sulfonic acid (25 µM), Indigo carmine (25 µM), 1,2-naphtoquinone (25 µM), 1,4-benzoquinone (20 µM) phenazine ethosulfate (20 µM), phenazine methosulfate (20 µM). Reductive potentiometric titrations were carried out using dithionite to reduce the ferricyanide oxidized sample and ferricyanide was used for oxidative titration of dithionite reduced sample. All titrations were performed at room temperature using a sealed anaerobic cuvette constantly flushed with argon. The midpoint potential of cytochrome c_1 head domain was calculated by fitting the redox titration data obtained to the Nernst equation for n = 1.

Differential scanning calorimetry (DSC) – DSC measurements were performed in a Nano-DSC II from Calorimetry Sciences Corp. The buffers used for reference and dilution of samples were phosphate buffer instead of Tris buffer to avoid the large pH changes during the processes of heating and cooling. Prior to loading into the cells of the DSC, all buffers were carefully degassed under vacuum to remove dissolved air. Sample proteins diluted in 550µL degassed buffer were loaded into the sample cell, and the same volume of the same buffer was loaded into the reference cell. During the scanning, both

the sample and reference buffer were heated from 10°C to 90°C, and then cooled back to 10°C, followed by being heated to 90°C again. The cells were equilibrated at 10°C and 90°C for 10°C minutes before the heating and cooling started, respectively. The difference of power input between the sample cell and reference cell was recorded in μW and plotted as a function of temperature by the data acquisition program DSCRun. One data point was taken in every 10 seconds as heating and cooling of cells were done in a steady rate of 1°C per-minute. There were no thermotransition peaks observed in the second heating scan since the protein sample was completely and irreversible denatured during the first heating scan. So the second heating was used as the baseline for analysis. The transition temperature and enthalpy change (ΔH) were calculated by using the CpCalc program from the Nano DSC program group.

Results and Discussion

Construction and isolation of cytochrome c_1 head domain - Figure 19 (Page 70) illustrates the steps followed to generate the truncated cytochrome c_1 head domain mutant. A detailed description of the protein expression in *R. sphaeroides* and the protein purification is included in the Materials and Methods section. Because the trans-membrane helix has been deleted, truncated cytochrome c_1 cannot be assembled into the complex with cytochrome *b* and ISP to form a functional protein complex on the membrane. The mutant $\Delta C_{(229\text{-}263)}$ can still grow semi-aerobically in the dark due to the alternative quinol oxidase pathway. Six-histidine tag was still attached on the C-terminus of the protein. The protein can be isolated from the periplasmic fraction through the affinity between the six-histidine tag and the Nickel column. During the process of

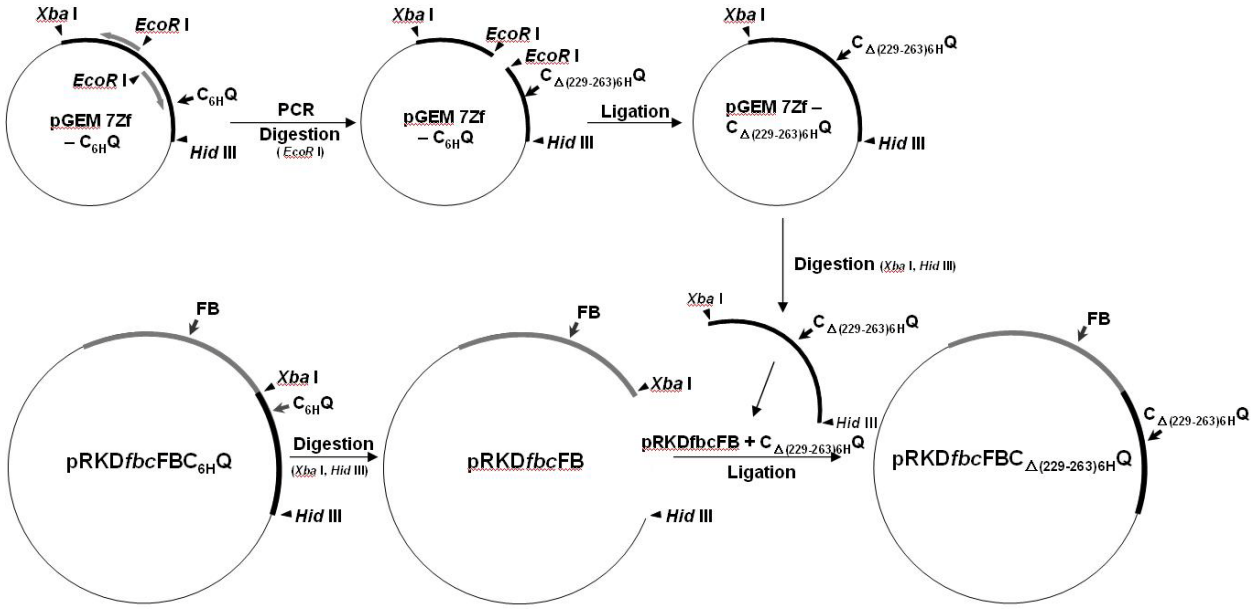

Figure 19. **Scheme showing construction of *fbc* operons encoding the mutant *R. sphaeroides* cytochrome bc_1 consisting of His-tagged cytochrome c_1 head domain**

purification, the purity of the mutated c_1 gradually increased after the steps of the Ni-NTA purification, ammonium sulfate precipitation and gel filtration. Finally, the fractions with high purity (soret/UV>4.2) were collected and concentrated.

Properties of cytochrome c_1 head domain - The isolated truncated cytochrome c_1 constitutes the soluble head domain of the cytochrome c_1 subunit, which comprises residues H1 to Q228 with an attached his-tag and has a theoretical molecular weight of 28KDa (Figure 20, Page 72). The soluble head domain was purified, as described in the previous section, to a Soret/UV ratio of 4.2. Without addition of β - mercaptoethanol, cytochrome c_1 head domain gave a smear band due to the covalently liked heme in the c-type cytochromes (17). The band is at a lower than but similar molecular weight to the wild type cytochrome c_1 on an SDS-PAGE gel. With the presence of β - mercaptoethanol, a band just below the authentic cytochrome c_1 on the SDS-PAGE gel shows a molecular weight of about 29KD under reducing conditions (Figure 21, Page 73).

The *c*-type of cytochrome has the heme covalently bound to the head domain of the *R. sphaeroides* cytochrome c_1 (17). To examine whether the deletion of the transmembrane helix affects the binding of the heme, the TBMZ (3,3',5,5'-tetramethylbenzidine dihydrochloride) heme staining was performed (18). Similar to the results of the SDS-PAGE, the heme staining shows a broad band under non-reducing condition and a sharp band under the reducing condition for both the *R. sphaeroides* soluble cytochrome c_1 and the wild type cytochrome c_1. The bands of soluble cytochrome c_1 are smaller than the bands of the wild type cytochrome c_1, indicating that the heme is still linked to the head domain of the truncated cytochrome c_1. Western blotting was performed with polyclonal rabbit antibodies being against cytochrome c_1. The similar

A B

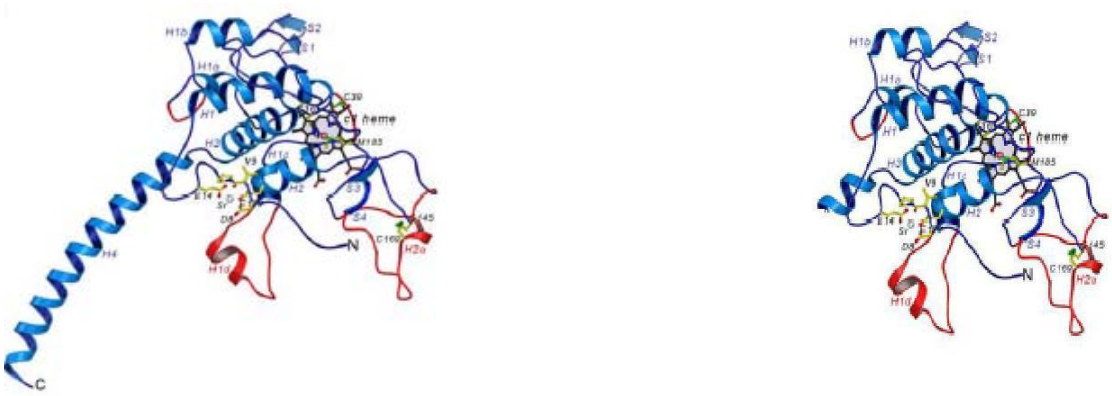

Figure 20. **Stuctures of the *R. sphaeroides* cytochrome c_1.** (A). Structure of the intact cytochrome c_1 in the ribbon form showing all secondary structure elements. (B). The mutant cytochrome c_1 head domain.

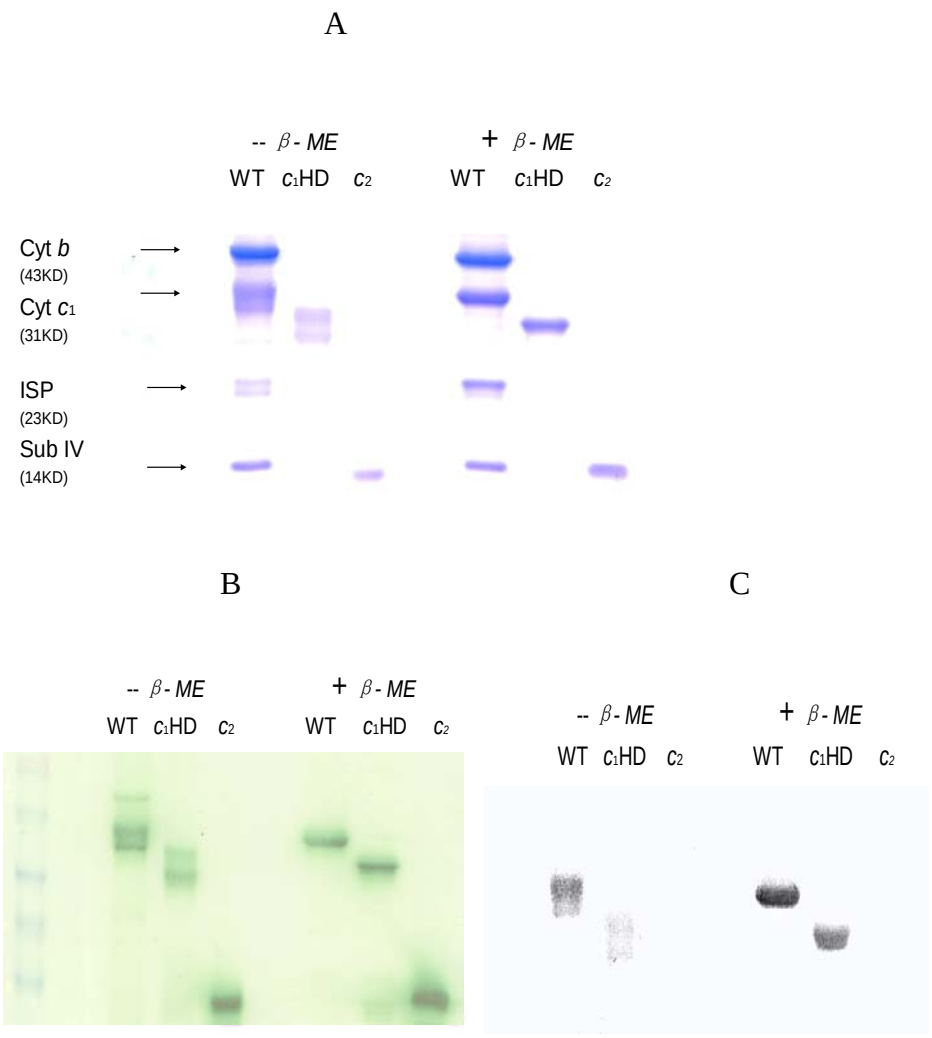

Figure 21. **Comparison of the complexed wild type c_1, cyotchrome c_1 head domain and cytochrome c_2.** (A) SDS-PAGE, (B) TMBZ heme staining, (C) Western blotting. Purified wild type *R.sphaeroides* bc_1 (WT), cytochrome c_1 head domain, and cytochrome c_2 are indicated. Samples of protein (200pmoles) were incubated in the presence or absence of β-mercaptoethanol as reducing agent at room temperature for 15min before being subjected to SDS-PAGE as described in the "Experimental Procedure".

bands are observed for the wild type cytochrome c_1 and soluble cytochrome c_1, which is corresponding to the heme staining. As expected, the cytochrome c_2 is not detected in the western blotting due to the antibody being against c_1.

After the purification, the ascorbate-reduced-minus-ferricyanide-oxidized spectra of the cytochrome c_1 head domain are comparable to that of the full length *R. sphaeroides* cytochrome c_1 (4,19,20), which implies a stable function of the head domain (Figure 22 B, Page 75). The spectrum of the reduced soluble fragment of cytochrome c_1 shows an absorption peak at 552 nm with an extinction coefficient of 17.5 mM^{-1} cm^{-1} and the soret absorptioin peak at 417 nm, which is similar to the membrane bound cytochrome c_1 (4,19,20). Reducibility by ascorbate implies a stably functional head domain, which was further confirmed by a negative reaction with carbon monoxide (data not shown) and by its midpoint potential, determined to be 225mV which is comparable to the wild type cytochrome c_1 potential of 235mV (Figure 23, Page 76).The gel filtration indicated the soluble fragment of cytochrome c_1 is a monomer with an apparent molecular weight of 28KD (Figure 22 A, Page 75).

Thermostalibility of isolated cytochrome c_1 head domain – Differential scanning calorimetry (DSC) is a prime technique to study the thermally induced transitions and conformational transitions of biological macromolecules (21,22). The thermotransition is observed as a sharp endothermic peak centered at a transition temperature. Generally, the higher transition temperature indicates the more thermodynamically stable macromolecules (21). Figure 24 (Page 78) shows the DSC thermograms for the reduced and oxidized cytochrome c_1 head domain in the 50mM phosphate buffer, pH7.5. Like mitochondrial cytochrome *c* and c_1 (23-25), the thermal denaturation of *R. sphaeroides*

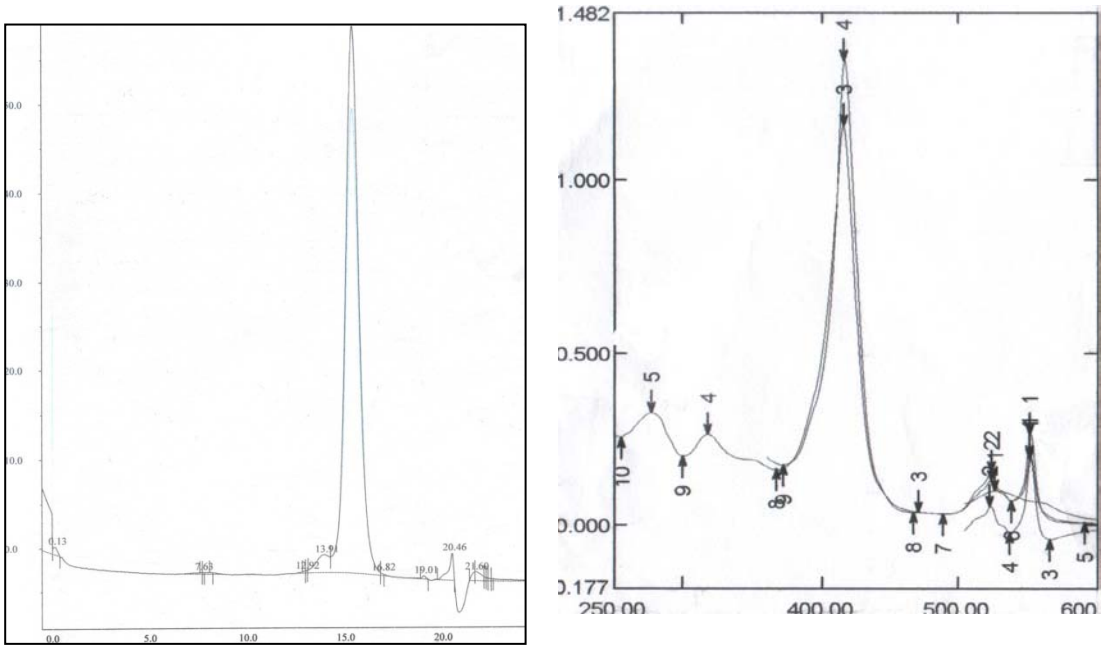

A B

Figure 22. **Characterization of the cytochrome c_1 head domain.** (A) Gel filtration of the pure soluble cytochrome c_1 head domain; (B) The absorption spectra of ferricyanide - oxidized and ascorbate -reduced 600nm-250nm) of the pure cytochrome c_1 head domain. The soret band wavelength for oxidized and reduced cytochrome c_1 head domain is 410nm and 417 nm, respectively. Its α-band wavelength is 552nm with an extinction coefficient of 17.5 $mM^{-1}.cm^{-1}$. Protein was diluted in 25mM TrisCl buffer, pH 8.0 at 4°C.

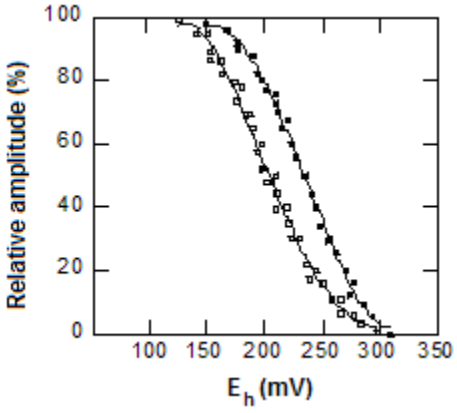

Figure 23. **Potentiometric titration of cyt c_1 in purified cytochrome bc_1 complexes from Wild type and from head domain**. [▪] Wild type cytochrome c_1; Em = 235mV, and [▫] cytochrome c_1 head domain; Em = 225mV. Oxidative and reductive titrations were performed as described in Materials and Methods. The data were fit to the Nernst equation for n=1.

cytochrome c_1 head domain was calorimetrically irreversible. The second heating of the protein solution had no thermal effect, which was used as the baseline. A sharp thermodenaturation peak for reduced c_1 head domain was found at 70.5°C. Oxidized c_1 head domain, however, underwent a thermal denaturation at 45°C. This suggested that the reduced form of cytochrome c_1 head domain possesses a more stable tertiary structure than the oxidized form.

The thermotropic properties of mitochondrial cytochrome *c* and c_1 have been studies decades ago (24). Under the condition of pH7.5, mitochondrial cytochrome *c* showed a transition temperature at 86.4°C for oxidized protein and denatures at 102°C when protein sample was reduced. Like mitochondrial cytochrome *c* and *R. sphaeroides* cytochrome c_1 head domain, mitochondrial cytochrome c_1 showed a single thermotransition peak. Oxidized mitochondrial c_1 denatured at 66°C whereas reduced mitochondrial c_1 underwent thermodenaturation at 70°C. For intact mitochondrial cytochrome c_1, the difference of thermodenaturation temperatures between reduced and oxidized proteins is only about 4°C. However, reduced and oxidized *R. sphaeroides* cytochrome c_1 head domains differ by 25°C at the given conditions. This suggests cytochrome c_1 head domain undergoes more conformational changes between reduced state and oxidized state than that between reduced and oxidized mitochondrial cytochrome c_1. This conformational change between reduced and oxidized form commonly exists among the *c*-type of cytochromes (26). Although *R. sphaeroides* cytochrome c_1 has been successfully purified more than a decade ago, it existed as an aggregated pentamer in aqueous solution (4,20). Due to the unavailability of the data of intact *R. sphaeroides* cytochrome c_1, we cannot compare it with its head domain so far.

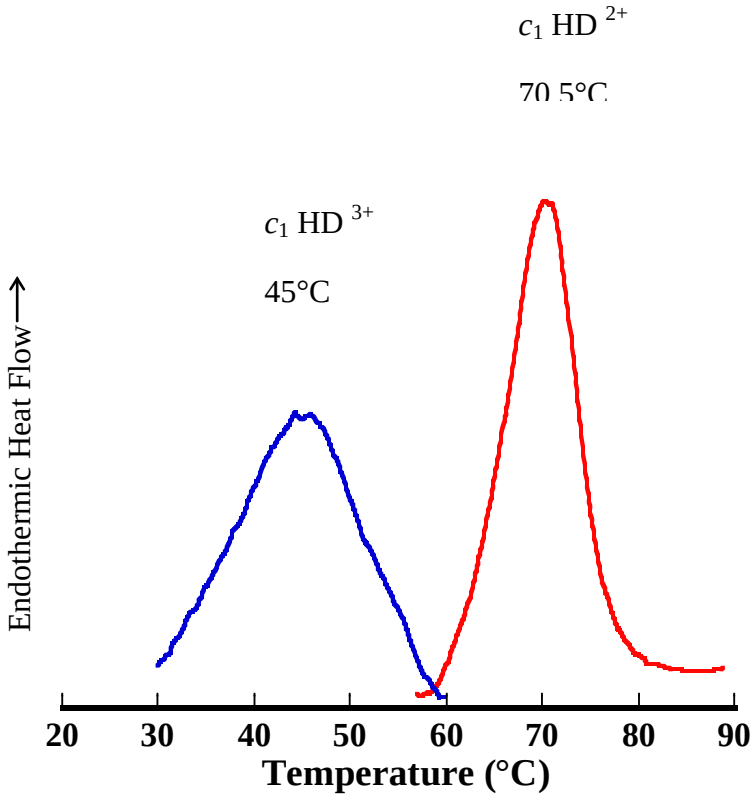

Figure 24. **DSC thermogram of *R. sphaeroides* cytochrome c_1 head domain**. Reduced (red) and oxidized cytochrome c_1 head domain (blue). Proteins were diluted in 50mM phosphate buffer, pH7.5 to 3mg/ml. As described in the "Experimental Procedure", 550µL of samples were scanned against the same volume of buffer from 20°C to 90°C. Oxidized cytochrome c_1 head domain shows a transition temperature at 45°C, reduced $c_1$head domain has a transition temperature at 70.5°C. For oxidized cytochrome c_1 head domain, 1mM potassium ferricyanide was included in the sample and buffer solutions.

Truncated cytochrome c_1 head domain is a suitable candidate to study the membrane bound c_1 - One method to study the structure and function of the bc_1 complex is to examine the individual subunits. The full length cytochrome c_1 has been successfully isolated from different species in aggregated form (27) (5-7,9) in aqueous solution. Constructions of single mutant generating the water soluble fragment of cytochrome c_1 – c_1 head domain have been attempted. Proteolysis of the cyrochrome c_1 released c_1 water soluble fragment from the bound of the membrane (27,28). However, the cytochrome c_1 was also degraded and heme was lost in some cases because the cytochrome c_1 is more sensitive to protease on the surface of the membrane than other subunits in the bc_1 complex. Then genetic engineering was employed to generate the c_1 head domain mutants by either introducing a stop codon at the neck of cytochrome c_1 following Q228 or by mutating Q228 itself to a stop codon, as reported by Konishi, K. et al (3) in 1991, have repeatedly failed due to the reversion of the mutants to wild type during semi-aerobic growth. Two decades has passed and no reproduced data has been reported of further head domain studies or to determine the structure of cytochrome c_1 head domain despite the lack of structure for most of those years. An additional attempt to isolate the head domain by engineering a triple mutation introducing Factor Xa IDGR cleavage consensus sequence at the neck of cytochrome c_1 followed by Factor Xa treatment was unsuccessful, most likely due to the inaccessibility of Factor Xa to the introduced site. The only successful way to isolate the soluble head domain was by engineering a mutant excluding the tail domain of cytochrome c_1 and attaching the histidine tag directly to the neck region. Due to the length of the tail domain of cytochrome c_1 (229-263), a deletion mutagenesis is unfeasible. Therefore, PCR was used to amplify the required fragments to

express the cytochrome c_1 head domain, ending at residue 228, with an attached his-tag, generating the truncated mutant.

Release of the cytochrome c_1 head domain from the *R. sphaeroides* cytochrome bc_1 resulted in a dysfunctional bc_1 complex since the bacteria could not grow photosynthetically, which suggests that the hydrophobic anchor of cytochrome c_1 and assembly of c_1 are essential for the function of the bc_1 complex. It has been reported that the intactness of cytochrome c_1 in the bc_1 complex also affected the stability of other subunits (29,30).

Although lacking a membrane anchor, the water soluble head domain of *R. sphaeroides* cytochrome c_1 still retains the functional redox center. The mutated protein is stable and maintains characteristics comparable to the intact membrane-bound counterpart. With the deletion of the membrane-spanning helix, the soluble fragment of the cytochrome c_1 can be easily isolated from the whole complex.

The cytochrome c_1 shuttles electron from hydrophobic environment of the cytochrome bc_1 to the hydrophilic environment of the cytochrome *c* or c_2. One would wonder if electron transfer is affected by the dramatic change of the cytochrome c_1 from membrane bound protein to soluble protein. Previous studies showed the interaction between the soluble cytochrome c_1 and its electron acceptor cytochrome c_2 in vitro (27,29). Although the co-crystal structures of the cytochrome bc1 and cytochrome c in some species have been resolved, the information about the structure of the soluble uncomplexed cyrtochrome c_1, the structure of complexed c_1 and c_2 in the aqueous environment is still unavailable. Our results demonstrated the soluble head domain of the cytochrome c_1 as a suitable candidate to obtain information on the structure and function

of cytochrome c_1 which cannot be obtained from the membrane bound full-length cytochrome c_1.

References

1. Andrews, K. M., Crofts, A. R., and Gennis, R. B. (1990) *Biochemistry* **29**, 2645-2651
2. Yun, C. H., Beci, R., Crofts, A. R., Kaplan, S., and Gennis, R. B. (1990) *Eur J Biochem* **194**, 399-411
3. Konishi, K., Van Doren, S. R., Kramer, D. M., Crofts, A. R., and Gennis, R. B. (1991) *J. Biol. Chem.* **266**, 14270-14276
4. Yu, L., Mei, Q.C., and Yu, C.A. . (1984) *Biochemical and Biophysical Research Communications* **118**, 964-969
5. Yu, C. A., Yu, L., and King, T. E. (1972) *J Biol Chem* **247**, 1012-1019
6. Robinson, N. C., and Talbert, L. (1980) *Biochem Biophys Res Commun* **95**, 90-96
7. Wakabayashi, S., Matsubara, H., Kim, C. H., and King, T. E. (1982) *J Biol Chem* **257**, 9335-9344
8. Ross, E., and Schatz, G. (1976) *J Biol Chem* **251**, 1991-1996
9. Yu, L., and Yu, C. A. (1984) *Biochem Biophys Res Commun* **123**, 1234-1239
10. Tian, H., Yu, L., Mather, M. W., and Yu, C.-A. (1997) *J. Biol. Chem.* **272**, 23722-23728
11. Donohue, T. J., McEwan, A. G., Van Doren, S., Crofts, A. R., and Kaplan, S. (1988) *Biochemistry* **27**, 1918-1925
12. Tian, H., Yu, L., Mather, M. W., and Yu, C. A. (1998) *J Biol Chem* **273**, 27953-27959
13. Laemmli, U. K. (1970) *Nature* **227**, 680-685
14. Feissner, R., Xiang, Y., and Kranz, R. G. (2003) *Anal Biochem* **315**, 90-94

15. Dutton, P. L. (1978) *Methods Enzymol.* **54**, 411-435

16. Guner, S., Robertson, D. E., Yu, L., Qiu, Z. H., Yu, C. A., and Knaff, D. B. (1991) *Biochim Biophys Acta* **1058**, 269-279

17. Elberry, M., Yu, L., and Yu, C.-A. (2006) *Biochemistry* **45**, 4991-4997

18. Goodhew, C. F., Brown, K.R. and Pettigrew, G.W. . (1986) *Biochim. Biophys. Acta* **852**, 288-294

19. Yu, C. A., Yu, L., and King, T. E. (1972) *J. Biol. Chem.* **247**, 1012-1019

20. Yu, L., Dong, J.-H., and Yu, C.-A. (1986) *Biochimica et Biophysica Acta (BBA) - Bioenergetics* **852**, 203-211

21. Bruylants, G., Wouters, J., and Michaux, C. (2005) *Curr Med Chem* **12**, 2011-2020

22. Cooper, A. (2005) *Biophys Chem* **115**, 89-97

23. al., A. A. M.-M. e. (2004) *Thermochimica Acata* **409**, 137-144

24. Yu, C. A., Steidl, J. R., and Yu, L. (1983) *Biochim Biophys Acta* **736**, 226-234

25. Yu, C. A., Gwak, S. H., and Yu, L. (1985) *Biochim Biophys Acta* **812**, 656-664

26. Salemme, F. R. (1977) *Annu Rev Biochem* **46**, 299-329

27. Li, Y., Leonard, K., and Weiss, H. (1981) *Eur J Biochem* **116**, 199-205

28. Theiler, R., and Niederman, R. A. (1991) *J Biol Chem* **266**, 23163-23168

29. Konishi, K., Van Doren, S. R., Kramer, D. M., Crofts, A. R., and Gennis, R. B. (1991) *J Biol Chem* **266**, 14270-14276

30. Gerhus, E., Steinrucke, P., and Ludwig, B. (1990) *J Bacteriol* **172**, 2392-2400

CHAPTER IV

THE INTERACTION BETWEEN *RHODOBACTER SPHAEROIDES* CYTOCHROME bc_1 COMPLEX AND CYTOCHROME *c* OR c_2

Abstract

The interaction between the cytochrome c_1 in the cytochrome bc_1 complex and cytochrome c_2 or cytochrome *c* has been studied. The results indicate this interaction is ionic strength dependent. Surprisingly, when oxidized cytochrome *c* was added to ascorbate reduced cytochrome bc_1 complex at low ionic strength (50mM phosphate buffer, pH7.5, containing 0.01% DM), both cytochrome c_1 in the bc_1 complex and cytochrome *c* showed a rapid oxidation. The extent of this oxidation decreased with the increased salt concentration in the reaction buffers. This oxidation was not sensitive to carbon monoxide, suggesting that this oxidation is not due to the presence of cytochrome *c* oxidase in the bc_1 preparation. The rate of the net oxidation was ten times slower when oxidized cytochrome *c* was added to the ascorbate reduced *Rs*ΔIV mutant complex. No net oxidation was observed when oxidized cytochrome *c* was added to reduced mitochondrial cytochrome bc_1 complex or isolated head domain of bacterial cytochrome c_1 under low ionic strength condition. Stigmatellin, which blocks electron transfer between the ISP and c_1, had no effect on the net oxidation of *R. sphaeroides* c_1 and *c*.

Introduction

The study of reaction mechanism of the interaction between cytochrome c_1 and its electron acceptor cytochrome *c* in mitochondria or cytochrome c_2 in bacteria has not been concluded. The results obtained from many groups demonstrated that the nature of this interaction is hydrophilic based on the studies of the proposed interacting surface of cytochromes c_1 and *c* or c_2. The X-ray structure of beef and yeast cytochrome bc_1 compex revealed the presence of acidic residues on the cytoplasmic side of cytochrome c_1 head domain which are believed to be at the cytochrome *c* docking site (1,2). Site-directed mutagenesis studies further proved that the two acidic regions rich in glutamate and aspartate residues located on the intra-membrane surface of bovine cytochrome c_1 are involved in directing the diffusion and binding of the cytochrome *c* from the intra-membrane space (3). These two regions were found to be conserved amongst most bacterial cytochrome c_1 sequences and thus believed to be involved in binding cytochrome c_2. In a complementary study, a water-soluble carbodiimide was used to show that specific carboxylate groups on cytochrome c_1 are involved in binding cytochrome *c* (4). Chemical modification and mutations of the lysine amino groups to negatively charged groups on the interface of cytochrome c_2 resulted in decreased binding between cytochrome c_2 and the cytochrome bc_1 complex. These results supported the involvement and importance of the positively charged residues in cytochrome c_2 in the interaction with the cytochrome bc_1 complex (1,5-11). In an independent study, the reaction of bovine heart cytochrome c_1 with a ruthenium - cytochrome *c* derivative by flash photolysis showed a progressive decrease of electron transfer rate constant within the complexes with increasing salt concentration indicating a dissociation of the complex

at increasing ionic strength (12). The effects of ionic strength on the complex formation between cytochrome c_2 and cytochrome bc_1 in photosynthetic bacteria *Rhodobacter capsulatus* were consistent with the previous results which showed that low ionic strength, but not the high ionic strength is favorable for the complex formation (13). However, in contrast to the considerable evidence supporting the electrostatic interaction between cytochrome c_1 and its electron acceptor, the co-crystal structure of the yeast cytochrome bc_1 and cytochrome *c* with bound stigmatellin from yeast, solved at 2.97 Å, revealed the binding of cytochrome *c* to one of the two possible cytochrome c_1 binding sites of the homodimeric complex, stabilized mainly by hydrophobic interactions (14-16). The oppositely charged residue pairs surrounding the non-polar interface with distances of 4.7-9.2 Å were not close enough to form stable salt bridges.

Herein we report the studies of electron transfer between cytochrome c_1 from *Rhodobacter sphaeroides* (*R. sphaeroides*) cytochrome bc_1 and cytochrome c_2 or horse cytochrome *c* under different ionic strength conditions. The interaction between the purified *R. sphaeroides* bc_1 mutants - cytochrome c_1 head domain, three-core-subunit (*Rs*ΔIV) and subunit IV fused bc_1 complex - and cytochrome c_2 or horse cytochrome *c* were also determined.

Experimental Procedure

Materials - Horse heart cytochrome *c* (type III) was purchased from Sigma and re-purified through a Superdex 200 FPLC column purchased from Pharmacia. The Ni-NTA resin used for purification of the His_6-tagged cytochrome bc_1 was purchased fromSigma. N-Dodecyl-β-D-maltoside (LM) and N-octyl- β-D-glucoside (OG) were

purchased from Anatrace. 2-Methyl-6- (4-methoxyphenyl)-3, 7-dihydroimidazol [1, 2-α] pyrazin-3-one, hydrochloride (MCLA) was obtained from Molecular Probes, Inc. 2, 3-Dimethoxy-5-methyl-6-bromodecyl-1, 4-benzoquinol ($Q_0C_{10}BrH_2$) was prepared in our laboratory as previously reported (17). All other chemicals were of the highest purity commercially available.

His_6-tagged cytochrome bc_1 complex preparation and activity assay - Cytochrome bc_1 complex from beef heart mitochondria (18,19), chromatophpores, intracytoplasmic membrane (ICM) and the His_6-tagged bc_1 complex from *Rhodobacter sphaeroides* (20,21) were prepared and assayed according to the method previous reported in our lab.

Frozen *R. sphaeroides* cells were suspended in 20mM Tris-succinate, pH7.5 at 4°C, in the presence of 1mM sodium ethylenediamminetetraacetate (EDTA) (3mL of buffer per gram of cells). After gradually adding a protease inhibitor phenylemethylsulfinyl fluoride (PMSF) dissolved in dimethylsuloxide (DMSO) to 1mM, a grain of DNase and RNase and stirring on ice for 20 minutes, the suspended cells were passed twice through French press at 1,000 psi to break the cells. The unbroken cells and cell debris were spun down and seperated from the broken cells after centrifugation at 40,000xg (18,000rpm with JA-20 rotor) for 30 minutes. After removing the precipitate, the supernatant was centrifuged at 220,000xg (60,000 rpm with Ti70 rotor or 49,000 rpm with Ti50.2 rotor) for 90 minutes to separate the chromatophore fraction from the soluble protein fraction. The pellet was homogenized in buffer 50mM TrisCl, pH8.0 at 4°C , containing 1mM $MgSO_4$ then subjected to centrifugation at 220,000 x g (60,000 rpm with Ti70 rotor or 49,000 rpm with Ti50.2 rotor) for 90 minutes to recover the

chromatophores. The resulting chromatophores were homogenized and suspended in buffer 50mM TrisCl, pH8.0 at 4°C, containing 1mM $MgSO_4$ and 20% glycerol. These chromatophores were ready to use or can be stored at -80°C until use.

To purify the His-tagged *R. sphaeroides* cytochrome bc_1 complex, the freshly prepared chromatophores or frozen chromatophores thawed on ice were adjusted to a cytochrome *b* concentration of 25 μM with buffer 50mM TrisCl, pH8.0 at 4°C, containing 1mM $MgSO_4$. 10% (w/v) Dodecylmaltoside (DM) was added to the chromatophore suspension to 0.56 mg/nmole of cytochrome *b* (0.14145x volume of suspension) to solubilize the protein. 4M sodium chloride solution was added into the suspension to a final concentration of 0.1M. After stirring on ice for 1 hour, the mixture was centrifuged at 220,000 x g (60,000 rpm with Ti70 rotor or 49,000 rpm with Ti50.2 rotor) for 90 minutes. The supernatant was collected and diluted with the same volume of buffer 50mM TrisCl, pH8.0 at 4°C, containing 1mM $MgSO_4$ followed by passing through the Ni-NTA agarose column (100nmole of cytochrome *b*/ml of resin) equilibrated with buffer 50mM TrisCl, pH8.0 at 4°C, containing 1mM $MgSO_4$ more than two volume of resin. After all the diluted supernatant flew through the column, the column absorbed with bc_1 complex was sequentially washed with following buffer until no greenish effluent, 50mM TrisCl, pH8.0 at 4°C, containing 100mM NaCl and 0.01%DM; 50mM TrisCl, pH8.0 at 4°C, containing 100mM NaCl, 0.01%DM and 5mM Histidine; 50mM TrisCl, pH8.0 at 4°C, containing 100mM NaCl and 0.5%OG; 50mM TrisCl, pH8.0 at 4°C, containing 100mM NaCl, 0.5%OG and 5mM Histidine. The cytochrome bc_1 complex was eluted with buffer 50mM TrisCl, pH8.0 at 4°C, containing 100mM NaCl, 0.5%OG and 200mM Histidine and collected fractionally. The pure fractions were

combined and concentrated by using Centriprep-30 concentrator. The purified bc_1 complex was added glycerol to a final concentration of 20% then stored at -80°C in 100µL aliquots.

The content of cytochrome c_1 was determined from the sodium ascorbate reduced-minus-potassium ferric cyanide oxidized spectrum and the extinction coefficient of 17.5 $cm^{-1}mM^{-1}$ was used for wavelength pair 552 nm and 540 nm (22). To determine the cytochrome *b* content, the spectrum of sodium dithionite reduced-minus-potassium ferric cyanide and the extinction coefficient of 28.5 $cm^{-1}mM^{-1}$ for wavelength pair 560 and 576 nm were used (23).

To assay the protein activity, the purified cytochrome bc_1 complex was diluted in 50mM TrisCl buffer, pH8.0 at 4°C, containing 100mM NaCl and 0.01%DM to a final cytochrome *b* concentration of 1µM. The reaction started by adding reduced $Q_0C_{10}BrH_2$ in ethanol into 1mL of assay mixture containing 100mM Na^+/K^+ phosphate buffer, pH 7.4, 300µM EDTA and 100µM cytochrome *c* (Horse heart, Sigma) to a final concentration of 25µM. Appropriate amounts of the diluted proteins were added to the assay mixture and the reduction of cytochrome *c* (the increase of absorbance at 550 nm) was measured in a Shimadzu UV 2101 PC spectrophotometer at 23°C. A millimolar extinction coefficient of 18.5 was used for calculation. The non-enzymatic reduction of cytochrome *c*, determined under same condition in the absence of bc_1 complex was subtracted from the calculation. To measure bc_1 activity in chromatophores, 30 µM potassium cyanide was added to the assay mixture to inhibit the cytochrome *c* oxidase activity.

Preparation of mutant R. sphaeroides cytochrome c_1 head domain - The construction, purification and characterization of water soluble cytochrome c_1 head domain were described in the previous chapter. The concentration of the isolated cytochrome c_1 head domain was determined by a difference spectrum between sodium ascorbate reduced minus potassium ferricyanide oxidized and a milimolar extinction coefficient of $17.5 mM^{-1}cm^{-1}$ for a wavelength pair 552nm and 540nm was used for calculating the cytochrome c_1 content.

Purification of cytochrome c_2 from R. sphaeroides - Cytochrome c_2 was purified according to Bartsch (24) with following modifications: The flow-through from the Ni-NTA column during the process of cytochrome c_1 purification was added pulverized solid ammonium sulfate to 80% saturation. The precipitate was removed by centrifugation and the pulverized solid ammonium sulfate was added supernatant to 100% saturation. The precipitate between 80% to 100% saturation, which contains most of the cytochrom c_2 was collected, dissolved in 25mM TrisCl, pH 8.0 at 4℃, and desalted. The sample was applied to a DEAE-cellulose column equilibrated with 25 mM TrisCl, pH8.0 at 4℃. The column was washed with 8-10 gel volumes of the same buffer. Cytochrome c_2 was eluted with the washing buffer containing 50mM KCl. The fractions with high purity (soret/UV>4) were combined and concentrated with YM-10 Amicon ultrafiltration membrane. The purified protein was divided into aliquots and saved at -80℃ until used.

The purified cytochrome c_2 is in reduced form. To obtain oxidized cytochrome c_2, the prepared cytochrome c_2 was added a slight excess of potassium ferricyanide ($K_3Fe(CN)_6$ and loaded onto a Superdex 200 column (Pharmacia) equilibrated with 50mMTrisCl, pH8.0 at 4°C, to remove excess $K_3Fe(CN)_6$.

To determine the concentration of cytochrome c_2, a difference spectra between sodium ascorbate reduced minus potassium ferricyanide oxidized was taken and a millimolar extinction coefficient of $18.5 mM^{-1}cm^{-1}$ for a wavelength pair 549nm and 540nm was used for calculation.

Gel electrophoresis - Sodium Dodecyl Sulfate - Polyacrylamide Gel Electrophoresis (SDS-PAGE) performed according to Laemmli (25) using a Bio-Rad Mini-Protean dual slab vertical cell. Samples were incubated with 10mM TrisCl buffer, pH 6.8 containing 1% SDS, 3% glycerol and 0.4% β – mercaptoethanol for 10 minutes at room temperature before being applied to electrophoresis.

Spectroscopic studies of the interaction - Samples were diluted in 50 mM phosphate buffer, pH 7.5, containing 0.01% DM and various concentrations of KCl to 10 μM of c_1 and *c*. A double-sector cuvette with 0.5 cm lightpath in each sector was used. Buffers were placed in the sample cell of the spectrophotometer and spectra were recorded from 500 nm to 600 nm as the base-line. The reduced cytochrome c_1 from wild type of *R. sphaeroides* bc_1 was obtained by adding equal molar of freshly prepared sodium ascorbate solution (based on cytochrome c_1). Reduced bc_1 complex or the cytochrome c_1 head domain was placed in one sector of the cuvette, and an equal volume of oxidized cytochrome *c* or c_2 was placed in another sector of the cuvette. Spectra were recorded from 500 nm to 600 nm in a Shimadzu UV-2101 PC spectrophotometer at 23 °C before and after mixing the samples in both sectors. The difference spectra were obtained by subtracting the spectra before mixing from the spectra after mixing.

Column cochromatography - Gel filtration co-chromatography studies were carried out on the Sephadex G100 column at 4°C. Samples of cytochrome bc_1 and *c* or c_2 were dissolved in 25 mM TrisCl, pH8.0 at 4°C, containing 0.01% DM, in the presence or absence of 250mM KCl to a final concentration of 150 µM for both samples. The column was equilibrated with the same buffer for at least 5 column volumes. Equal molar amounts of *R. sphaeroides* bc_1 and c_2 were mixed under low and high ionic strength conditions and incubated on the ice for 30 minutes before applying onto the Sephadex G100 column. The column was washed and the proteins were eluted with the same buffer. Control experiments were carried out by using individual components under same conditions.

Co-precipitation studies - Pull down experiments were carried out in a desktop Optima TLX Ultracentrifuge at 4°C. The samples were dissolved in 25mM TrisCl, pH8.0 at 4°C, containing 0.05% OG, in the presence or absence of 250mM KCl. Equal molar amount of *R. sphaeroides* bc_1, based on cytochrome c_1, and cytochorme *c* or c_2 were mixed in 500 µL of buffer and incubated on ice for 20 minutes. The mixtures were subjected to ultracentrifugation at 170,000 x g for 2 hours. The amounts of cytochrome *c* or c_2 in the supernatants were measured after ultracentrifugation. An equal amount of individual cytochrome *c* or c_2 was used in the same procedure as the control experiments. When an inhibitor Stigmatellin was used, the wild type *R. sphaeroides* bc_1 was treated with 3 fold molar excess of inhibitor over cytochrome *b* for 20 minutes at 4°C, prior to mixing with cytochrome *c* or c_2.

Differential scanning calorimetry (DSC) - DSC measurements were performed in a Nano-DSC II from Calorimetry Sciences Corp. The buffers used for reference and

dilution of samples were phosphate buffer instead of Tris buffer to avoid the large pH change during the processes of heating and cooling. Prior to loading into the cells of the DSC, all buffers were carefully degassed under vacuum to remove dissolved air. Sample proteins diluted in 550μL degassed buffer was loaded into the sample cell, and the same volume of the same buffer was loaded into the reference cell. For interaction experiments, two components were incubated in the buffers for 30 minutes before applying to DSC. 1mM potassium ferricyanide was added into both the sample and reference buffer. During the scanning, both the sample and reference buffer were heated from 10°C to 90°C, and then cooled back to 10°C, followed by being heated to 90°C again. The cells were equilibrated at 10°C and 90°C for 10°C minutes before the heating and cooling started, respectively. The difference of power input between the sample cell and reference cell was recorded in μW and plotted as a function of temperature by the data acquisition program DSCRun. One data point was taken in every 10 seconds as heating and cooling of cells were done in a steady rate of 1°C per-minute. There were no thermotransition peaks observed in the second heating scan since the protein sample was completely and irreversible denatured during the first heating scan. So the second heating was used as the baseline for analysis. The transition temperature and enthalpy change (ΔH) were calculated by using the CpCalc program from the Nano DSC program group.

Fast Kinetics Study - To determine electron transfer rates between the cytochrome c_1 in *R. sphaeroides* bc_1 complex and the cytochrome *c* or c_2, the sodium ascorbate reduced *R. sphaeroides* bc_1 was mixed with the oxidized cytochrome *c* or c_2 in equal volume at room temperature in an Applied Photophysics stopped-flow reaction analyzer SX.18MV (Leatherhead, United Kingdom). The concentrations of protein

samples were 10 μM, based on cytochrome c_1, in 50 mM phosphate buffer, pH 8.0, at 4 °C, containing 0.01% DM and various concentration of KCl from 0 mM to 500 mM. When an inhibitor Stigmatellin was used, the bc_1 complex was treated with 3 fold molar excess of inhibitor over cytochrome *b* for 20 minutes at 4°C, prior to mixing with cytochrome *c* or c_2. Reduction of cytochrome *c* or c_2 was monitored by the change of absorption at 550 nm. Oxidations of cytochrome c_1 head domain and reductions of cytochrome *c* or c_2 were measured in 50 mM phosphate buffer, pH 7.5, containing various amount of KCl and monitored by the absorption change at A_{552} and A_{549}, respectively, with a photodiode array scan between 600 and 500 nm.

Results and Discussions

Column cochromatographic and coprecipitation studies of the interation between cytochrome c_1 and c or c_2 - The molecular weight of *R. sphaeroides* cytochrome bc_1 is about 110KD while cytochrome c_2 is about 14KD. The significant size difference makes size exclusion column chromatography a suitable method to study the interaction. If cytochrome c_1 interacts with c_2 electrostatically, the environment with low ionic strength will be favorable to c_1-c_2 complex formation; high ionic strength will prevent them from interacting with each other. Therefore, cytochrome c_2 will co-migrate with the cytochrome bc_1 complex under low ionic strength; cytochrome bc_1 complex and cytochrome c_2 will be eluted separately under high ionic strength. If the nature of the interaction is hydrophobic, the reverse results will be observed.

As summarized in Table 4 (Page 96), after equimolar amount of *R. sphaeroides* cytochrome bc_1 complex and cytochrome *c* were mixed in a buffer containing 25 mM

TrisCl (pH8.0), 250 mM KCl, 0.01% DM, the sample was loaded onto the Sephadex G100 column and eluted with the same buffer. The cytochrome bc_1 and cytochrome *c* eluted separately, two clear bands was observed. Ninety-seven percent of cytochrome *c* was detected in the eluate as uncomplexed form. When the same procedure was performed at low ionic strength, in the buffer in the absence of 250 mM KCl, only one major broad band was eluted. Less than 4% uncomplexed cytochrome *c* was observered. When same procedure was carried between *R. sphaeroides* cytochrome bc_1 complex and cytochrome c_2, a similar pattern of co-elution of the two components was observed under low ionic strength condition. No co-elution was observed under the high ionic strength condition. Cytochrome *c* was detected uncomplexed 97% in the eluate at high ionic strength. In control experiments, more than 98% of individual cytochrome *c* or c_2 was recovered under both high and low ionic strength conditions. This suggested that both cytochrome *c* and c_2 associate with *R. sphaeroides* cytochrome bc_1 electrostatically. The low ionic strength condition is in favor of the association of the two components. As expected, the effect of ionic strength on the interaction between *R. sphaeroides* cytochrome bc_1 and cytochrome *c* is more apparent than that between bc_1 complex and cytochrome c_2.

This was further supported by the results of pull down experiments (Table 5, Page 98). Cytochrome *c* and c_2 are soluble proteins with very high solubility. *R. sphaeroides* bc_1 only is dispersed in the solutions containing detergent. When subjected to ultracentrifugation, the cytochrome bc_1 will become precipitated in the absence of detergent but the cytochrome *c* or c_2 will still stay in the supernatant solution if there is no interaction between them. If the cytochrome bc_1 and *c* or c_2 form a complex under

Table 4. **Recovered cytochrome *c* or c_2 in gel filtration cochromatography**

Preparation	Recovered cytochrome *c* or c_2 (%)			
	Low salt (25mM TrisCl/0.01% DM)		high salt (25mM Tris/250mM KCl/0.01% DM)	
	Free	Complex	Free	Complex
Cytochrome *c*	98	0	98	0
Cytochrome c_2	97	0	98	0
Cytochrome bc_1+*c*	4	94	97	0
Cytochrome bc_1+c_2	30	68	97	0

certain condition, in this case, either in the low or the high ionic strength condition, the cytochrome *c* or c_2 will be pulled down by the bc_1 and no or a lesser amount of *c* or c_2 will be detected in supernatants. If no complex is formed between the cytochrome bc_1 and *c* or c_2, these two components will be separated and cytochrome *c* or c_2 will stay in the supernatant solution.

When *R. sphaeroides* bc_1 and cytochrome *c* were incubated in 25mM TrisCl, pH8.0 at 4°C, the supernatant is clear after 2 hour ultracentrifugation. Less than 1% of cytochrome *c* and no cytochrome $bc_1$was detected in the supernatant. In contrast to this, when these two proteins were mixed in the buffer in the presence of 250 mM KCl, the supernatant showed red color and contained more than 95% of cytochrome *c* and no cytochrome bc_1. When only cytochrome *c* was used under both low and high ionic strength conditions, no precipitate was observed and all the cytochrome *c* remained in the supernatants. These results showed that cytochrome *c* formed a complex with cytochrome bc_1 and co-precipitated at low ionic strength. At high ionic strength, no complex formation happened and cytochrome bc_1 and *c* were separated as precipitate and supernatant.

When the cytochrome *c* was replaced by c_2 to interact with *R. sphaeroides* bc_1, analysis of the spectra of the supernatant indicated about 28% and 93% of cytochrome c_2 were detected in the supernatants under low and high ionic strength conditions, respectively. Similar as cytochrome *c*, when only cytochrome c_2 was used in the control experiments, all of the c_2 stayed in the supernatant after ultracentrifugation at both low and high ionic strength. This co-precipitation of two components at low ionic strength but not high ionic strength further suggested the hydrophilic interaction between

Table 5. **Recovered cytochrome *c* or c_2 in co-precipitation experiments**

	Recovered cytochrome *c* or c_2 in supernatant (%)			
Preparation	Low salt (25mM TrisCl)		high salt (25mM Tris/250mM KCl)	
	Free	Complex	Free	Complex
Cytochrome *c*	100	0	100	0
Cytochrome c_2	100	0	100	0
Cytochrome bc_1+*c*	0.8	99	95	0
Cytochrome bc_1+c_2	28	70	95	0

R. sphaeroides bc_1 and cytochrome *c* or c_2. The complex formation between cytochrome bc_1 and *c* showed to be more sensitive to high ionic strength than that between the bc_1 and c_2.

The effect of stigmatellin was tested under these two different conditions. The results demonstrated that the complex formation between the cytochrome bc_1 and *c* or c_2 was not affected by the presence of Stigmatellin.

Spectroscopic studies of the interaction between R. sphaeroides c_1 *and cytochrome c or* c_2 - Forward reactions between *R. sphaeroides* bc_1 and cytochrome *c* or c_2 were studied by direct spectrophotometric measurements in a double-sector cuvette. When 10 µM of ascorbate-reduced *R. sphaeroides* bc_1 and 10 µM of oxidized cytochrome *c* or c_2 in 50mM phosphate buffer, pH7.5, containing 0.01% DM (low ionic strength) were placed in two separate sectors of the cuvette, the recorded spectrum showed a peak at 552nm, which is the absorption peak of reduced cytochrome c_1. Then the samples in both sectors were mixed together and the spectrum was recorded. It was to our surprise that, after mixing, the peak at 552nm disappeared and no other peak was observed. Both cytochromes c_1 and *c* showed a rapid oxidation (See Figure 25, Page 102). When the interaction was carried out in the same buffer in the presence of 500 mM KCl (high ionic strength), the peak shifted from 552 nm to 551 nm. When the interactions were carried out between the wild type *R. sphaeroides* bc_1 and cytochrome c_2, or with the cytochrome c_1 head domain and cytochrome *c*, the net oxidation was not observed under low ionic strength condition. The difference spectra were shown in Figure 26 (Page 103).

These results are different from the interaction between mitochondrial cytochrome c_1 and cytochrome *c*. When reduced mitochondrial cytochrome c_1 was

interacting with cytochrome *c* or vice versa in 50mM phosphate buffer, pH 7.4, electron transfer took place and cytochrome c_1 became partially oxidized and cytochrome *c* partially reduced or vice versa, the difference spectra showed a peak at 548 nm and a trough at 554 nm (26), no net oxidation of the cytochromes was observed.

Kinetic study of electron transfer between cytochrome c_1 and c or c_2 - Surprised by the observation of net oxidation after mixing reduced *R. sphaeroides* bc_1 and cytochrome *c*, we wondered if this still exists when the mixing of these components was tested by the stopped-flow spectrophotometer. The kinetics of electron transfer at physiological direction in which electron goes from reduced cytochrome c_1 to oxidized *c* or c_2 was examined by monitoring the absorption changes at 550 nm which is the α band belong to cytochrome *c* or c_2.

$$c_1^{2+} + c^{3+} (c_2^{3+}) \rightleftharpoons c_1^{3+} + c^{2+} (c_2^{2+})$$

The effect of ionic strength on the interaction was assayed by using various concentrations of KCl from 0 to 500mM in the 50mM phosphate buffer, pH7.5 containing 0.01% DM. As shown in Figure 27 (Page 105), when reduced wild type *R. sphaeroides* bc_1 mixed with oxidized cytochrome *c*, a rapid decrease was seen at 550 nm in the absence of KCl in phosphate buffer. Increases of KCl concentration in the reaction buffers resulted in the increases of absorption at 550 nm. When reduced cytochrome c_1 from wild type *R. sphaeroides* bc_1 was mixed with oxidized c_2 at low ionic strength, the extent of decrease at 550 nm was much less than that in the interaction between wild type *R. sphaeroides* bc_1 and cytochrome *c*. These were consistent with previous results that the interaction between *R. sphaeroides* bc_1 and cytochrome *c* is more dependent on ionic

strength than that between *R. sphaeroides* bc_1 and cytochrome c_2. The electron transfer between mitochondrial bc_1 and cytochrome *c* was also measured under the same conditions and the ionic strength dependent interactions were observed. The more KCl present in the buffer, the slower cytochrome *c* reduced, as monitored at 550 nm. When there was no KCl in 50mM phosphate, the electron transfer was too fast to be detected by the stopped-flow spectroscopy. This net oxidation of cytochrome c_1 and *c* was not affected by Stigmatellin (Figure 28, Page 106). Interestingly, this net oxidation was related with the activity of the bc_1 complex. *R. sphaeroides* mutant *Rs*ΔIV lacking subunit IV has only 30% of activity compared with the wild type complex. As shown in Figure 29 (Page 107), the interaction between reduced *Rs*ΔIV and oxidized cytochrome *c* was ionic strength dependent. The net oxidation was also observed when electron transfer took place between *Rs*ΔIV and cytochrome *c* under low ionic strength condition, but much slower than in the interaction between reduced wild type *R. sphaeroides* bc_1 and oxidized cytochrome *c.* In contrast to this, the interaction between reduced cytocrhome c_1 from *Rs*ΔIV and cytochrome c_2 showed no rapid oxidation and was ionic strength independent under all conditions examined. *R. sphaeroides* bc_1 mutant Subunit IV-fused bc_1 complex in which the subunit was linked to the cytochrome c_1 through 14 glycine residues has 90% higher activity than Wild Type bc_1 complex. This mutant showed faster and stronger oxidation after mixing with cytochrome *c* at low ionic strength (Figure 30, Page 109). From the comparison of the interactions between cytochrome c_1 from three bacterial bc_1 complex preparations with cytochrome *c*, the bc_1 complex with higher activity is more sensitive to ionic strength than that ones with lower activity. Because the purified bacterial complex is somewhat deficient in subunit IV as the interaction between

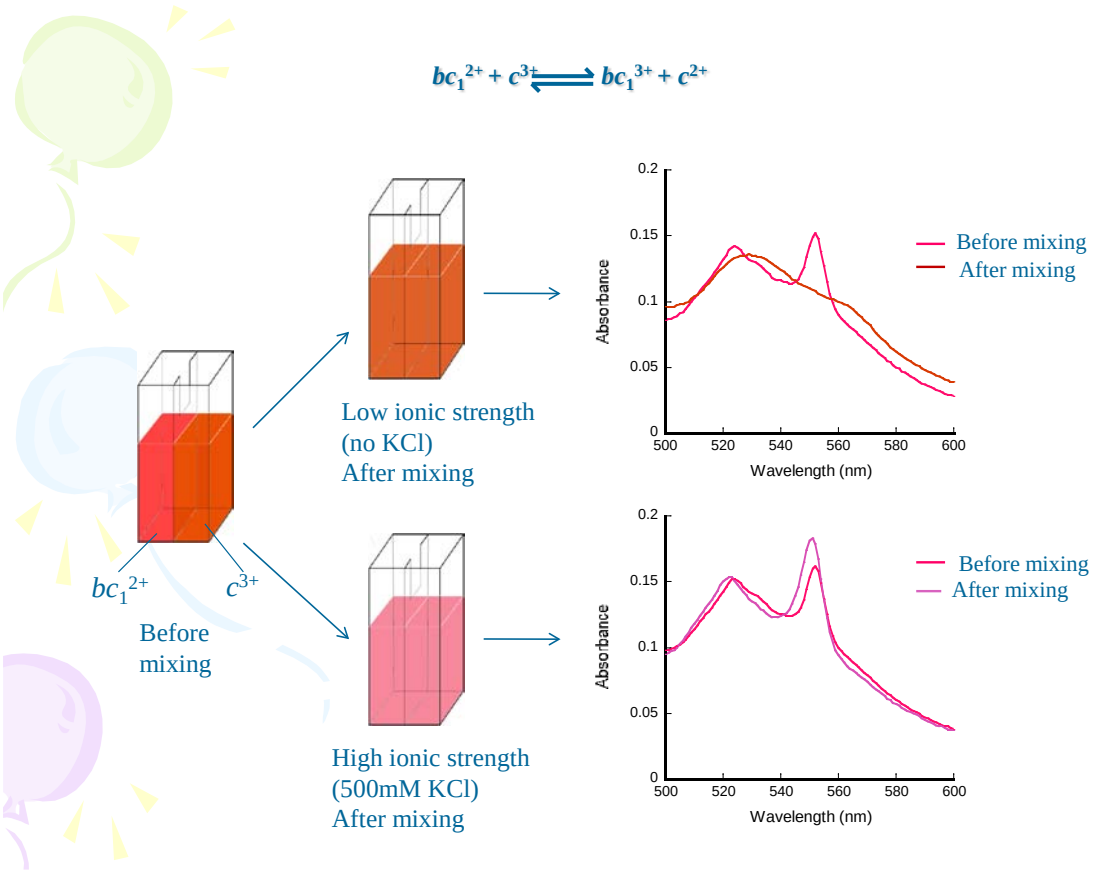

Figure 25. **Spectra of the interaction of reduced wild type *R. sphaeroides* bc_1 and oxidized cytochrome *c* under low ionic and high ionic strength conditions.**

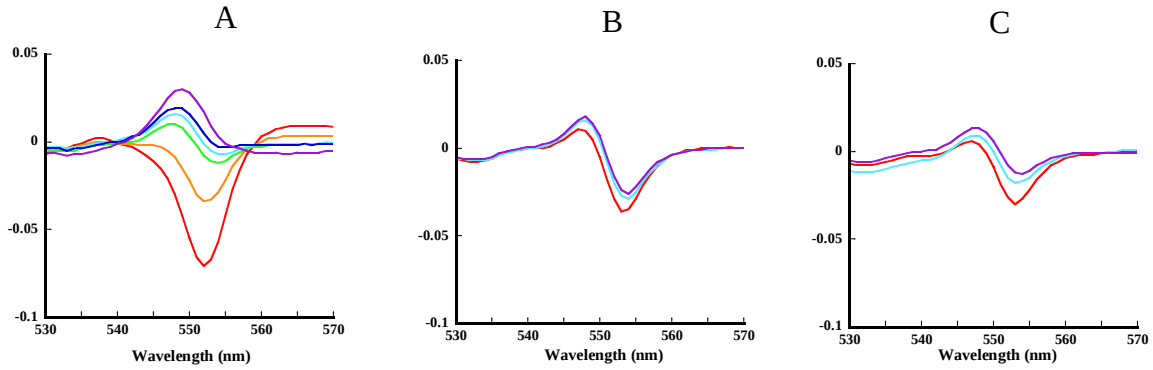

Figure 26. **Difference spectra of effect of salt concentration on electron transfer between cytochrome c_1^{2+} and cytochrome c^{3+}.** (A) wild type *R. sphaeroides* bc_1 and cytochome *c*; (B) wild type *R. sphaeroides* bc_1 and cytochrome c_2; (C) mutant cytochrome c_1 head domain and cytochrome *c*. 10μM of cytochrome c_1^{2+} and 10uM of cytochrome c^{3+} in the same buffer 50mM Phosphate, pH7.5, containing 0.01% LM and no (red), 125 (orange), 200 (green), 250 (cyan), 300 (blue) and 500 (purple) mMKCl were placed in two separate cells of a double-sector cuvette. Spectra were recorded before mixing and after mixing.

subunit IV and other core subunit is very sensitive to detergent used during purification, its activity is enhanced substantially upon the addition of recombinant subunit IV.

When the soluble cytochrome c_1 head domain was released from the transmembrane helix by mutagenesis method, it has been shown that the purified soluble head domain of *R. sphaeroides* c_1 maintains the same properties as the membrane bound cytochrome c_1. Therefore, the cyotchrome c_1 head domain provides a good opportunity to study interaction between cytochrome c_1 and *c* or c_2 in aqueous solution. The electron transfer between reduced cytochrome c_1 head domain and oxidized cytochrome *c* or c_2 was measured as a function of ionic strength. As shown in Figure 31 (Page 110), the interaction between these two components is ionic strength dependent. The higher ionic strength, the slower oxidation of cytochrome c_1 and reduction of cytochrome *c* or c_2. The interaction was too fast to be well recorded by the Stopped-flow analyzer in the absence of KCl in the buffer. When KCl concentration was increased over 200mM, the cytochrome *c* reduction slowed down significantly. The interactions between cytochrome c_1 head domain and cytochrome c_2 are less affected by the ionic strength than that between c_1 head domain and *c*. In the range of 200 to 500 mM KCl, electron transfer between cytochrome c_1 head domain and c_2 were more independent of ionic strength.

The observed net oxidation of cytochromes c_1 and *c* upon mixing at low ionic strength was unexpected. One possible reason would be the contamination of cytochrome *c* oxidase in the bc_1 preparation caused the oxidation of cytochrome *c* after electron was transferred from cytochrome c_1 to *c*. To test the possibility of existence of the cytochrome *c* oxidase in *R. sphaeroides* bc_1 preparation, the cytochrome bc_1 was diluted in 50mM phosphate buffer, pH7.5, containing 0.01% DM to 40 μM to record the spectra from 250

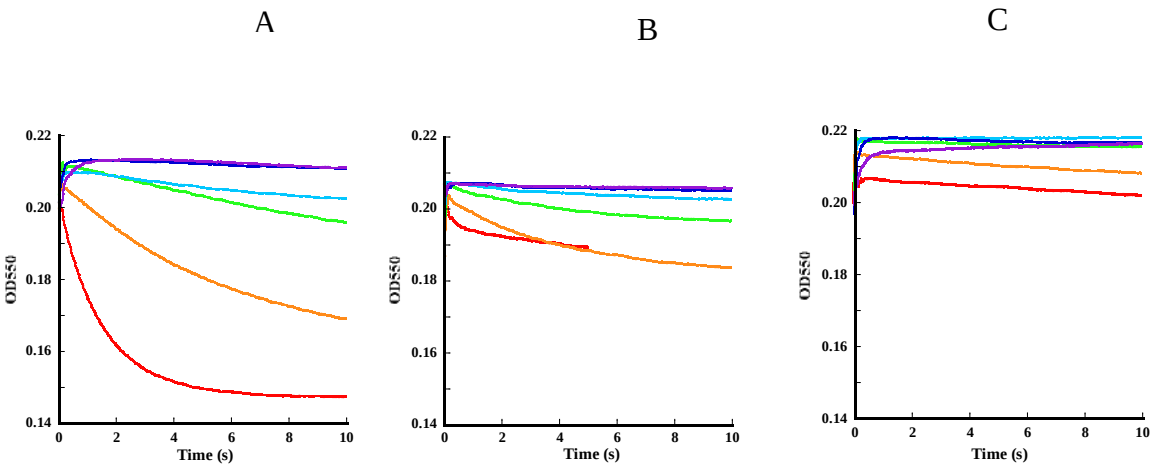

Figure 27. **Kinetics of effect of ionic strength on the interaction between wild type cytochrome c_1 and c or c_2.** (A) *R. sphaeroides* bc_1 and cytochrome *c*, (B) *R. sphaeroides* bc_1 and cytochrome c_2; (C) mitochondrial bc_1 and cytochrome *c*. 10 µM of cytochrome c_1^{2+} from *R. sphaeroides* or mitochondria and 10µM of cytochrome c^{3+} or cytochrome c_2^{3+} in the same buffer 50mM Phosphate, pH7.5, containing 0.01% LM and no (red), 125 (orange), 200 (green), 250 (cyan), 300 (blue) and 500 (purple) mMKCl were mixed in an Applied Photophysics stopped-flow reaction analyzer SX.18MV.

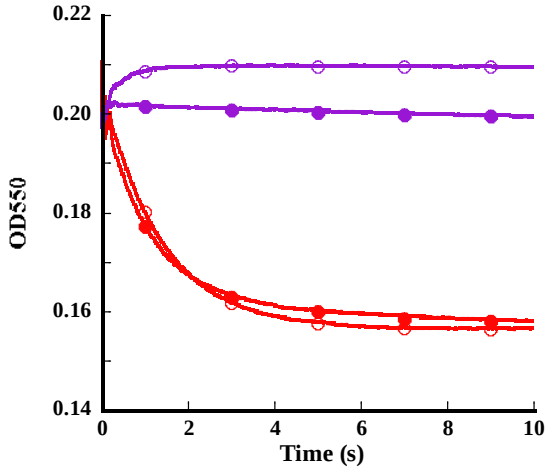

Figure 28 **. Effect of Stigmatellin on the interaction between *R. sphaeroides* bc_1^{2+} and cytochrome c^{3+} under low and high ionic strength conditions**. 10 µM of wild type *R. sphaeroides* bc_1, based on c_1, in buffer 50mM Phosphate, pH7.5, containing 0.01% DM, no or 500 mM KCl was incubated with 3 fold cytochrome *b* of Stigmatellin for 20 minutes before mixing with cytochrome c^{3+} in the same buffer in the stopped flow reaction analyzer.

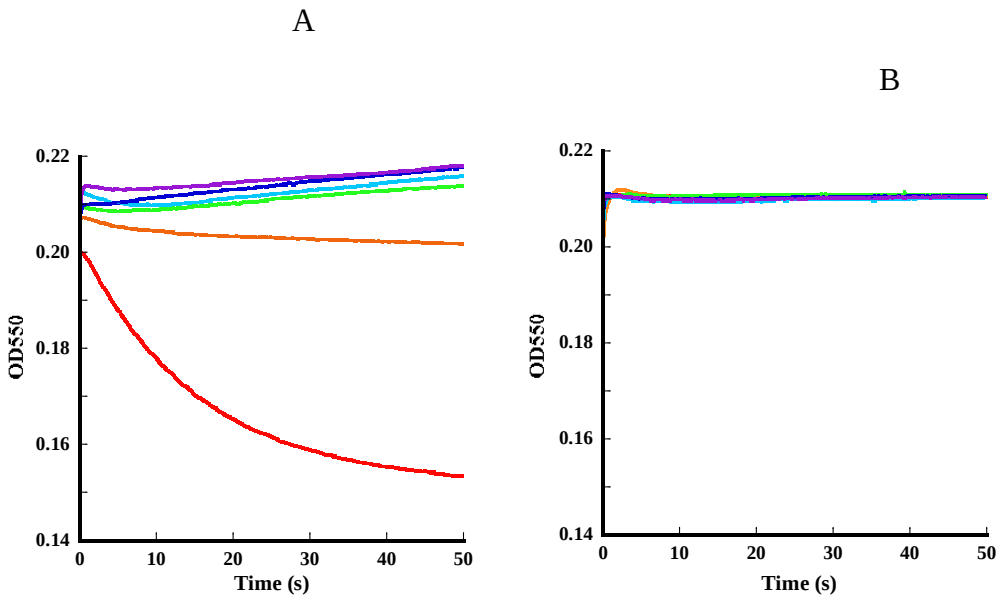

Figure 29. **Effect of Ionic strength on the interaction** between **cytochrome c_1^{2+} from mutant *R. sphaeroides* ΔIV and cytochrome c^{3+} or c_2^{3+}. (**A) 10 µM of cytochrome c_1^{2+} was mixed with 10uM of cytochrome c^{3+} or (B) 10µM cytochrome c_2^{3+} under the same conditions described in Figure 3. 10uM of cytochrome c_1^{2+} and 10uM of cytochrome c^{3+} in the same buffer 50mM Phosphate, pH7.5, containing 0.01% LM and no (red), 125 (orange), 200 (green), 250 (cyan), 300 (blue) and 500 (purple) mMKCl.

nm to 700 nm. Sodium hydrosulfite was added to reduce the sample, according to previously reported method (27). No absorption around 600nm was observed, which indicated no detectable cytochrome *c* oxidase in the sample. When sodium azide (NaN_3), an inhibitor of the cytochrome *c* oxidase, was incorporated in the interaction buffer, the net oxidation of cytochrome c_1 and *c* after mixing was still observed under low ionic strength condition. Carbon monoxide was used to further test the possible presence of cytochrome *c* oxidase in the samples. Reduced wild type *R. sphaeroides* bc_1 was diluted in 50mM phosphate buffer, pH7.5, containing 0.01% DM, to 10μM of cytochrome c_1 and the sample was bubbled with carbon monoxide gently. Then electron transfer was measured during the course of bubbling by mixing the sample with 10μM of oxidized cytochrome *c* in the same buffer. Purified cytochrome *c* oxidase was also treated with carbon monoxide simultaneously and the oxidation of cytochrome *c* by treated cytochrome *c* oxidase under the same condition was measured at same time as control. The net oxidation of cytochrome c_1 and cytochrome *c* in the interaction between reduced *R. sphaeroides* bc_1 and oxidized cytochrome *c* at low ionic strength was not eliminated by carbon monoxide, even after 3 hour-bubbling. However, the oxidation of cytochrome *c* by cytochrome *c* oxidase was completely inhibited by carbon monoxide in the control experiment after bubbling for 70 minutes. These results demonstrate that the net oxidation of the cytochrome c_1 and *c* in the interaction between reduced *R. sphaeroides* bc_1 and oxidized cytochrome *c* was not due to the contamination of the cytochrome *c* oxidase in the cytochrome bc_1 preparation.

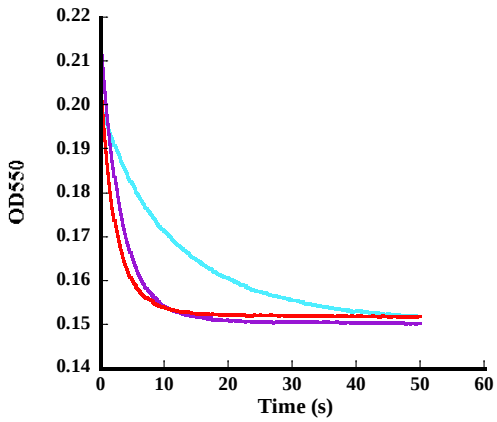

Figure 30**. Comparison of the interaction between cytochrome c_1^{2+} in the wild type *R. sphaeroides* bc_1 or Subunit IV fused bc_1 complex and cytochrome c^{3+} under low ionic strength condition.** Ten µM of cytochrome c_1^{2+} was mixed with 10µM of cytochrome c^{3+} in the same buffer 50mM Phosphate, pH7.5, containing 0.01% DM and 8mMKCl.

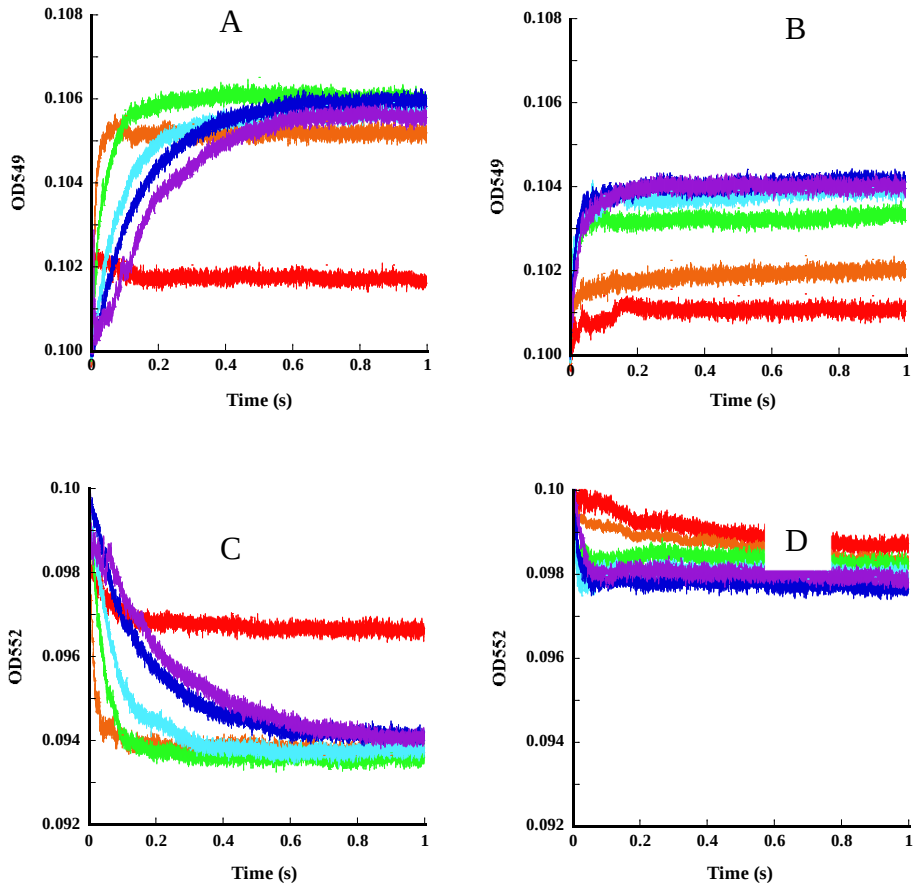

Figure 31. **Fast kinetic studies of electron transfer between *R. sphaeroides* cytochrome c_1 head domain and cytochrome *c* or c_2.** (A) Reduction of the cytochrome *c* and (C) oxidation of the cytochrome c_1 in the interactions between c_1 head domain and *c*; (B) Reduction of the cytochrome c_2 and (D) Oxidation of the cytochrome c_1 in the interactions between c_1 head domain and c_2; The colors representing different salt concentrations in the buffers are: red for without KCl, orange for 100mMKCl, green for 200mMKCl, cyan for 300mMKCl, blue for 400mMKCl and purple for 500mMKCl. Experimental conditions were described in the "Experimental Procedure." All protein concentrations were 10uM. Reaction carried at 22°C.

Thermotropic studies of the complex formation between R. sphaeroides cytochrome c_1 and c or c_2 - (Summary in Table 6, Page 114) Generally speaking, if a ligand binds to the native conformation of a protein or a complex forms between two proteins, a higher thermal stability of the protein-ligand or protein-protein complex than either of the two individual components will be observed. DSC is a popular method to measure protein - ligand and protein - protein interactions (28,29).

In 50 mM phosphate buffer, pH 7.5, containing 0.01% DM (low salt) (Figure 32, Page 112), the wild type *R. sphaeroides* cytochrome bc_1 complex showed a thermal transition temperature at 43°C and an enthalpy change of 126.5 kcal/mol, compared with those of 46.8°C and 155.3 kcal/mol when 250mM KCl (high salt) was added into the same buffer. Under the same low or high salt condition, when the equal concentration of cytochrome *c* was mixed with the wild type *R. sphaeroides* bc_1, a transition temperature at 43.8°C and an enthalpy change of 95.4 kcal/mol at low salt, a transition temperature at 46.8°C and an enthalpy change of 144.4 kcal/mol at high salt were observed. Besides the transition peaks of the wild type bc_1 complex, another transition peaks of 69.5°C and 71°C appeared in the thermogram in the interactions between cytochrome bc_1 and *c* under both low and high ionic strength conditions, respetively. The peaks at higher temperature were different from the thermal transition peak of native cytochrome *c* because it undergoes thermal-denaturation at 83.1°C at low ionic strength and 80.6°C at high ionic strength. This suggested that although no stable complex formed between *R. sphaeroides cytochrome* bc_1 and cytochrome *c*, there were still interactions which destabilized cytochrome *c* under both low and high ionic strength conditions. Apparently, the cytochrome *c* was not as stable in the mixture as in its native state.

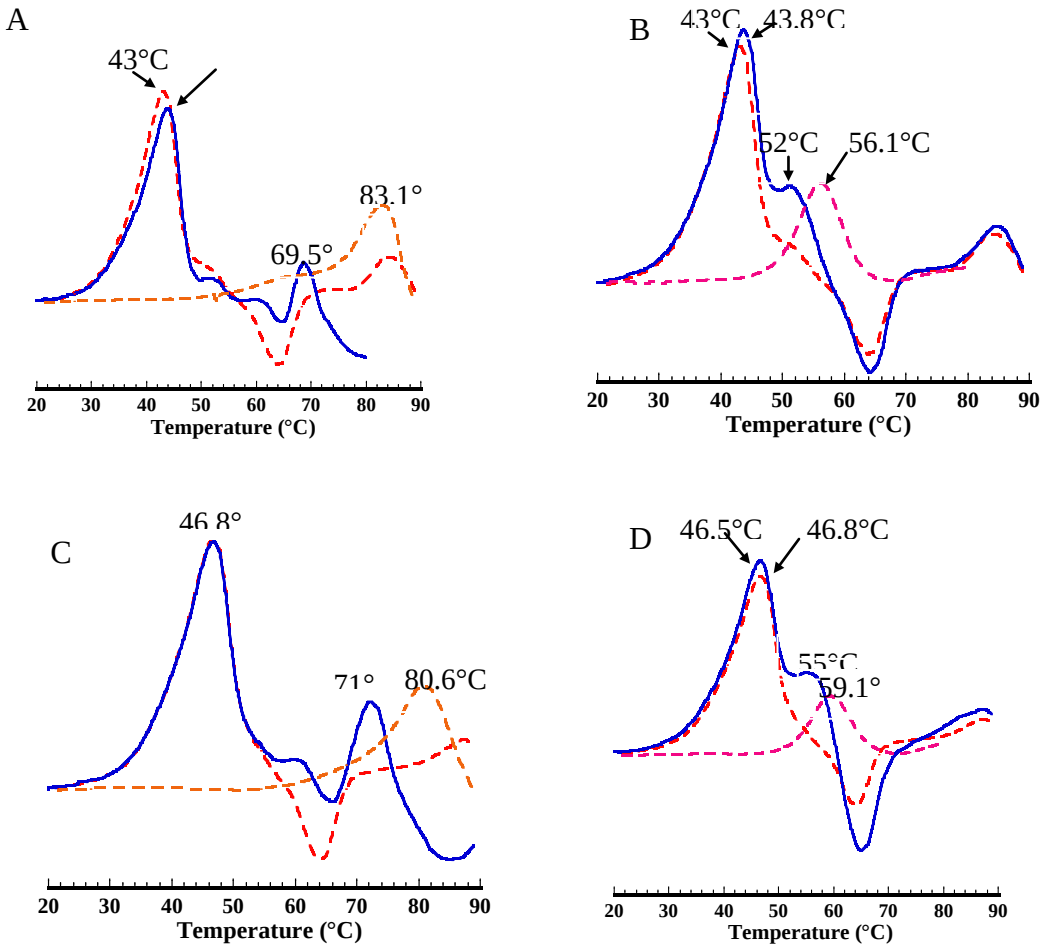

Figure 32. **Effect of the ionic strength on the complex formation between *R. sphaeroides* cytochrome bc_1 and cytochrome *c* or c_2.** (A) bc_1+*c* at low ionic strength (50mM phosphate, pH7.5, containing 0.01%DM); (B) bc_1+c_2 at low ionic strength; (c) bc_1+*c* at high ionic strength(50mM phosphate, pH7.5, containing 250mM KCl and 0.01%DM); (D) bc_1+c_2 at high ionic strength. Solid blue lines, equal molar concentration (50μM) of oxidized wild type *R. sphaeroides* cytochrome bc_1 and the oxidized cytochrome *c* or c_2 mixed in low or high ionic strength buffers, the mixture was incubated at 4°C for 30 minutes prior to measuring the DSC thermograms. All the dashed lines represent: red, the wild type *R. sphaeroides* cytochrome bc_1; orange, the cytochrome *c*; rose, the cytochrome c_2, measured separately under same conditions.

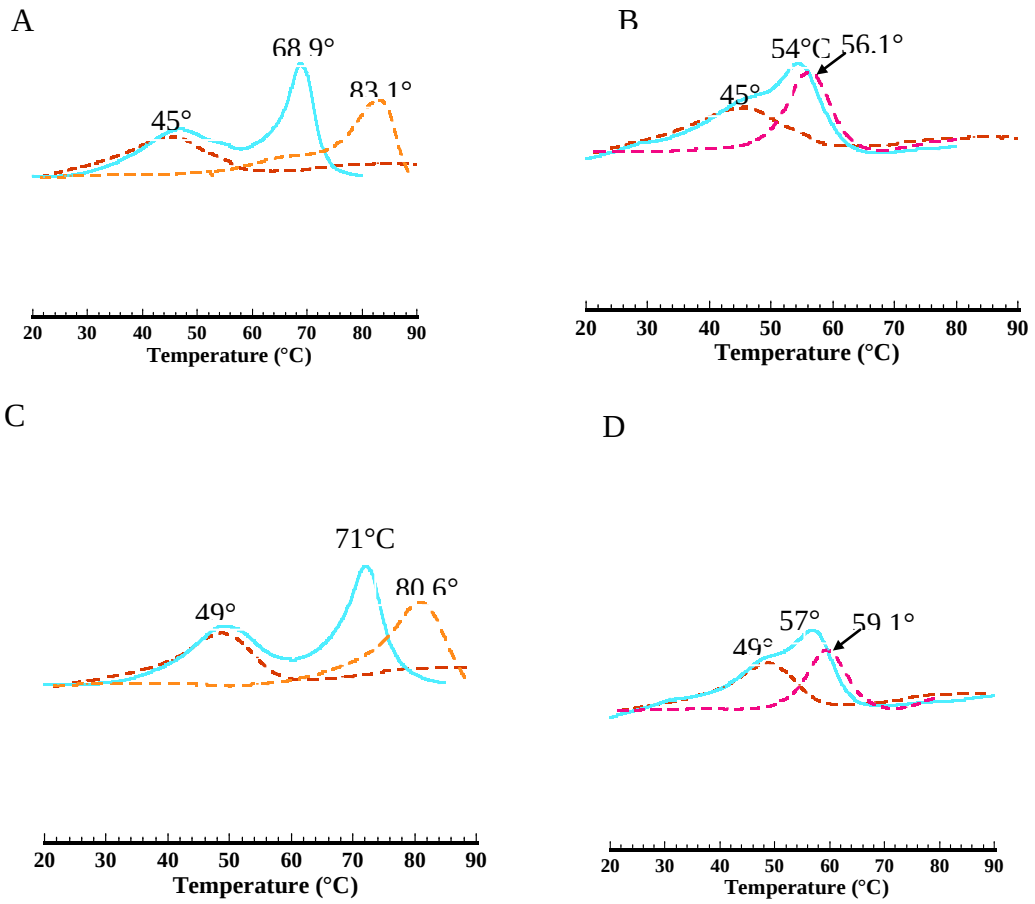

Figure 33. **Effect of the ionic strength on the complex formation between *R. sphaeroides* cytochrome c_1 head domain and cytochrome *c* or c_2.** (A) c_1 head domain+*c* at low ionic strength (50mM phosphate, pH7.5); (B) c_1 head domain+c_2 at low ionic strength; (c) c_1 head domain+*c* at high ionic strength(50mM phosphate, pH7.5, containing 250mM KCl); (D) c_1 head domain+c_2 at high ionic strength. Solid cyan lines, equal molar concentration (250μM) of oxidized c_1 head domain and the oxidized cytochrome *c* or c_2 mixed in low or high ionic strength buffer, the mixture was incubated at 4°C for 30 minutes prior to measuring the DSC thermograms. All the dashed lines represent: brown, the cytochrome c_1 head domain; orange, the cytochrome *c*; rose, the cytochrome c_2, measured separately under same conditions.

Table 6. **Thermal denaturation temperature and change in enthalpy of interaction between *R. sphaeroides* cytochorme c_1 and *c* or c_2 under low and high ionic strength conditions**.

Preparation	Low ionic strength (50mM Na^+/K^+/0.01% DM)		High ionic strength (50mM Na^+/K^+/0.01% DM/250mM KCl)	
	Tm (°C)	ΔH (kcal/mol)	Tm (°C)	ΔH (kcal/mol)
Cytochrome *c*	83.1	78	80.6	66.1
Cytochrome c_2	56.1	54.5	59.1	40.9
Cytochrome c_1 head domain	45	75.3	49	86.6
Cytochrome bc_1	43	126.7	46.8	155.3
Cytochrome bc_1 + *c*	43.8	95.4	46.8	144.4
Cytochrome bc_1 + c_2	43.8	158.2	46.5	186.9
Cytochrome c_1 head domain + *c*	68.9	126.9	72.1	128.5
Cytochrome c_1 head domain + c_2	54.4	91.1	56.9	105.5

When the cytochrome c_2 was applied to the interaction, the thermogram was found to be different from the interaction between bc_1 and *c*. In the mixture, the cytochrome bc_1 showed a thermal denaturation temperature at 43.8°C and an enthalpy change of 158.2 kcal/mol at low salt and those of 46.5°C and 186.9 kcal/mol at high salt. The shoulders were observed on the right side of the transition peaks of the wild type bc_1 with temperatures of 51°C and 55°C under low and high ionic strength conditions, respectively. Under same conditions, the cytochrome c_2 had transition temperature at 56.1°C at low ionic strength and 59.5°C at high ionic strength. This indicated that the complexes formed between *R. sphaeroides cytochrome* bc_1 and c_2 under both low and high ionic strength conditions but cytochrome c_2 was more sensitive to heat upon mixing with cytochrome bc_1 complex than it was in the solution alone.

The cytochrome c_1 head domain showed a thermal denaturation temperature at 45°C and an enthalpy change of 75.3 kcal/mol at low ionic strength (50 mM phosphate, pH7.5), compare with 49°C and 86.6 kcal/mol at high ionic strength (50 mM phosphate, pH7.5, containing 250 mM KCl) (Figure 33, Page 113). When the cytochrome c_1 head domain and was mixed cytochrome *c*, a peak appeared with an enthalpy change of 126.9 kcal/mol a temperature of 68.9°C in the low salt buffer or 128.5 kcal/mol and 72.1°C in high salt buffer besides the peak of 45°C or 49°C which belonged to the cytochrome c_1 head domain. Similar to the interaction between the cytochrome bc_1 complex and *c*, these higher temperature peaks were different from ones of the native cytochrome *c* under same conditions. These results suggested that the interactions between these components under at both low and high ionic strength did not result in stable complex formation but the destabilized cytochrome *c*.

When the c_1 head domain and c_2 were applied to the same conditions, the thermal properties of the mixtures developed differently from the ones with cytochrome *c*. A peak were detected at with 91.1 kcal/mol and 54°C at low salt or 105.1 kcal/mol and 57°C at high salt, companied with left side shoulders of 45°C and 49°C belonged to the cytochrome c_1 head domain. These demonstrated that the complexes formed between the cytochrome c_1 head domain and c_2 at both low and high ionic strength during the process of DSC. The formation of complexes caused the c_2 to be more labile to the heat.

The results of thermal properties of the interactions between *R. sphaeroides* cytochrome bc_1 or the soluble c_1 head domain and the cytochrome *c* are different from interactions in mitochondria. When the interaction between isolated mitochondrial cytochrome c_1 and *c* at low ionic strength (10mM phosphate buffer, at neutral pH), studied by DSC, a single peak showing higher thermal stability appeared. In high ionic strength buffer (100mM phosphate buffer, pH7.0), two peaks were observed but cytochrome *c* was destabilized upon mixing (30). These results indicated that the complex formation in vitro between mitochondrial cytochrome c_1 and *c* is ionic strength dependent.

Although DSC is a powerful technique to measure the complex formation between proteins, the thermal properties of the protein and protein interaction are often very complicated. Many factors can affect the result of the complex formation during the process of DSC. The interaction between *R. sphaeroides* cytochrome bc_1 and cytochrome *c* or c_2 showed different DSC patterns. This is not unusual since the electron transfer and complex formation between cytochrome bc_1 and *c* or c_2 are dynamic processes. In electron transfer process in vivo, the electron is passed from reduced cytochrome c_1 to

oxidized *c* or c_2. However, it takes place so fast that the transient complex formed is undetectable by DSC. When oxidized cytochrome c_1, either complexed or uncomplexed, and cytochrome *c* or c_2 were mixed in DSC, they reached a dynamic equilibrium state during the long heating process of DSC. They may associate together as a complex in solution (bc_1 and c_2) or stay mostly independent but still affect each other somehow (bc_1 and *c*). Once two components reach the equilibrium, the ionic strength might not affect this equilibrium as much as on the transient complex formation.

From the DSC patterns, we also can see the cytochrome *c* is more labile to heat under low ionic strength than high ionic strength upon mixing with cytochrome bc_1 or c_1 head domain. The transition temperature of cytochrome *c* dropped about 14°C under low ionic strength condition but 9°C under high ionic strength condition in the interactions. In contrast to this, the transition temperature of cytochrome c_2 only decreased 4°C interacting with cytochrome c_1 from bc_1 complex or 2°C interacting with c_1 head domain under both conditions. This suggested that interaction between cytochrome c_1 and *c* is more affected by ionic strength, which is consistent with previous results. Upon mixing with cytochrome c_1, the cytochrome *c* undergoes more conformational change at low ionic strength than high ionic strength, which is indicated by the larger difference of transition temperature on DSC patterns. This might be related to the observation of net oxidation in the kinetics studies.

Interaction between cytochrome c_1 and c or c_2 - The electron transfer between cytochrome c_1 and *c* or c_2 is hydrophilic or electrostatic, which has been under debate for decades. Both opinions agree to the formation of a transient 1:1 complex between reduced cytochrome c_1 and oxidized *c* or c_2. This process includes the interaction

between c_1 and its electron acceptor, the transient complex formation, rapid electron transfer and complex dissociation and reduced product release. In mitochondria, most studies supported the ionic strength dependent reactions. In bovine heart, the reaction is too fast to be measured by stopped flow technique below 200mM ionic strength since it takes place within microseconds. Increase of ionic strength decreased the reaction rate substantially (26,31). Photosynthetic purple bacteria *Rhodobacter capsulatus* and *Rhodopseudomonas viridis*, the cytochrome bc_1 has three core subunits and no supernumerary subunit, *Rhodospirillum rubrum* bc_1 complex has the similar operon arrangement as *R. sphaeroides* cytochrome bc_1. It has been proven that electrostatic interaction between the cytochrome bc_1 complex and cytochrome c_2 is important (13,32-34).

A mechanism of interaction between cytochrome c_1 and cytochrome *c* has been proposed in which that the electrostatic interaction steers the docking of cytochrome *c* to the specific configuration stabilized by the central hydrophobic domain that is optimized for rapid electron transfer. This biphasic mechanism is supported by several different electron transfer systems including *R. sphaeroides* cytochrome c_2 - Reaction Center complex, and cytochrome *c* - cytochrome *c* oxidase complex (35). Recently, it was found the binding of cytochrome c_1 and c_2 in *Rhodobacter capsulatus* is mediated by the conformational change of the ISP. The binding of Stigmatellin affects the interaction via fixing the ISP head domain at *b* position (36).

The hydrophobic core interface between cytochrome c_1 from yeast bc_1 complex and *c* in the co-crystal structure also provided the evidence for this mechanism. However, sequence alignment showed that some of residues involved in the interaction between

yeast cytochrome c_1 and *c* complex are not conserved (37). Since co-crystals of cyrochrome bc_1 and c_2 from *R. sphaeroides* are still unavailable, it is difficult to conclude if the mechanism of yeast cytochrome c_1 - c_2 interaction applies to *R. sphaeroides.* It is also possible that the structure in the crystal is different from the one in the solution.

In our study, the results supported the hydrophilic interaction between *R. sphaeroides* cytochrome c_1 and *c* or c_2. As shown in gel filtration and pull down experiments, the wild type of *R. sphaeroides* cytochrome bc_1 formed complex with the cytochrome *c* or c_2 at low ionic strength but not high ionic strength. When reduced *R. sphaeroides* cytochrome c_1 head domain and oxidized cytochrome *c* or c_2 were mixed in the low salt buffer, the fast oxidation of cytochrome c_1 and reduction of cytochrome *c* or c_2 were observed. The reactions were affected by the concentrations of the KCl present in the buffer. Our results also indicated that the ionic strength does not affect the interaction between bc_1 complex and *c* or c_2 in bacteria as much as in mitochondria. It was found that, in BLAST database, *R. sphaeroides* and a member of the marine *Roseobacter* clade are close relatives (38). Higher salt tolerance might be the heritage from its ancestor living in the saline environment. It also gives *R. sphaeroides* an advantage to adapt the different environments.

However, it was to our surprise that a net oxidation of cytochrome c_1 and *c* was observed after mixing reduced c_1 and oxidized *c* together under low ionic strength conditions. The induced oxidation is not sensitive to carbon monoxide, suggesting that the oxidation was not due to the presence of cytochrome *c* oxidase in the *R. sphaeroides* cytochrome bc_1 complex preparation. No net oxidation was observed when reduced isolated mitochondrial cytochrome c_1 or head domain of bacterial cytochrome c_1 and

cytochrome *c* were mixed at low ionic strength. The presence of Stigmatellin had no effect on the appearance of net oxidation of *R. sphaeroides* c_1 and *c* under low ionic strength condition. The higher the electron transfer activity of the *R. sphaeroides* bc_1, the faster the oxidation occurred. So far we do not have a reasonable explanation how this net oxidation took place. Since it did not happen to the mixture of either mitochondrial bc_1 complex or *R. sphaeroides* cytochrome c_1 head domain but happen in the *R. sphaeroides* bc_1 complex and cytochrome *c*, there must be some influences from other subunits in the complex system. One possibility is that mixing of the *R. sphaeroides* bc_1 and cytochrome *c* under low ionic strength condition caused the change of redox potential of the cytochome *c* or other components. It has been proven that the cyrochrome *c* under dymamic conformational change between reduced and oxidized states (39,40). Our results indicated the conformational change of cytochrome *c* is more sensitive to ionic strength when it is interacting with *R. sphaeroides* cyrochrome c_1. Possibly, this conformational change caused the decrease of redox potential of cytochrome *c* upon mixing with *R. sphaeroides* cyrochrome bc_1 complex, resulting in the observed net oxidation in the interacting system. The understanding the mechanism of this net oxidation will give us valuable information in elucidating the interaction between the cytochrome c_1 and *c*.

References

1. Xia, D., Yu, C. A., Kim, H., Xia, J. Z., Kachurin, A. M., Zhang, L., Yu, L., and Deisenhofer, J. (1997) *Science* **277**, 60-66
2. Hunte, C., Koepke, J., Lange, C., Rossmanith, T., and Michel, H. (2000) *Structure* **8**, 669-684
3. Tian, H., Sadoski, R., Zhang, L., Yu, C. A., Yu, L., Durham, B., and Millett, F. (2000) *J Biol Chem* **275**, 9587-9595
4. Stonehuerner, J., O'Brien, P., Kendrick, L., Hall, J., and Millett, F. (1985) *J Biol Chem* **260**, 11456-11460
5. Stonehuerner, J., O'Brien, P., Geren, L., Millett, F., Steidl, J., Yu, L., and Yu, C. A. (1985) *J Biol Chem* **260**, 5392-5398
6. Guner, S., Willie, A., Millett, F., Caffrey, M. S., Cusanovich, M. A., Robertson, D. E., and Knaff, D. B. (1993) *Biochemistry* **32**, 4793-4800
7. Millett, F., and Durham, B. (2004) *Photosynth Res* **82**, 1-16
8. Broger, C., Salardi, S., and Azzi, A. (1983) *European Journal of Biochemistry* **131**, 349-352
9. Speck, S. H., Ferguson-Miller, S., Osheroff, N., and Margoliash, E. (1979) *Proc Natl Acad Sci U S A* **76**, 155-159
10. Iwata, S., Lee, J. W., Okada, K., Lee, J. K., Iwata, M., Rasmussen, B., Link, T. A., Ramaswamy, S., and Jap, B. K. (1998) *Science* **281**, 64-71
11. Hunte, C. (2001) *FEBS Lett* **504**, 126-132
12. Heacock, D. H., 2nd, Liu, R. Q., Yu, C. A., Yu, L., Durham, B., and Millett, F. (1993) *J Biol Chem* **268**, 27171-27175

13. Guner, S., Willie, A., Millett, F., Caffrey, M. S., Cusanovich, M. A., Robertson, D. E., and Knaff, D. B. (1993) *Biochemistry* **32**, 4793-4800

14. Hunte, C., and Michel, H. (2002) *Curr Opin Struct Biol* **12**, 503-508

15. Hunte, C., Solmaz, S., Palsdottir, H., and Wenz, T. (2008) *Results Probl Cell Differ* **45**, 253-278

16. Solmaz, S. R., and Hunte, C. (2008) *J Biol Chem* **283**, 17542-17549

17. Yu, C. A., and Yu, L. (1982) *Biochemistry* **21**, 4096-4101

18. Yu, C. A., and Yu, L. (1980) *Biochim Biophys Acta* **591**, 409-420

19. Yu, L., Yang, S., Yin, Y., Cen, X., Zhou, F., Xia, D., and Yu, C. A. (2009) *Methods Enzymol* **456**, 459-473

20. Tian, H., Yu, L., Mather, M. W., and Yu, C. A. (1998) *J Biol Chem* **273**, 27953-27959

21. Tso, S. C., Yin, Y., Yu, C. A., and Yu, L. (2006) *Biochim Biophys Acta* **1757**, 1561-1567

22. Yu, L., Dong, J. H., and Yu, C. A. (1986) *Biochim Biophys Acta* **852**, 203-211

23. Berden, J. A., and Slater, E. C. (1970) *Biochim Biophys Acta* **216**, 237-249

24. Bartsch, R. (1978) *Plenum Press New York*

25. Laemmli, U. K. (1970) *Nature* **227**, 680-685

26. Yu, C. A., Yu, L., and King, T. E. (1973) *J Biol Chem* **248**, 528-533

27. Yu, C. A., and King, T. E. (1977) *Biochem Biophys Res Commun* **74**, 670-676

28. Bruylants, G., Wouters, J., and Michaux, C. (2005) *Curr Med Chem* **12**, 2011-2020

29. Celej, M. S., Montich, G. G., and Fidelio, G. D. (2003) *Protein Sci* **12**, 1496-1506

30. Yu, C. A., Steidl, J. R., and Yu, L. (1983) *Biochim Biophys Acta* **736**, 226-234

31. Konig, B. W., Wilms, J., and Van Gelder, B. F. (1981) *Biochim Biophys Acta* **636**, 9-16

32. Ambler, R. P., Meyer, T. E., and Kamen, M. D. (1976) *Proc Natl Acad Sci U S A* **73**, 472-475

33. Hall, J., Zha, X. H., Yu, L., Yu, C. A., and Millett, F. (1987) *Biochemistry* **26**, 4501-4504

34. Hall, J., Zha, X. H., Yu, L., Yu, C. A., and Millett, F. (1989) *Biochemistry* **28**, 2568-2571

35. Kefei Wang, e. a. (1999) *THE JOURNAL OF BIOLOGICAL CHEMISTRY* **274**, 38042-38050

36. Devanathan, S., Salamon, Z., Tollin, G., Fitch, J. C., Meyer, T. E., Berry, E. A., and Cusanovich, M. A. (2007) *Biochemistry* **46**, 7138-7145

37. Millett F, D. B. (2004) *Photosynth Res.* **82(1)**, 1-16

38. Mackenzie, C., Eraso, J. M., Choudhary, M., Roh, J. H., Zeng, X., Bruscella, P., Puskas, A., and Kaplan, S. (2007) *Annual review of microbiology* **61**, 283-307

39. Liu, W., Rumbley, J. N., Englander, S. W., and Wand, A. J. (2009) *Protein Sci* **18**, 670-674

40. Yeh, S. R., and Rousseau, D. L. (1998) *Nat Struct Biol* **5**, 222-228

VITA

FEI ZHOU

Candidate for the Degree of

Doctor of Philosophy

Thesis: OXYGEN DEPENDENT ELECTRON TRANSFER IN THE CYTOCHROME BC1 COMPLEX AND THE INTERACTION BETWEEN *RHODOBACTER SPHAEROIDES* bc_1 COMPLEX AND CYTOCHROME *c* OR c_2

Major Field: Biochemistry and Molecular Biology

Biographical:

Education:

Completed the requirements for the Doctor of Philosophy degree with a major in Biochemistry and Molecular Biology at Oklahoma State University in Dec. 2011;
Completed the requirements for the Master of Science in Cell Biolgy at Lanzhou University, Lanzhou, Gansu, P.R.China in 2004;
Completed the requirements for the Bachelor of Engineering in Machinery and its Automation at Jiangsu University, Zhenjiang, Jiangsu, P.R.China in 2000.

Professional Memberships:

American Biophysical Society
Biochemistry & Molecular Biology Graduate Student Association at Oklahoma State University

Publications:

Zhou, F., Yin, Y., Su, T., Yu. L., and Yu, C.A. Oxygen dependent electron transfer in the cytochrome bc_1 complex (Manuscript submitted)

Zhou, F., Yu. L., and Yu, C.A. The interaction between *Rhodobacter sphaeroides* cytochrome bc_1 and c or c_2 (Manuscript in preparation)

Qu, Y., **Zhou, F.**, Yu. L., and Yu, C.A. Involvement of R94 of the cytochomre *b* in porton pumping in the cytochomre bc_1 complex from *Rhodobacter sphaeroides* (Manuscript in preparation)

Xia, D., Esser, E., Elberry, M., **Zhou, F.**, Yu, L., and Yu, C-A. (2008). *J. Bioenergetic Biomembrane*. **40**, 485-492.

Esser, L., Elberry, M., **Zhou, F.**, Yu, C-A., and Di Xia (2008). *J. Biol. Chem.* **283,** 2846-2857.

Yu, L., Yang, S., Yin, Y., Cen, X., **Zhou, F.**, Yu, C-A. *Methods Enzymol.* (2009) 456 :459-73

Name: FEI ZHOU Date of Degree: December, 2011

Institution: Oklahoma State University Location: Stillwater, Oklahoma

Title of Study: OXYGEN DEPENDENT ELECTRON TRANSFER IN THE CYTOCHROME bc_1 COMPLEX AND THE INTERACTION BETWEEN *RHODOBACTER SPHAEROIDES* BC_1 COMPLEX AND CYTOCHROME *c* OR c_2

Pages in Study: 123 Candidate for the Degree of Doctor of Philosophy

Major Field: Biochemistry and Molecular Biology

Scope and Method of Study:

Although it has been well recognized that the bc_1 complex also generates a small amount of superoxide anion during the catalytic reaction, the involvement of molecular oxygen in the regulation of the bc_1 electron transfer reaction was never noticed until now. The mechanism of interaction between cytochromes c_1 in bc_1 complex and *c* (or c_2 in bacterial system) has been extensively studied but not been concluded. To elucidate the role of oxygen in the electron transfer catalyzed by cytochrome bc_1 complex and superoxide generation, we assayed the electron transfer activity of bc_1 complexes, measured pre-steady *b* and c_1 reduction in wild type of *Rhodobacter sphaeroides* cytochrome bc_1, b_L or b_H lacking mutants by ubiquino as well as superoxide generation under aerobic and anaerobic conditions. To clarify nature of interaction between cytochrome c_1 and *c* or c_2, we examined the interaction under ionic strength conditions by using gel filtration, co-precipitation, fast kinetics and DSC. We also constructed mutant cytochrome c1 water soluble head domain to test the cytochrome c_1 and *c* or c_2 interaction under different ionic strength conditions.

Findings and Conclusions:

Our results demonstrated that oxygen is involved in the regulation of the electron transfer catalyzed by cytochrome bc_1 complex. Oxygen increases the electron transfer activity of the bc_1 complex up to 50%, depending on the intactness of the complex. Oxygen enhances the pre-steady reduction rate of cytochrome b_L and has no effect on the reduction of cytochrome b_H. By using a heme b_L or b_H knockout *R. sphaeroides* bc_1 mutant complex, the site affected by oxygen in the electron transfer sequence was identified to be cytochrome b_L. The interaction between *Rhodobacter sphaeroides* cytochrome bc_1 and *c* or c_2 is electrostatic. A net oxidation of cytochrome c_1 and *c* was observed after mixing reduced c_1 and oxidized *c* together under low ionic strength condition. The effect of ionic strength on the interaction between bc_1 and *c* is more than the interaction between bc_1 and c_2.

ADVISER'S APPROVAL: Dr. Chang-An Yu